

Copyright  
by  
LaNisha LaTice Patterson  
2022

The Dissertation Committee for LaNisha LaTice Patterson certifies that this  
is the approved version of the following dissertation:

***Ehrlichia chaffeensis* Activates Notch Signaling Through  
SLiM Mimicry to Inhibit Apoptosis**

Committee:

*Jere W. McBride*

---

Jere W. McBride, Ph.D.

*Andres Oberhauser*

---

Andres Oberhauser, Ph.D.

*Thomas J. Smith*

---

Thomas Smith, Ph.D.

*Gracie Vargas*

---

Gracie Vargas, Ph.D.

*Joya Chandra*

---

Joya Chandra, Ph.D.

*Spyros Artavanis-Tsakonas*

---

Spyros Artavanis-Tsakonas, Ph.D.

***Ehrlichia chaffeensis* Activates Notch Signaling Through  
SLiM Mimicry to Inhibit Apoptosis**

by

**LaNisha LaTice Patterson, B.S., M.S.**

**Dissertation**

Presented to the Faculty of the Graduate School of  
The University of Texas Medical Branch  
in Partial Fulfillment  
of the Requirements  
for the Degree of

**Doctor of Philosophy**

**The University of Texas Medical Branch  
November 2022**

## **Dedication**

I would like to dedicate this dissertation to my deceased father,  
Myron Wade Patterson.

## **Acknowledgements**

My research herein is dedicated to my entire support system that has helped me complete this journey in various ways. I would like to thank the Most High for guiding me through this journey during very hard times which gave me the strength necessary to obtain this accomplishment. A big thank you to my principal investigator, Jere McBride, who has played a huge role in my success as a Ph.D. student. A special thank you to Xiaofeng Zhang who has also been essential to my success in the laboratory. Thank you to current and previous lab members who have assisted me in several experiments necessary for the completion of degree. Your hard work and collaboration are much appreciated.

I would like to especially thank my parents who have set the educational foundation that was necessary for me to complete my Ph.D. Without their love and guidance, my journey in research would have never been. I would especially like to dedicate this research project to my father, Myron Wade Patterson, who recently passed away from cholangiocarcinoma in 2020. Thank you for all of your love, supportive words, life lessons and study sessions. To my beautiful mother, thank you for constantly checking on me and during difficult times and life-coaching me through my Ph.D. experience. Your love and support cannot be replaced.

To my significant other, Adrian Green, thank you for your support and blessing me with our beautiful daughter, Alaysia Amani Green. It is the constant love and memories that our family shares and builds that have pushed me to complete my Ph.D. journey. To my family, especially my sisters and mother-in-law, thank you for your help and support especially with encouraging talks, advice, and taking care of Alaysia while I pursued my Ph.D. To my friends, thank you for cheering me on and being the extra support system necessary for me to fulfill my obligations as a Ph.D. student. Without the love and laughs from each of you, this journey would have been more challenging.

# ***Ehrlichia chaffeensis* Activates Notch Signaling Through SLiM Mimicry to Inhibit Apoptosis**

Publication No. \_\_\_\_\_

LaNisha LaTice Patterson

The University of Texas Medical Branch, 2022

Supervisor: Jere W. McBride

*Ehrlichia chaffeensis* is a small, obligately intracellular gram-negative bacterium, and the etiological agent of human monocytotropic ehrlichiosis (HME), an emerging, life-threatening tick-borne zoonosis. *E. chaffeensis* infects mononuclear phagocytes and has evolved molecular strategies to reprogram the host cell involving secreted effectors that interact directly with the host cell targets. Recently, we have shown *E. chaffeensis* evasion of innate defenses of the macrophage involve activation of Wnt, Hedeghog and Notch signaling pathways. Interestingly, the *E. chaffeensis* tandem repeat effector, TRP120, has been shown to interact with host proteins important for activation and regulation of conserved signaling pathways including Wnt, Notch and Sonic Hedgehog. In this study, we investigated the molecular interactions and functional implications of Notch activation during *E. chaffeensis* infection.

The **objective** of this research project is to identify the SLiM ligand mimetic in *E. chaffeensis* TRP120 and the functional implications of TRP120 Notch activation. Two aims were originally proposed to investigate this hypothesis. **Aim 1** was to elucidate the molecular interactions required for TRP120 Notch activation. **Aim 2** was to investigate the role of *E. chaffeensis* Notch stabilization of XIAP and inhibition of caspase activation. Based on the evidence collected during my research, I have concluded that a TRP120-TR Notch SLiM mimetic motif directly binds Notch-1 at a region containing the LBD to activate Notch signaling. TRP120 Notch activation results in an anti-apoptotic program involving inhibitor of apoptosis proteins (IAPs) that inhibits caspase activation for intracellular survival.

We demonstrate sequence homology between TRP120 and Notch ligands and determined that the TRP120-TR shares significant identity with known Notch ligands. We determined direct interactions between TRP120 and NECD recombinant protein containing ligand interaction domain, EGFs 1-13. We further defined the TRP120-TR domain as being capable of Notch activation and have defined the TRP120 Notch SLiM mimetic motif required for Notch activation. Furthermore, we determined a direct correlation between Notch activation and inhibition of apoptosis linked to an increase in XIAP expression during *E. chaffeensis* infection. Increased XIAP levels correlated with increased NICD levels during *E. chaffeensis* infection and after TRP120 Notch ligand mimetic peptide treatment. Additionally, increased XIAP expression was consistent with increased pro-caspase levels. siRNA knockdown or inhibition of XIAP with small molecule inhibitor significantly increased apoptosis and Caspase-3, -7 and -9 levels and decreased ehrlichial load. This investigation reveals a mechanism whereby *E. chaffeensis* repurposes Notch signaling to stabilize XIAP and inhibit apoptosis. Understanding the molecular basis of *Ehrlichia*-Notch ligand mimicry is important for

understanding the survival strategies of intracellular pathogenesis. Defining such interactions may lead to the development of novel therapeutics that target host-pathogen protein-protein interactions.

The proposed study is highly significant in revealing a molecular mechanism whereby obligately intracellular pathogens, with small genomes and limited protein effectors, have evolved moonlighting proteins and molecular mimicry to rewire conserved signaling pathways and cellular functions to ensure persistent infection and survival. The identification of a short linear motif found within a non-canonical Notch ligand gives more insight into the underlying molecular mechanisms of aberrant Notch activation and may therefore lead to therapeutic approaches for diseases by which constitutively activated Notch signaling leads to disease onset and progression. Understanding Notch activation during *E. chaffeensis* infection will allow for the development of agents targeting critical steps of Notch signaling to inhibit infection and survival in the macrophage.

## TABLE OF CONTENTS

List of Tables .....	xi
List of Figures .....	xii
List of Abbreviations.....	xiv
Chapter 1. Introduction.....	18
Human monocytic ehrlichiosis (HME).....	18
<i>Ehrlichia chaffeensis</i> .....	19
Physical characteristics and intracellular development of <i>E. chaffeensis</i> .....	20
<i>E. chaffeensis</i> genome.....	21
Type I secretion system and effectors.....	21
Tandem repeat protein (TRPs).....	22
TRP120 is a moonlighting protein.....	23
TRP120 Nucleomodulin Activity .....	24
TRP120 Ligand Mimicry.....	25
Bacterial Pathogen SLiM Mimicry .....	26
TRP120 activation of Wnt signaling.....	27
TRP120 activation of Hedgehog signaling.....	28
TRP120 activation of Notch signaling.....	28
Notch activation by pathogens.....	29
The Notch signaling pathway.....	29
Canonical Notch signaling activation.....	30
Notch Regulation .....	32
Notch ligand-receptor structure and interaction.....	33
Non-canonical Notch-ligand interaction.....	38
Integral membrane-tethered non-canonical Notch ligands.....	38

GPI-linked non-canonical ligands.....	40
Secreted non-canonical Notch ligands.....	41
<i>E. chaffeensis</i> TRP120 interacts with Notch pathway proteins.....	42
Apoptosis as a survival mechanism for intracellular pathogens.....	42
Inhibitor of Apoptosis proteins (IAPs).....	43
Notch activation interferes with XIAP ubiquitination and degradation.....	44
Project introduction.....	45
Chapter 2. Material and Methods.....	48
Chapter 3. <i>Ehrlichia</i> SLiM ligand mimetic activates Notch signaling in human monocytes.....	58
Introduction.....	58
Results.....	60
<i>E. chaffeensis</i> TRP120 shares sequence homology and predicted Notch ligand function.....	60
<i>E. chaffeensis</i> TRP120 directly interacts with the Notch-1 ligand binding region (LBR).....	62
<i>E. chaffeensis</i> TRP120-TR Notch ligand IDD-mimetic activates Notch.....	66
<i>E. chaffeensis</i> TRP120-TR Notch Ligand SLiM mimetic activates Notch.....	68
TRP120 Notch SLiM antibody blocks <i>E. chaffeensis</i> Notch activation.....	71
Discussion.....	73
Chapter 4. <i>Ehrlichia</i> Notch signaling induction promotes XIAP stability and inhibits apoptosis.....	80
Introduction.....	80
Results.....	82
<i>Ehrlichia chaffeensis</i> infection and TRP120 increases XIAP levels...	82

NICD interacts with XIAP during infection.....	84
Notch activation and XIAP stabilization by NICD.....	85
Notch stabilization of XIAP results in antiapoptotic activity and increased infection.....	86
XIAP stabilizes pro-caspase levels to inhibit apoptosis.....	87
Pro-caspase levels during <i>E. chaffeensis</i> infection.....	89
<i>Ehrlichia chaffeensis</i> TRP120 mediated FBW7 ubiquitination and proteasomal degradation stabilizes XIAP.....	92
Discussion.....	93
Chapter 5. Summary, Conclusions and Future Directions.....	101
Appendices.....	105
Appendix A: Fig S1. TRP120 shares biological function with canonical and noncanonical Notch ligands.....	105
Appendix B: Fig S2. Purification of recombinant TRP120 Proteins.....	106
Appendix C: Fig S3. Jagged-1 activates Notch gene expression in a concentration -dependent manner.....	107
Appendix D: Table S1. TRP120 IDD and SLiM mimetic peptides activates Notch gene expression in a concentration dependent manner.....	108
Appendix E: Fig S4. Inhibition of XIAP enhances apoptosis in <i>E. chaffeensis</i> -infected cells.....	111
Appendix F: Fig S5. Pro-caspase transcript levels are increased during <i>E.</i> <i>chaffeensis</i> infection.....	112
Bibliography/References.....	113
Vita.....	127

## List of Tables

Table 1. Canonical and Non-canonical Notch Ligands.....	39
Table 2. TRP120 Synthetic Peptides .....	53

## List of Figures

Figure 1: <i>E. chaffeensis</i> infected cells.....	19
Figure 2: <i>E. chaffeensis</i> Life cycle.....	20
Figure 3: <i>E. chaffeensis</i> TRP120 Identified Short Liner Motifs (SLiMs).....	27
Figure 4: The Notch signaling pathway.....	32
Figure 5. <i>E. chaffeensis</i> TRP120 shares sequence homology and biological function with canonical and noncanonical Notch ligands. ....	62
Figure 6. <i>E. chaffeensis</i> TRP120-TR interactions with the Notch receptor ligand- binding region (LBR). ....	64
Figure 7. TRP120-TR activates Notch and NICD nuclear translocation in primary human monocytes.....	65
Figure 8. A TRP120-TR Notch-1 memetic IDD peptide stimulates NICD nuclear translocation.....	67
Figure 9. TRP120-N1-P3 IDD peptide stimulates Notch gene expression. ....	68
Figure 10. A TRP120-TR Notch-1 memetic SLiM peptide activates Notch signaling. .....	70
Figure 11. TRP120-N1-P6 SLiM Notch memetic peptide stimulates Notch gene expression.....	71
Figure 12. Amino acids critical to TRP120-N1-P6 memetic SLiM activity and anti- SLiM antibody blocks Notch activation. ....	72
Figure 13. Proposed model of <i>E. chaffeensis</i> TRP120 Notch activation. ....	79

Figure 14: XIAP is increased during <i>E. chaffeensis</i> infection. ....	83
Figure 15: NICD interaction of XIAP during <i>E. chaffeensis</i> infection. ....	84
Figure 16: Notch activation stabilizes XIAP during <i>E. chaffeensis</i> Infection. ....	86
Figure 17: XIAP enhances cell viability to promote <i>E. chaffeensis</i> infection. ....	87
Figure 18: XIAP stabilizes pro-caspase levels to inhibit apoptosis. ....	89
Figure 19: XIAP stabilizes pro-caspase levels -3, -7 and -9 to inhibit apoptosis during <i>E. chaffeensis</i> infection. ....	91
Figure 20: FBW7 degradation during <i>E.ch.</i> Infection enhances XIAP stability and caspase-3 and -9 activation. ....	92
Figure 21. Model of <i>E. chaffeensis</i> TRP120 Notch-mediated apoptosis inhibition. ....	100

## List of Abbreviations

ABC	ATP binding cassette
ADAM	A disintegrin and metalloproteinase
Anks	Ankyrin proteins
ASI	Alpha secretase inhibitor
BIR	Baculovirus IAP repeat
BCL2	B-cell lymphoma 2
BSA	Bovine serum albumin
CADASIL	Cerebral autosomal dominant arteriopathy with subcortical infarcts and leukoencephalopathy
CASP	Caspase
CRD	Cysteine-rich domain
DC	Dense-cored
DLL	Delta-like ligand
DNER	Delta/Notch-like EGF-related receptor
DOS	Delta and OSM-11-like proteins
DSB	Disulfide bond formation protein
DSV	<i>Desulfovibrio vulgaris</i>
Dx	Deltex
<i>E. chaffeensis</i>	<i>Ehrlichia chaffeensis</i>
<i>E.ch.</i>	<i>Ehrlichia chaffeensis</i>
<i>E. coli</i>	<i>Escherichia coli</i>
EGF	Epidermal growth factor-like repeats
EGFL7	Epidermal growth factor-like domain 7
EIIP	Electron-ion interaction potential
ERK1/2	Extracellular signal-regulated kinase 1/2

FBS	Fetal bovine serum
FBW7	F-box and WD repeat domain-containing 7
Fzd	Frizzled receptor
GPI	Glycosyl phosphatidylinositol
GSI	Gamma secretase inhibitor
H&E	Hematoxylin and eosin
HCK	Hematopoietic cell kinase
HD	Heterodimer
<i>Hes</i>	Hairy and enhancer of split 1
<i>Hey</i>	Hairy/enhancer-of-split related with YRPW motif 1
HME	Human monocytotropic ehrlichiosis
IAPs	Inhibitor of apoptosis proteins
IDD	Intrinsically disordered domain
IM-1	Intermediate form-1
IM-2	Intermediate form-2
IMM	Inner mitochondrial membrane
ISM	Informational spectrum method
Jag1	Jagged-1
LBD	Ligand binding domain
LBR	Ligand binding region
LNR	Lin12/Notch repeats
LPS	Lipopolysaccharide
MAPK	Mitogen-activated protein kinase
MAML	Mastermind-like
MFP	Membrane fusion protein

MNNL	Module at the N-terminus of Notch ligand
MnSOD	Manganese superoxide dismutase
MOI	Multiplicity of infection
MPT	Mitochondrial permeability transition
NIAID	National Institute of Allergy and Infectious Diseases
NECD	Notch extracellular domain
NICD	Notch intracellular domain
Ni-NTA	Nickel-nitrilotriacetic acid
NLS	Nuclear localization sequence
NRR	Negative regulatory region
OMP	Outer membrane protein
PBS	Phosphate-buffered saline
PCGF5	Polycomb group RING finger protein 5
PDZ	PSD-95/Dlg/ZO-1
PEST	Proline (P), Glutamic acid (E), Serine (S), and Threonine (T)
PMSF	Phenylmethylsulfonyl fluoride
PTCH2	Patched-2
PTM	Posttranslational modification
RBPjK	Recombination signal binding protein for immunoglobulin kappa J region
RC	Reticulate cell
RTX	Repeats in toxin
SCF	Skp1-cullin-1-FBOX
SLiM	Short linear motif
SUMO	Sumoylation
Su(dx)	Suppressor of Deltex

tBID	truncated p15 BID
TAD	Transcription activation domain
TBST	Tris-buffered saline containing Triton
TRPs	Tandem repeat proteins
TRX	Thioredoxin
TxDSHS	Texas Department of State Health Services
T1SS	Type I secretion system
T4SS	Type IV secretion system
TLR2/4	Toll-like receptor 2/4
TR	Tandem repeat
TSP2	Thrombospondin2
Ub	Ubiquitin
VWFC	von Willebrand factor type C domain
XIAP	X-linked inhibitor of apoptosis protein
YB-1	Y-box protein-1

## CHAPTER 1. INTRODUCTION

### Human Monocytic Ehrlichiosis (HME)

Human monocytic ehrlichiosis (HME) is an emerging tick-borne zoonotic disease caused by *Ehrlichia chaffeensis* (*E. chaffeensis*; *E.ch.*) [1]. The first case of HME was reported in the United States in 1986 and the disease became reportable to the Centers for Disease Control (CDC) in 1994 [2, 3]. Since the first reported case, HME has become the most prevalent life-threatening tick-borne disease in the United States. Over the last 20 years, reported cases has been steadily increasing with the largest number (>2000) reported in 2019; however, due to underreporting, passive surveillance, and underdiagnosis, the incidence of HME is likely underestimated by 100 to 200 cases per million[4-6].

HME is prevalent in both the southcentral and southeastern United States [6]. As of 2019, Missouri, Arkansas, North Carolina, and New York accounted for about half of all reported cases. Of these reported cases, ehrlichiosis is reported more frequently diagnosed in men than women, and in individuals between 60 to 69 years of age [7]. In addition, most cases are reported in the spring and summer (April-September), correlating with the seasonal increase in tick activity [7].

HME manifests as an undifferentiated febrile illness with symptoms that include fever, chills, headache, myalgia, nausea, vomiting, diarrhea, confusion, malaise, and rash, with rash being more common among children [3, 8, 9]. Laboratory manifestations of HME include thrombocytopenia, leukopenia, and elevated hepatic transaminases [10]. HME is a severe disease and can be lethal if not treated in a timely manner with the appropriate therapeutic. Life-threatening outcomes, such as kidney failure, acute respiratory distress and multiorgan failure may lead to death within two weeks of illness onset. [10]. The preferred treatment for HME is doxycycline [11, 12], which is most effective when administered shortly after the onset of

symptoms; however, it is not effective during later stages of the disease. Therefore, improved diagnostic and therapeutic approaches are needed for HME. By understanding the molecular and cellular pathobiology of *E. chaffeensis*, we may develop new countermeasures to prevent onset of severe illness or death.

### ***Ehrlichia chaffeensis***

*Ehrlichia chaffeensis* is a Gram-negative, aerobic, obligately intracellular bacterial pathogen and the etiological agent of the tick-borne zoonosis, human monocytic ehrlichiosis (HME) [8, 13]. *E. chaffeensis* is an  $\alpha$ -proteobacteria belonging to the family Anaplasmataceae in the order Rickettsiales [14]. *Ehrlichia chaffeensis* is transmitted by the lone star tick, *Amblyomma americanum* [13, 15] and is one of five *Ehrlichia* species that exhibits tropism for mononuclear phagocytes. *E. chaffeensis* resides and replicates in cytoplasmic membrane-bound vacuoles forming microcolonies known as morulae (inclusion bodies). Infected mononuclear phagocytes may contain multiple morulae with each containing from 1 to 400 bacteria (Fig. 1)

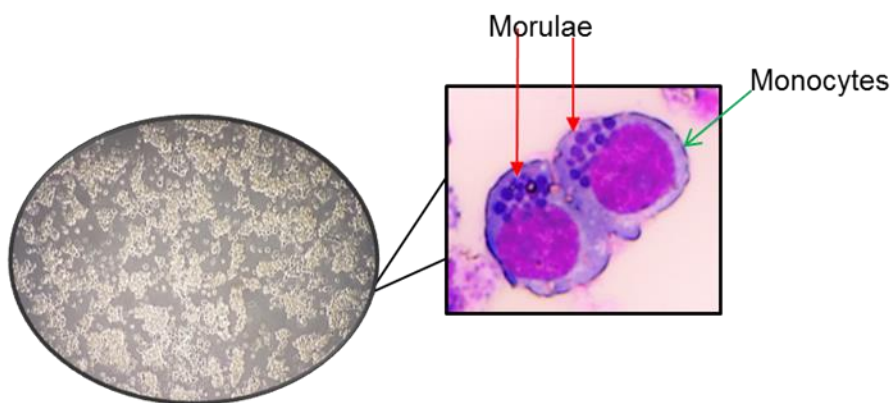


**Figure 1: *E. chaffeensis* infected cells.**

Light microscopy and H&E stained THP-1 cells (3 dpi) with cytoplasmic morulae containing *E. chaffeensis*. Image created by L. Patterson using Microsoft Powerpoint.

## Physical Characteristics and Intracellular Development of *E. chaffeensis*

The life cycle of *E. chaffeensis* involves both a tick vector and a mammalian host [16-19]. Transmission of *E. chaffeensis* between the tick vector and mammalian hosts occurs through the bite of infected ticks [18, 20]. *E. chaffeensis* infects and replicates within mononuclear phagocytes and within salivary glands and midgut cells of the tick [21]. There are two morphologically distinct forms of *E. chaffeensis* identified by electron microscopy [22]. The infectious or dense-cored (DC) cell form of *E. chaffeensis* is 0.4 to 0.6  $\mu\text{m}$  in diameter and exhibits a condensed nucleoid DNA. In comparison, the replicative form or reticulate cell (RC) is  $\sim 0.7$  to 1.9  $\mu\text{m}$  in diameter and has a uniformly dispersed nucleoid DNA associated with DNA replication [22]. Attachment to the host cell is associated with an *E. chaffeensis* adhesins EtpE and the tandem repeat protein 120 (TRP120) [23]. Host cell entry occurs within 1 h through receptor-mediated endocytosis [24]. After entry the DC transitions into an intermediate form (IM)-1 and then into the RC form which replicates by binary fission, doubling every 8 h for 48 h [24]. RCs subsequently transform into the second intermediate form IM-2, followed by maturation into the infectious DC form that is released by cell lysis by 72 h [24].

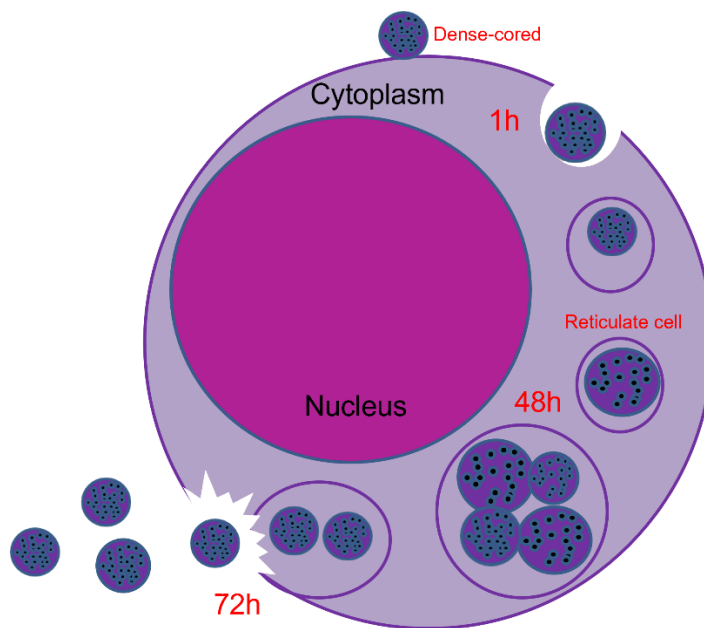


## Figure 2: *E. chaffeensis* Life cycle

The life cycle of *E. chaffeensis* begins with dense-cored (DC) ehrlichiae entering into the host cell through receptor-mediated phagocytosis, involving *E. chaffeensis* TRP120 and EtpE interacting with host receptors DnaseX (1h). Once inside the cell, DC ehrlichiae transition into reticulate cell (RC) form to replicate by binary fission and form microcolonies known as morulae (48h). Upon completion of replication, RC ehrlichiae mature back into the DC form and exit the cell via whole cell lysis. Image created by L. Patterson using Microsoft Powerpoint

## *E. chaffeensis* Genome

*E. chaffeensis* has a relatively small genome (~1.3 Mb) encoding ~850 proteins. The small genome of these host-adapted bacteria is attributed to a reductive evolutionary process resulting in a significant reduction in genes associated with various metabolic processes. Characteristics of the *Ehrlichia* genome include a low GC content (~30%), long intergenic regions which are important for size plasticity associated with the presence of long tandem repeats, and long non-coding regions. *Ehrlichia* genomes also have genes that are associated with tandem repeat proteins (TRPs), ankyrin proteins (Anks), type IV secretion system (T4SS) proteins, and outer membrane proteins (OMPs). Despite the small genome size of *E. chaffeensis*, it has evolved highly sophisticated mechanisms to subvert host immune defenses within mammalian and arthropod hosts. TRPs, OMPs, and various hypothetical proteins are differentially expressed in arthropod and mammalian hosts and may therefore be important for host adaptation. *E. chaffeensis* lacks genes for the biosynthesis of the lipopolysaccharide (LPS) and peptidoglycan; genes associated with the onset of innate immunity [25].

## Type I Secretion System and Effectors

*E. chaffeensis* has both type I and type IV secretion systems (T1SS and T4SS, respectively) [26, 27]. The T1SS is a multi-protein secretion system consisting of two inner membrane proteins: an ATP binding cassette (ABC) transporter and membrane fusion protein (MFP), as well as an outer membrane protein (OMP) of the TolC class [28, 29]. The ABC transporter is linked to the MFP spanning the initial part of the periplasm and forming a

continuous channel to the surface with the trimeric OMP [30]. The T1SS is independent of the Sec-system, functions to secrete proteins from the cytoplasm to the extracellular space in a single step and is essentially promiscuous in the proteins it secretes [31]. T1SS components contain a 50 amino acid, non-consensus signal sequence at the C-terminus [32]. These substrates tend to be acidic and contain tandem repeats. The repeats in toxin (RTX) proteins of *Escherichia coli* (*E. coli*) are well defined T1SS substrates [33]. Identified *E. chaffeensis* T1SS substrates include the 200 kDa ankyrin repeat protein (Ank200) and tandem repeat protein (TRP) effectors [34]. Various studies of *E. chaffeensis* effectors have focused on T4SS effectors and their roles in *E. chaffeensis* pathogenesis [35-37]. By comparison, until recently, less was known about T1SS effectors; however, they are now known to play important roles in reprogramming the host cell for intracellular survival.

### **Tandem Repeat Proteins (TRPs)**

It is well documented that pathogens use sophisticated molecular strategies to exploit host cell functions and alter host pathways to promote infection [38-40]. Pathogens have evolved various effector proteins to modulate the host through interactions with posttranslational modification, lipids and cellular membranes, cellular metabolism, vesicular trafficking, degradative pathways (autophagy), transcription, translation, innate and cellular immune response and signaling pathways [36, 41-49]. *E. chaffeensis* evades innate host defenses partly by secreting effector proteins into the host cell [50, 51]. Over 200 *E. chaffeensis* effector proteins have been predicted with tandem repeat proteins (TRPs) being the best studied *E. chaffeensis* effector proteins [34, 50]. TRPs are major immunoreactive proteins that elicit strong and robust host antibody responses [52]. Host antibody responses are directed at linear species-specific epitopes located in the tandem repeat region [53]. Four TRPs have been identified and characterized including TRP32, TRP47, TRP75 and TRP120 [53-55]. Consistent with other known T1SS substrates, TRP32, -47 and -120 are highly acidic (pI, 4.1 to 4.2), as

well as serine-rich [8, 55]. In contrast, TRP75 contains lysine-rich repeats and is slightly acidic (pI, ~5.5) [56, 57]. TRPs migrate at a higher molecular mass than predicted by their amino acid sequence due to their acidic pIs [58]. Although similar in nature, TRPs vary in their amino acid sequences and number of tandem repeats; however, each TRP contains a predicted carboxy-terminal T1S signal [51]. TRPs are differentially expressed on the surface of dense-cored (DCs) and reticulate cells (RCs). TRP32, TRP47, TRP75 and TRP120 are all expressed by DCs, while TRP32 and TRP75 are additionally expressed by RCs [57, 59]. Recently studies have demonstrated that TRPs interact with a diverse array of host proteins associated with various biological functions critical for cell fate determination and homeostasis [56, 60-62]. Interactions were identified by yeast-two hybrid analysis were investigated using siRNA [51, 56, 60, 61]. Interestingly, siRNA knockdown of 89% of TRP target host proteins significantly influenced infection, confirming the importance of TRP-host interactions for intracellular survival [51]. TRP-host interactions are mediated in some instances by post-translational modifications [63-65]. Specifically, TRP120 is sumoylated at a canonical consensus SUMO conjugation motif located in the C-terminus which is important for interactions with numerous host proteins [63]. Additionally, TRP120 is posttranslationally modified by ubiquitin (Ub) at a multiple conserved sites including the TR and C-terminal domains [65]. Both PTMs have been demonstrated to play key roles in effector-host protein interactions and are critical for ehrlichial intracellular survival.

### **TRP120 is a Moonlighting Protein**

TRP120 is an immunoprotective effector protein secreted by *E. chaffeensis* [59]. Interestingly, recent studies have revealed that TRP120 has multifunctional roles or “moonlighting” capabilities. The first reported function of TRP120 was as an adhesin responsible for host cell attachment and entry [59]. Within the past decade, other TRP120 functions have been reported which include functions as a nucleomodulin [66, 67], DNA binding protein [66, 67], a ubiquitin ligase [64, 65] and a conserved signaling pathway ligand mimic. Therefore,

TRP120 has been defined as a multifunctional effector protein that has essential cellular reprogramming functions for *E. chaffeensis* survival.

### **TRP120 Nucleomodulin Activity**

Effector proteins known as nucleomodulins localize to the host cell nucleus to repurpose nuclear processes and is a strategy utilized by many bacterial pathogens. Detection of *E. chaffeensis* TRP120 in the host cell nucleus has recently been demonstrated [62, 66, 67]. Nuclear localization of TRP120 occurs as early as 3 hpi and accumulates over the course of infection [67]. The tandem repeat domain of TRP120 is a DNA binding domain that targets conserved G-C rich motifs [68]. Approximately 2,000 host target genes containing at least one TRP120 binding site have been identified [68]. Interestingly, several target genes were associated with conserved signaling pathways, including *JAK2* and *NOTCH1* [68]. Moreover, TRP120 target genes were associated with various biological functions that are imperative for cellular homeostasis, including 21 target genes associated with apoptosis [68]. TRP120 DNA binding function is vital to the pathogenesis of *E. chaffeensis* by manipulating host cell gene transcription and altering numerous cellular processes for infection.

Another well-defined TRP120 function is as a HECT E3 ligase that ubiquitinates host proteins for degradation [64, 65, 69]. TRP120 has both intrinsic (autoubiquitination) and extrinsic ligase activity [65]. A conserved C-terminal HECT E3 ligase domain was identified and shown to be essential for ubiquitin ligase activity [65]. TRP120 is known to degrade two nuclear host proteins, polycomb group RING finger protein 5 (PCGF5) and F-box and WD repeat domain-containing 7 (FBW7)[64, 69]. FBW7 controls proteasome-mediated degradation of oncoproteins such as cyclin E, c-Myc, Mcl-1, mTOR, Jun and Notch [64]. Interestingly, degradation of FBW7 was demonstrated to occur by TRP120 ubiquitin ligase activity to stabilize Notch intracellular domain (NICD) expression for *E. chaffeensis* survival [64]. Collectively, these data demonstrate

the importance of TRP120 nucleomodulin activity for manipulation of host gene transcription and degradation of nuclear host proteins associated with various signaling pathways.

### **TRP120 Ligand Mimicry**

Hijacking host pathways for survival is essential for obligately intracellular pathogens. As such, these endosymbionts have evolved highly sophisticated strategies to repurpose host cell networks for survival. Modulation of host pathways may occur through molecular mimicry and protein interaction modules. There are three classifications of protein interaction modules; globular domains, intrinsically disordered domains (IDDs) and short linear motifs (SLiMs) [70, 71]. Globular domains are about 50-200 amino acids in size, have a stable tertiary structure in their native state and have affinities in the picomolar range [71]. In comparison both IDDs and SLiMs are found in intrinsically disordered regions [71, 72]. IDDs are about 20-50 amino acids in size, have disordered conformations in their native states and the affinity of their interactions tends to be in the nanomolar range [71]. Similarly, SLiMs have disordered conformations, are shorter in length, ranging between 3-12 amino acids with typical interactions within the micromolar range [38, 71-74]. SLiMs are normally found within intrinsically disordered domains. Importantly, both IDDs and SLiMs lack stable tertiary structure until bound to a binding partner [71].

Recently, SLiMs have been identified as a mechanism to hijack host pathways utilized by pathogens to escape innate immune defense [38-40]. Various pathogens have convergently evolved eukaryotic-like mimicry modules *de novo* to interact with host proteins [71]. Effector interactions with host proteins that have been described include proteins involved in processes such as transcription and translation, post-translational modification, protein trafficking, cell signaling, actin cytoskeleton organization and immune response [75].

## Bacterial Pathogen SLiM Mimicry

Eukaryotic-like SLiM mimicry is a host hijacking mechanism utilized by various pathogens, including bacterial pathogens [76]. With over 100,000 SLiMs predicted in the human proteome, obligately intracellular pathogens also utilize SLiMs to interface with host cell networks and interfere with important processes to the host cell, including metabolism, cell cycle, PTMs and signal transduction [38-40, 75, 77, 78]. Interestingly, bacterial pathogens have been shown to use intrinsically, disordered secreted protein effectors containing functionally diverse SLiMs to bind host proteins [79-81]. The ability of secreted protein effectors to bind to their target is related to SLiMs being located in intrinsically disordered regions [82]. Identified SLiMs in proteins secreted by bacteria range from 3-20 amino acids in size and may be repeated within the sequence [75]. By identifying SLiMs that are utilized in effector-host protein interactions, we may gain a better understanding of the molecular mechanisms responsible for bacterial escape of innate immunity and may identify potential therapeutic targets to combat infection.

Within the past decade, various SLiMs have been identified in *E. chaffeensis* TRP120 that are important for intracellular survival. The first identified SLiM was a TRP120 SUMO conjugation motif important for pathogen-host interactions [63]. Another identified SLiM motif found within TRP120 was a functional HECT E3 ligase conserved catalytic site in the C-terminal region of TRP120 [65]. The HECT E3 ligase conserved catalytic site is important for autoubiquitination and ubiquitination of host proteins to promote infection. Additionally, several TRP120 SLiMs that mimic host ligands of evolutionarily conserved signaling pathways have been identified [79-81, 83]. These SLiMs are found within the intrinsically disordered tandem repeat domain of TRP120 and activate Wnt, Notch and Hedgehog signaling pathways [79-81]. Importantly, activation of these conserved signaling pathways, through SLiM mimicry, has various outcomes on innate immune responses that promote survival.

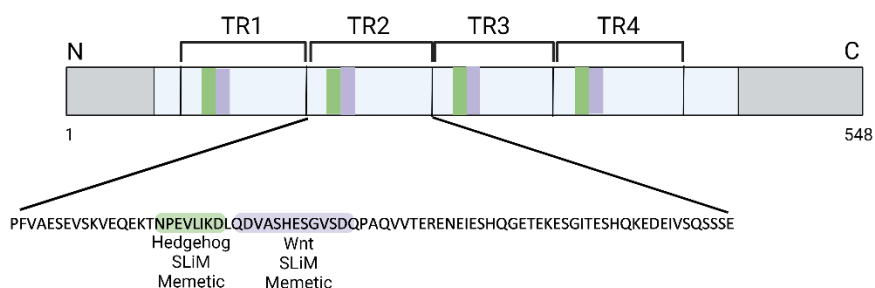


**Figure 3: *E. chaffeensis* TRP120 Identified Short Linear Motifs (SLiMs)**

Short linear motifs (SLiMs) that mimic ligands of evolutionarily conserved signaling pathways, Wnt and Hedgehog. SLiMs are found within the intrinsically disordered tandem repeat domain of TRP120. Image created by L. Patterson using BioRender.com.

### TRP120 Wnt Signaling Activation

TRP120 activates the evolutionarily conserved Wnt signaling pathway [79, 84, 85]. The Wnt signaling pathway governs a myriad of biological processes important for cell fate determination and embryonic development, amongst various other functions [86-88]. The initial discovery of TRP120-mediated Wnt activation determined that *E. chaffeensis* exploits both canonical and noncanonical Wnt signaling to stimulate phagocytosis for host cell entry [85]. Importantly, activation of Wnt signaling was linked to TRP120 interaction with Wnt pathway proteins [60]. Further studies determined TRP120-mediated Wnt activation occurs through direct interaction of TRP120 with cognate Wnt receptors [79]. There are 10 Fzd homologues in the mammalian genome, and TRP120 colocalizes with various Fzd receptors, including Fzd2, 4, 5, 7, and 9 [79, 89]. Therefore, these receptors were concluded to play a role in *E. chaffeensis* host cell entry. Direct interaction of TRP120 and Fzd5 was confirmed by co-immunoprecipitation and surface-plasmon resonance (SPR) [79]. Direct interaction of Fzd5 was determined to occur with the TRP120 repeat domain (TRP120-TR), particularly through a SLiM homologous to Wnt ligands [79]. Inhibition of the TRP120-Wnt SLiM using  $\alpha$ -TRP120-Wnt-SLiM against the SLiM

region reduced Wnt pathway activation, demonstrating the necessity of the TRP120 Wnt SLiM to activate Wnt/ $\beta$ -catenin signaling during *E. chaffeensis* infection.

### **TRP120 Hedgehog Signaling Activation**

TRP120 also activates the conserved Hedgehog signaling pathway [80]. Consistent with Wnt signaling, Hedgehog signaling plays essential roles in embryonic development and cellular homeostasis across metazoan species [90, 91]. Importantly, Hedgehog signaling has been specifically shown to be important for cell survival through regulation of apoptosis [92, 93]. Activation of Hedgehog signaling during *E. chaffeensis* infection occurs through direct interaction of TRP120-TR and Hedgehog receptor, Patched-2 (PTCH2) [80]. An eight amino acid SLiM (NPEVLIKD) sharing 87% sequence homology with Hedgehog ligand is the motif responsible for TRP120-PTCH2 interaction [80]. Importantly, this SLiM was found to be associated with the Hh-PTCH binding [80]. TRP120-mediated Hedgehog activation is important for inhibition of apoptosis through the anti-apoptotic protein B-cell lymphoma 2 (BCL-2) [80].

### **TRP120 Notch Signaling Activation**

TRP120 activates the evolutionarily conserved Notch signaling pathway during *E. chaffeensis* infection [94]. As previously mentioned, inhibition of Notch signaling by siRNA knockdown of Notch activating components dramatically reduces ehrlichial load, confirming the importance of Notch signaling for *E. chaffeensis* survival [51]. Studies determined that TRP120-mediated Notch activation inhibits extracellular signal-regulated kinase 1/2 (ERK1/2) and p38 mitogen-activated protein kinase (MAPK) pathways required for the expression of transcription factor PU.1 [94]. PU.1 downregulation subsequently leads to inhibition of Toll-like receptor 2/4 (TLR2/4) expression [94]. Although Notch signaling has been shown to downregulate TLR expression, other potential purposes for Notch activation may assist in intracellular survival of *E. chaffeensis*.

## Notch Activation by Pathogens

Previous studies have reported modulation of the Notch signaling pathway by pathogens [95-97]. *Desulfovibrio vulgaris* was shown to induce Notch-1 signaling in RAW 264.7 macrophages, mouse primary BMMs, HCT116 epithelial, and in the mouse small intestine [97]. *D. vulgaris* differentially positively regulated expression of Notch ligands and receptors [97] including DLL1, Jagged-1, and receptor Notch-1, but downregulated ligands DLL3, DLL4, Jagged-2 and Notch-4 receptor [97]. *D. vulgaris* also increased NICD expression in the proximal region of the small intestine [97]. Modulation of Notch signaling by *D. vulgaris* influences expression of proinflammatory cytokine pro-IL-1 $\beta$  and a cytokine signaling regulator SOCS3; however, the mechanism of how Notch is activated during infection remains unknown [97]. Similarly, *Mycobacterium bovis Bacille Calmette-Guérin* (*M. bovis BCG*) was shown to activate Notch signaling and cause upregulation of Notch-1 expression to increase SOCS3 expression within macrophages [98]. *M. bovis BCG* Notch activation involves the activation of PI3K and MAPK as downstream regulators of SOCS3 expression [98]. Notch activation occurs through direct TLR2-Notch-1 interaction, by which TLR2-MyD88 is stimulated by *M. bovis BCG* [98]. Although pathogens have been shown to modulate the Notch signaling pathway during infection, the molecular details as to how Notch is activated within these studies need further investigation.

## The Notch Signaling Pathway

The Notch signaling pathway is a highly evolutionarily conserved signaling pathway across metazoan species [99-101]. Notch signaling plays crucial roles in cell-fate determination during embryonic development, including differentiation, proliferation, apoptotic events, and stem cell maintenance during metazoan development [101-108]. Notch was first discovered through the Notch gene in *Drosophila melanogaster* as a sex-linked mutation displaying a

serrated wing margin phenotype [108]. Over the past 40 years, Notch biology has expanded from understanding its normal function in embryonic development to recent research which has linked Notch signaling with the regulation of innate and adaptive immune responses including inflammation, autophagy, apoptosis, and TLR expression, and T and B cell development [104, 105, 109-112]. The importance of Notch signaling can be inferred from perturbations in Notch signaling resulting in the genesis of various diseases, including cancer, Alagille syndrome, spondylocostal dysostosis and cerebral autosomal dominant arteriopathy with subcortical infarcts and leukoencephalopathy (CADASIL) [113-116]. Notch signaling has also recently become of emerging interest as a mechanism to evade innate immune responses by intracellular pathogens [94, 98, 117].

### **Canonical Notch Signaling Activation**

Canonical Notch activation is initiated by direct cell-to-cell interactions between a Notch sending cell and a Notch receiving cell. Notch sending cells contain canonical Notch ligands referred to as Delta-Serrate-Lag (DSL) ligands [118]. There are five canonical Notch ligands; Delta-like ligands; DLL1, DLL3, DLL4, and Serrate-like ligands; Jagged-1 and Jagged-2 [119]. Notch receiving cells contain single-pass type I transmembrane Notch receptors that transduce signals by binding directly to a Notch ligand on a receiving cell [99, 120]. Four Notch paralogs (Notch 1-4) have been identified that have both redundant and unique functions [121].

Canonical Notch activation involves receptor proteolysis which is essential for transducing a signal. Notch receptors are synthesized as ~300- to 350-kDa single-pass transmembrane proteins [122-126]. Following synthesis, the Notch receptor is cleaved in the Golgi apparatus. The Notch receptor is initially cleaved by a furin-like protease in the ectodomain (S1) of the full-length Notch receptor during maturation [127]. This cleavage step produces a heterodimer that traffics to the cell surface in a protease-resistant conformation. The second cleavage event occurs when canonical Notch ligands (i.e Delta-like ligands; DLL1,

DLL3, DLL4, and Serrate-like ligands; Jagged-1 and Jagged-2) bind the extracellular domain of the Notch receptor, resulting in cleavage by A disintegrin and metalloproteinase (ADAM) proteases in an extracellular juxtamembrane domain of the Notch receptor (S2) [125, 126] (Fig. 2). DSL ligands bind to the Notch receptor at epidermal growth factor-like (EGF) repeats 11-13, the identified ligand-binding domain (LBD) [119, 128]. Following Notch ligand-receptor binding, endocytosis of the ligand on the signal sending cell, and Notch extracellular domain (NECD) on the signal-receiving cell are thought to produce a mechanical force in the negative regulatory region (NRR) of the Notch receptor that exposes the S2 site for ADAM cleavage [129]. ADAM cleavage exposes S3 and S4 cleavage sites which are subsequently cleaved by  $\gamma$ -secretase to release the Notch Intracellular Domain (NICD) from the membrane [130]. NICD is the intracellular domain of the Notch receptor that functions as a biologically active signal transducer after complete cleavage of the NECD [100, 125, 127, 131]. NICD translocates to the nucleus and initiates the assembly of a transcription complex, including a DNA binding protein and a coactivator, recombination signal binding protein for immunoglobulin kappa J region (RBPjK) and mastermind-like (MAML), respectively [132]. Assembly of the transcription complex activates Notch downstream targets such as hairy and enhancer of split 1 (*hes*) and hairy/enhancer-of-split related with YRPW motif 1 (*hey*) (Fig. 4) [133, 134]. Notably, the activation of Notch through cell-cell interactions is referred to as trans-activation. Ligands can also interact with Notch receptors cell-autonomously, resulting in inhibition (cis-inhibition) [118].

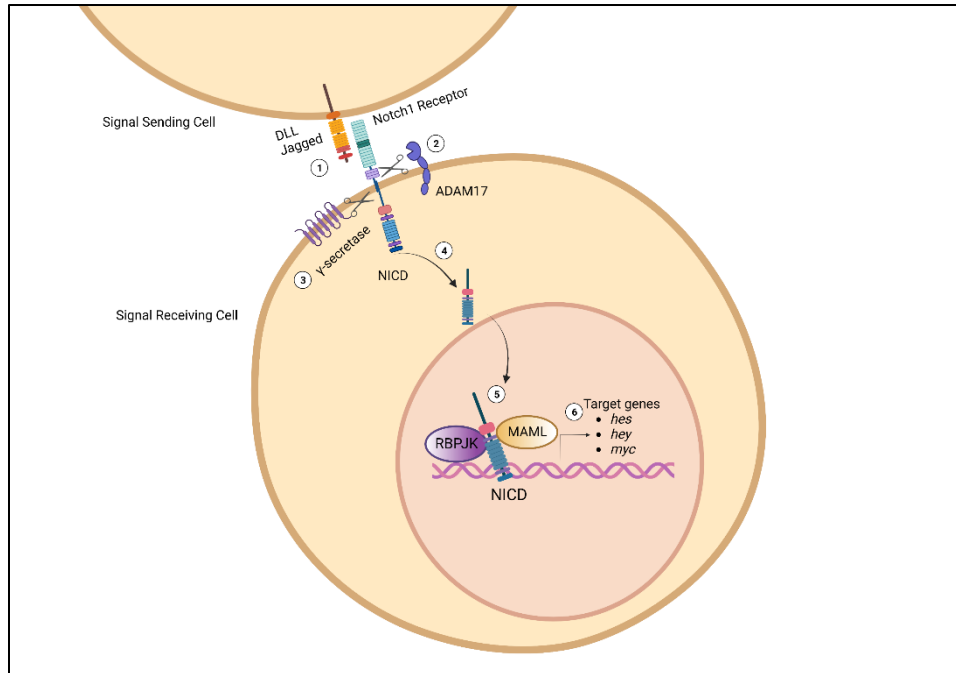


**Figure 4: The Notch signaling pathway.**

Canonical Notch activation occurs through direct cell-cell interactions. (1) Notch signaling is initiated when a mature Notch receptor located on a signal receiving cell binds to a canonical DSL ligand on a signal sending cell. (2) Notch receptor-ligand interaction results in exposure of the S2 site of the Notch receptor which is cleaved by an ADAM metalloprotease. (3) S2 site cleavage results in intracellular S3 cleavage by  $\gamma$ -secretase. (4)  $\gamma$ -secretase cleavage of the S3 site results in the full cleavage and translocation of the NICD to the nucleus, (5) where it binds to the CSL transcriptional complex containing a DNA binding protein, RBPJK and a co-activator, Mastermind-like. (6) Formation of the CSL transcriptional complex leads to transcription of the downstream Notch targets, such as *Hes1*, *Hey1* and *c-Myc*. Image created by L. Patterson using BioRender.com.

## Notch Regulation

Various fundamental mechanisms contribute to the regulation of Notch signaling that ensure tight spatial-temporal control of Notch activity. Critical mechanisms for regulation of Notch signaling include glycosylation of specific serine and threonine residues in the Notch receptor EGF-like repeats, endocytosis of both intracellular and extracellular Notch domains, and ubiquitination of Notch receptors and ligands [135-137]. Regulation of Notch signaling by E3 ubiquitin ligases has been proven to be important for tight regulation of Notch signaling. Identified E3 ligases that are implicated in Notch regulation include HECT E3 ligases Suppressor of Deltex Su(dx) in fruit flies/Itch in mammals and Nedd4, and RING family 3

ligases, Deltex (Dx), c-Cbl and Mdm2 [138-141]. Su(dx), c-Cbl, and Nedd4 are Notch antagonists, while Deltex and Mdm2 act as Notch agonists. Additionally, F-BOX and WD domain repeating-containing 7 (FBW7), the substrate recognition subunit of the eukaryotic Skp1-cullin-1-FBOX E3 ubiquitin (Ub) ligase complex (SCF) is a nuclear tumor suppressor and Notch negative regulator [142]. FBXW7 controls proteasome-mediated degradation of oncoproteins such as cyclin E, c-Myc, Mcl-1, mTOR, Jun, and Notch [143, 144]. Transcriptionally active Notch1 intracellular domain (NICD) is ubiquitylated by SCF-FBW7 by the attachment of K48 poly-ubiquitin chains to the PEST domain [145]. Therefore, the stabilization of both NICD and its principal downstream targets are dependent on FBW7 ubiquitin ligase activity.

### **Notch Ligand-Receptor Structure and Interaction**

Studies on the Notch signaling pathway have sought to unfold the molecular details responsible for Notch ligand-receptor interaction. Prior to integration into the plasma membrane, Notch is cleaved inside the trans-Golgi network by a furin-like protease. The cleavage event occurs 70 amino acids N-terminal of the transmembrane domain at the S1 site, resulting in the formation of a heterodimer that is held together by calcium-dependent ionic bonds [146, 147]. The Notch heterodimer is comprised of a Notch extracellular domain (NECD) which contains 29-36 tandem epidermal growth factor-like (EGF) repeats, and a Notch intracellular domain (NICD) [124]. The NECD mediates interactions with Notch ligands using EGFs 11-13, the defined ligand-binding domain (LBD) [124]. Interestingly, the LBD was found to be sufficient to bind to Notch ligands in a calcium-dependent manner but has not shown full functionality *in vivo*; therefore, additional sites may be involved in Notch activation and regulation [124]. Notch EGF domains are modified with O-linked glycans that influence receptor sensitivity to ligand stimulation [148]. The transmembrane domain is connected to the extracellular domain by the negative regulatory region (NRR) [126, 129]. The NRR consists of three cysteine-rich

Lin12/Notch repeats (LNR) and the fragment-spanning heterodimer (HD) domain [129]. The NRR is important for regulation of Notch activation, in that it prevents the S2 site from being cleaved by ADAM metalloproteases [126, 129]. Various studies have indicated the importance of the NRR in preventing Notch activation in the absence of ligand. Mutations causing destabilization of the NRR have been demonstrated to cause ligand-independent Notch signaling, which has most frequently been shown to be mutated in T cell acute lymphocytic leukemia [149, 150]. Pulling forces by Notch receptor-ligand interaction results in LNR destabilization and S2 site exposure for ADAM cleavage [126, 129]. ADAM metalloprotease cleavage results in exposure of the S3 site, located in the transmembrane domain of the Notch receptor. Full exposure of the S3 site results in proteolysis by  $\gamma$ -secretase [130]. S3 proteolysis causes full cleavage of NICD, which translocates to the nucleus to activate Notch downstream targets [130].

NICD also contains several domains important for its eventual function as a transcription factor. NICD is composed of a RAM domain, a nuclear localization sequence (NLS), seven ankyrin repeats (ANK), a transcription activation domain (TAD) and PEST domain [151]. RAM and ANK domains are important for interactions with CSL transcription factors, and the PEST domain is important for NICD degradation via proteolysis [151].

Canonical Notch ligands are type I transmembrane proteins that are structurally similar. All canonical Notch ligands contain an N-terminal domain, a variable amount of EGFs, and a DSL domain located at the N-terminus [152]. Studies have shown that the DSL domain of Notch ligands is required for Notch trans-activation or cis-inhibition, while the EGFs mediate Notch binding [153-155]. Additionally, a conserved motif, known as the Delta and OSM-11-like proteins (DOS), is found within the first EGF repeats and has been suggested to cooperate with the DSL domain for Notch binding and signaling [152, 155]. Canonical Notch ligands DLL3 and DLL4 lack a DOS motif and have been suggested to cooperate with DOS domain containing non-canonical ligands for Notch activation [156].

Although canonical DSL ligands are similar in structure, differences can be found in the number of EGF-like repeats. Jagged ligands have a cysteine-rich region sharing partial homology with a domain found in multi-protein/multi-functional proteins known as the von Willebrand factor type C domain (VWFC) that is absent from Delta ligands [152, 157]. The most diversity in DSL ligand structure is within the intracellular domain which contains various lysine residues in their intracellular domains. Lysine residues have been identified as potential sites for ubiquitination which is critical for canonical DSL ligand Notch activation [158]. DLL3 is the only DSL ligand absent of multiple lysine residues. Additionally, most DSL ligands have a C-terminal PSD-95/Dlg/ZO-1(PDZ)-ligand motif that plays a Notch independent role by promoting actin cytoskeleton interaction, however functional relevance of this domain is still under investigation [159]. The major difference between Serrate/Jagged ligands from the Delta ligands is a juxtamembrane cysteine-rich domain (CRD) found in the extracellular domain of Serrate/Jagged ligands [159, 160] .

Importantly, other major distinctions have been identified between canonical Notch ligand DLL3. DLL3 is the most structurally dissimilar Notch ligand in that it contains a degenerate DSL domain and lacks a DOS motif [120, 161]. DLL3 does not bind to the Notch receptor itself but instead inhibits Notch signaling cell-autonomously [162]. The majority of DLL3 is expressed in the Golgi apparatus and appears on the cell surface when overexpressed [162]. DLL3 is the only canonical Notch ligand shown to act solely as a Notch antagonist [163].

Various structural studies have attempted to identify critical residues within Notch ligands that are important for Notch-ligand binding. The most studied interactions have been both Jagged-1 and DLL4 binding to the Notch receptor. Chillakuri et. al. identified a group of highly conserved residues found within the DSL domain of Jagged-1 (human Jagged1 F<sup>199</sup>, R<sup>201</sup>, R<sup>203</sup>, F<sup>207</sup>) [153]. Sequence alignment identified these residues to be highly conserved in the DSL domains across both families of Notch ligands [153]. They also reported that site-directed mutagenesis studies confirmed the importance of these residues for Notch-ligand interactions;

however, various structural data has suggested that other residues that are important for receptor-ligand interactions. Although the DSL domain plays the most prominent role in binding, Jagged-1 EGF1 and EGF2 also participate in interface formation [153]. These findings are consistent with reports from Shimizu et al., where deletion mutagenesis demonstrated that the DSL domain was indispensable for Notch binding; however, EGF1 and EGF2 were also necessary for native-like affinity for the Notch receptor [164].

A Notch binding site on the DSL domain from human Jagged-1 is a part of an interface that is responsible for regulating both cis- and trans-interactions. A highly conserved series of residues within the DSL domains of both Jagged/Serrate and DLLs were identified through sequence alignment. Mutation analysis studies revealed that there is a highly conserved phenylalanine residue (F207/257) which abrogates both trans-activation and cis-inhibition when mutated [153]. Crystallography studies revealed the phenylalanine residue packs against a hydrophobic interface between Notch-1 11-12 and Notch-1 12–13, acting as a pivot [153]. Additionally, alanine mutagenesis revealed other residues that have been shown to be essential for ligand dependent activation, including residues F207, F199, R203 of DLL ligands and F257, F249, R253 found within Serrate ligands [124]. These residues are extensively buried, in comparison to R201 and D205 (R251 and D255 in Serrate), which have minor contacts with Notch-1 11-13 [153]. In addition, contacts between Jagged-1 DSL and Notch-1 EGF 11 are made through an H-bond and salt bridge between Glu424 of Notch-1 and Tyr210 and Arg203 of Jagged-1, and a hydrophobic polyethylene (glycol) formed by insertion of Jagged-1 residues Phe206 and 207 into a pocket in Jagged-1 [165]. Notch-1 EGFs 9 and 10 have also been shown to anchor Jagged-1 EGFs 1 and 2 through residues Tyr255, His268, Pro269, Trp280 and Leu292 [165]. Tyr255 was shown to be specific to Jagged-1 and thus thought to facilitate biased engagement of the Jagged-1 surface [165].

A mutant Jagged-1 variant was found to bind to Notch-1 EGFs 8-12 with an affinity of 0.81  $\mu$ M and to EGFs 11-12 with an affinity of 5.4  $\mu$ M [165]. The difference in affinity was

determined to indicate that EGFs 8-10 are important for binding, in addition to the DSL domain. In comparison, DLL4 was shown to bind to Notch-1 EGFs 8-12 with an affinity of 9.7  $\mu\text{M}$  and to EGFs 11-12 with an affinity of 12.8  $\mu\text{M}$  [165]. Therefore, EGFs 8-10 has a minimal role in Notch1-DLL4 engagement. Importantly, Notch-1 8-10 were shown to be required for maximal DLL4-mediated Notch-1 activation. Therefore, Jagged and DLL ligands were determined to show different binding affinities for different Notch-1 domains [155, 165, 166]. Despite kinetic differences, both Jagged and DLL ligands contain a conserved hydrophobic patch on their surface, which is predicted to be a common interaction site [167].

Other discontinuous DLL residues have been shown to be important for receptor-ligand interactions. For example, Tyr179, Arg191, and Phe195 are conserved DLL ligands, in which Arg191 and Phe195 are important for interaction based on site-directed deletion in the equivalent positions in Jagged1 in the *D. melanogaster* ligand Serrate [167]. These interactions occur at the EGF 11-DSL interface. Furthermore, this study revealed that EGF12-MNNL interface is more variable and facilitates ligand pleiotropy [166]. Collectively, the data demonstrated that Notch-1 EGF-like repeats 11 and 12 interact with DLL4 DSL domain and the MNNL domains, respectively.

Despite various crystallography and cellular-based studies that have attempted to find a consensus sequence important for Notch ligand binding, there has been no conclusive data as to the residues required for all canonical Notch ligands. Additionally, various non-canonical Notch ligands have also been shown to activate Notch signaling. These non-canonical Notch ligands share very little sequence similarity to canonical Notch ligands, therefore further investigation is needed in elucidating how various ligands are able to activate the Notch signaling pathway [152].

## **Non-Canonical Notch Ligand Interaction**

It is well documented that secreted and membrane-bound proteins activate Notch signaling. The interactions between non-canonical Notch ligands and Notch receptors are not well-defined. Non-canonical Notch ligands are a group of structurally diverse proteins that activate Notch signaling [152]. The structure of non-canonical Notch ligands are unrelated to canonical Notch ligands in that they lack the DSL domain required for Notch interaction [152]. A non-canonical consensus Notch binding site has not been identified; however, some non-canonical ligands activate Notch through  $\gamma$ -secretase activity and CSL-dependent transcription [168, 169]. Non-canonical Notch ligands include integral- and GPI-linked membrane proteins as well as secreted proteins (Table 1).

## **Integral Membrane Tethered Non-Canonical Notch Ligands**

Two documented integral membrane-tethered non-canonical Notch ligands are Dlk-1 and DNER. Mammalian Dlk-1 was shown to share sequence homology, containing 6 EGF-repeats that are almost identical to canonical Notch ligands; however, Dlk-1 lacks the essential DSL domain required for canonical Notch-ligand interaction [170]. Interestingly, yeast-two hybrid analysis has demonstrated that despite the lack of the DSL domain, Dlk-1 can bind to the Notch receptor. Studies revealed that Dlk-1 binds to the Notch receptor and acts as an antagonist to Notch signaling, possibly by competing with DSL-containing ligands for Notch binding [170, 171]. Membrane-tethered Dlk-1 was first shown to contain autonomous cis-inhibitory activity that affects Notch targets in the wing imaginal disk of *Drosophila* [170]. In addition, a recent study identified a critical role of Dlk1 in temporally downregulating Notch signaling and promoting AT2-to-AT1 transition and alveolar epithelial repair during *Pseudomonas aeruginosa* lung injury [172]. Interestingly, Dlk-1 and Dlk-2 were shown to activate Notch signaling through an identified DOS domain, allowing these non-canonical ligands to act as co-activators [173].

Therefore, the DOS-domain may be conserved across metazoan species. Two documented integral membrane-tethered non-canonical Notch ligands are Dlk-1 and DNER. Mammalian Dlk-1 was shown to share sequence homology, containing 6 EGF-repeats that are almost identical to canonical Notch ligands; however, Dlk-1 lacks the essential DSL domain required for canonical Notch-ligand interaction [170].

Ligand	Canonical/Non-Canonical?	Classification	Notch binding Region of Ligand	Outcome
DLL1	Canonical	Integral Membrane-bound	DSL domain	Trans-activation
DLL3	Canonical	Integral Membrane-bound	DSL domain	Cis-inhibition
DLL4	Canonical	Integral Membrane-bound	DSL domain	Trans-activation
Jagged-1	Canonical	Integral Membrane-bound	DSL domain	Trans-activation
Jagged-2	Canonical	Integral Membrane-bound	DSL domain	Trans-activation
Dlk-1/Pref-1	Non-canonical	Integral Membrane-bound	EGF 1-2 or EGF 5-6	Cis-inhibition/Trans-activation?
DNER	Non-canonical	Integral Membrane-bound	EGF 1-2	Trans-activation
Jedi	Non-canonical	Integral Membrane-bound	Not-tested	inhibition
F3/Contactin-1	Non-canonical	GPI-linked Membrane-bound	Full-length	Trans-activation
NB3/Contactin6	Non-canonical	GPI-linked Membrane-bound	Full-length	Trans-activation
scabrous	Non-canonical	Secreted	Full-length	Trans-activation
wingless	Non-canonical	Secreted	Full-length	Trans-activation
OSM-11	Non-canonical	Secreted	Full-length	Trans-activation
CCN3/NOV	Non-canonical	Secreted	C-terminal cysteine knot	Cis-activation
MAGP-2	Non-canonical	Secreted	Matrix binding domain	Cis-activation
MAGP-1	Non-canonical	Secreted	Full-length	Cis-activation
TSP2	Non-canonical	Secreted	Full-length	Cis agonist
YB-1	Non-canonical	Secreted	Full-length	Cis-activation
EGFL7	Non-canonical	Secreted	Emilin domain and EGF 1-2	Cis and trans antagonist/ Cis agonist

**Table 1. Canonical and Non-canonical Notch Ligands**

Interestingly, yeast-two hybrid analysis has demonstrated that despite the lack of the DSL domain, Dlk-1 can bind to the Notch receptor. Studies revealed that Dlk-1 binds to the Notch receptor and acts as an antagonist for Notch signaling, possibly by competing with DSL-containing ligands for Notch binding [170, 171]. Membrane-tethered Dlk-1 was first shown to contain autonomous cis-inhibitory activity that affects Notch targets in the wing imaginal disk of *Drosophila* [170]. In addition, a recent study identified the critical role of Dlk1 in temporally downregulating Notch signaling and promoting AT2-to-AT1 transition and alveolar epithelial repair during *P. aeruginosa* lung injury [172]. Interestingly, Dlk-1 and Dlk-2 activate Notch signaling through an identified DOS domain, allowing these non-canonical ligands to act as co-activators [173]. Therefore, the DOS-domain may be conserved across metazoan species.

DNER was initially recognized as a neuron-specific Notch ligand during Bergmann glial development by inducing process extension through  $\gamma$ -secretase- and Deltex-dependent Notch signaling activation [169]. DNER contains extracellular EGF repeats, but also lacks the DSL domain [169]. DNER was demonstrated to bind to the Notch receptor by the extracellular domain, specifically at the first and second EGF-like repeats to bind Notch-1 [169]. Although these studies identified DNER as a non-canonical Notch ligand that binds to Notch-1, a conflicting study demonstrated that DNER does not induce Notch activation in a luciferase assay in contrast to DLL1 and was unable to prevent the differentiation of cultured myoblasts like DLL1 [174]. This study strongly suggested that DNER is not a non-canonical Notch ligand, despite the strong sequence homology with such ligands.

### **GPI-Linked Non-Canonical Ligands**

F3/contactin1 is glycosyl phosphatidylinositol (GPI)-anchored neural cell adhesion molecule that has been shown to activate Notch signaling in trans to induce oligodendrocyte (OL) differentiation [168]. *In silico* studies have revealed F3/contactin1 to share similar biological

function with TRP120 (Appendix A, p. 117). F3/contactin1 can form complexes with Notch-1 and Notch-2; however, the domain of F3/contactin-1 that is interacting with Notch has not been elucidated [120]. Importantly, the Notch ligand binding regions responsible for F3/contactin1 interaction are EGFs 1-13 and distal EGFs 22-34. The role of binding to EGFs 22-34 has not been determined [168]. F3/contactin1 can form complexes with Notch-1 and Notch-2; however, the F3/contactin-1 interacting domain has not been elucidated [120]. Importantly, the Notch ligand binding regions responsible for F3/contactin1 interaction are EGFs 1-13 and distal EGFs 22-34. The role of binding to EGFs 22-34 has not been determined [168]; however, this study revealed that F3/contactin-1 initiates the Notch signaling pathway via Deltex1 (DTX1) that promotes oligodendrocyte maturation and myelination [168].

### **Secreted Non-Canonical Notch Ligands**

Various secreted non-canonical Notch ligands have been identified. Notably, thrombospondin2 (TSP2), Y-box protein-1 (YB-1) and epidermal growth factor-like domain 7 (EGFL7) all share significant sequence homology with TRP120 (data not published). TSP2 potentiates notch3/jagged1 signaling by directly binding to Notch-3 and Jagged1 [175]. Notch activation was shown to be  $\gamma$ -secretase dependent and require the extracellular domain of the Notch receptor [175]. Interaction between TSP2 and the Notch-3 receptor occurs between the first 11 EGF-like repeats of Notch-3 [175]. Interestingly, TSP2 shares a significant amount of sequence homology with *E. chaffeensis* TRP120 (data not published).

YB-1 and EGFL7 also share a significant sequence homology with TRP120. YB-1 belongs to the DNA- and RNA-binding proteins with an evolutionarily ancient and conserved cold shock domain [176]. YB-1 interacts with EGF repeats 13-33 of Notch-3 and activates in a  $\gamma$ -secretase dependent manner [177]. YB-1/Notch-3 interaction are thought to promote dissociation of the Notch-3 heterodimer [177]. In comparison, EGFL7 interacts EGF-like repeats inclusive of the DSL binding sites of Notch receptors and antagonizes Notch signaling [178].

Moreover, EGFL7 competes with Jagged-1 for Notch binding [120, 178]. YB-1 and EGFL7 also share a significant amount of sequence homology with TRP120, and YB-1 belongs to the DNA- and RNA-binding proteins with an evolutionarily ancient and conserved cold shock domain [176].

### ***E. chaffeensis* TRP120 Interactions with Notch Pathway Proteins**

Over a decade ago (2011), yeast-two hybrid analysis demonstrated that TRP120 directly binds to 98 host proteins associated with various biological functions, two of which were Notch regulatory proteins [60]. Both ADAM17, a Notch activating, and FBW7, a Notch negative regulator were identified as TRP120 interacting partners [60]. Furthermore, siRNA knockdown of Notch activating components significantly reduced *E. chaffeensis* infection, demonstrating the importance of these host-protein interactions for intracellular survival [51]. Therefore, studying these effector-host protein interactions became of significant interest for understanding the sophisticated strategies utilized by *E. chaffeensis* for intracellular survival.

### **Apoptosis: A Survival Mechanism for Intracellular Pathogens**

Apoptosis is an anti-microbial defense mechanism and various pathogens have developed strategies to inhibit apoptosis as a survival strategy. Intracellular pathogens have especially found apoptosis inhibition a useful strategy to utilize the host as a niche for intracellular survival [179-181].

Apoptosis is triggered by multi-signal pathways with proteins specific for each pathway. The extrinsic pathway initiates outside of the cell whereby a death ligand receptor is bound by specific ligands resulting in activation of Caspase-8 and induction of the execution pathway leading to apoptosis [182-184]. The intrinsic pathway is initiated by various non-receptor mediated stimuli, including oncogenes, direct DNA damage, and hypoxia that result in mitochondrial permeability transition (MPT) [185]. MPT alters the permeability of the inner

mitochondrial membrane (IMM) resulting in cytochrome c release. The release of cytochrome c triggers formation of a complex known as an apoptosome and subsequent Caspase-9 activation resulting in apoptosis [186]. Caspases or cysteine-aspartic proteases are proteolytic enzymes important for the execution of apoptosis [187]. Active Caspase-8 and/or -9 cleave inactivated executioner pro-Caspase-3/7 into their active forms, leading to the degradation of cellular components important for cell survival [184, 187, 188]. Modulation of several proteins that control and regulate apoptotic mitochondrial events (intrinsic apoptosis) occur during *E. chaffeensis* infection including Bcl-2 and BirC3, and have further demonstrated downregulation of apoptotic inducers, such as Bik, BNIP3L, and hematopoietic cell kinase (HCK) [180, 189]. *E. chaffeensis* is also known to suppress apoptosis by secreting the T4SS effector, ECH0825, which localizes to the mitochondria and inhibits Bax-induced apoptosis by increasing mitochondrial manganese superoxide dismutase (MnSOD) to decrease reactive oxygen species-mediated damage [190].

### **Inhibitor of Apoptosis Proteins (IAPs)**

Caspases are zymogens that are primarily responsible for apoptosis, therefore inhibition of apoptosis requires inhibiting caspase activation. One of the key regulators of apoptosis are inhibitor of apoptosis proteins (IAPs). IAPs are a family of antiapoptotic proteins that inhibit caspase activation [191] by binding Caspases-3, -7 and/or 9, but not Caspase-8 [192]. Mammalian IAPs include XIAP, cIAP1, and cIAP2 and they are structurally defined by the presence of the baculovirus IAP repeat (BIR) domain(s) [193]. The BIR domains are responsible for mediating protein–protein interactions [193-196].

Various studies have demonstrated XIAP as the most potent endogenous inhibitor of caspases due to weaker binding and inhibition of caspases by other IAP proteins [196-201]. XIAP is an E3 RING ubiquitin ligase with 3 BIR domains (BIR1-3), a RING domain and an evolutionarily conserved ubiquitin-associated (UBA) domain [202]. XIAP inhibits apoptosis

through directly binding to Caspases-3, -7 and -9 through different BIR domains [194, 196, 197]. The linker region located between BIR1 and 2 has been shown to directly bind to Caspases-3 and -7 and inhibit their caspase activity [197]. In comparison, The BIR3 domain of XIAP directly binds to Caspase-9 to inhibit its activation [203]. Interestingly, XIAP may be cleaved by upstream caspases not inhibited or by Caspase-3 and -7 when their molar concentration exceeds that of XIAP [196]. The resulting XIAP fragments are BIR1-2 and BIR3-RING fragments. The BIR1-2 fragment may inhibit Caspase-3 and -7; however, it is less potent than full-length XIAP and may be more susceptible to degradation [196]. In contrast, the BIR3-RING fragment may inhibit Caspase-9 activity, and is more stable [196]. Multiple studies have concluded that XIAP is the most potent endogenous inhibitor of caspases due to weaker binding and inhibition by other IAP proteins [196-201]. XIAP is an E3 RING ubiquitin ligase with 3 BIR domains (BIR1-3), a RING domain and an evolutionarily conserved ubiquitin-associated (UBA) domain [202]. XIAP inhibits apoptosis by directly binding Caspases-3, -7 and -9 through interactions with different BIR domains [194, 196, 197]. The linker region located between BIR1 and 2 is known to bind Caspases-3 and -7 and inhibit their activity [197]. In comparison, The BIR3 domain of XIAP directly binds to Caspase-9 to inhibit activation [203]. Interestingly, XIAP may be cleaved by upstream caspases not inhibited or by Caspase-3 and Caspase-7 when their molar concentration exceeds that of XIAP [196]. The resulting XIAP fragments are BIR1-2 and BIR3-RING fragments. The BIR1-2 fragment may inhibit Caspase-3 and Caspase-7; however, it is less potent than full-length XIAP and may be more susceptible to degradation [196]. In contrast, the BIR3-RING fragment may inhibit Caspase-9 activity and is more stable [196].

### **Notch Activation Interferes with XIAP Ubiquitination and Degradation**

A recent study confirmed that Notch signaling inhibits apoptosis by directly interfering with XIAP ubiquitination and degradation [204]. NICD was shown to bind directly to the RING domain of XIAP and interfere with E2 conjugation and ubiquitination [204]. Interference of

ubiquitination of XIAP inhibited autoubiquitination leading to increased XIAP expression [204]. Whether or not *E. chaffeensis* may activate Notch to inhibit apoptosis through XIAP has never been studied.

Importantly, NICD levels increase during *E. chaffeensis* infection though TRP120 HECT E3 ligase activity [64]. TRP120 ubiquitinates the Notch negative regulator, FBW7, during infection to maintain and increase NICD levels [64]. Whether increases in NICD levels through TRP120 FBW7 degradation leads to increased XIAP levels during *E. chaffeensis* infection needs to be investigated.

## **Project Introduction**

Human monocytotropic ehrlichiosis (HME) is an emerging tick-borne zoonotic disease caused by *E. chaffeensis* [8]. In the year 2000, only 200 cases of ehrlichiosis were reported; however, by 2019 the number of reported cases increased to over 2000. Notably, the number of reported cases is underestimated by 100-fold due to underreporting and underdiagnosing [205, 206]. HME is a severe disease and can be lethal if not treated in a timely manner with the appropriate therapeutic. Life-threatening outcomes, such as kidney failure, acute respiratory distress, neurological manifestations and multiorgan failure may lead to death within two weeks of illness [207, 208]. Currently, doxycycline is the only antibiotic treatment available for HME [209]. Understanding the pathobiology of ehrlichiosis will provide clear rationale for the developing novel therapeutic targets.

Our laboratory has identified several *E. chaffeensis* type 1 secretion system (T1SS), tandem repeat protein effectors (TRPs), several which have been determined to be involved in a diverse array of host-pathogen protein-protein interactions [51, 52, 56, 61, 69]. We have specifically investigated TRP interactions with host proteins involved in cytoskeleton rearrangement, cell signaling, transcriptional and translational regulation, post-translational modification, and apoptosis [52, 56, 60, 61]. The interactions of TRPs with host proteins are

important for ehrlichial survival [51]. Several studies from our laboratory have demonstrated that TRPs activate highly conserved host signaling pathways to promote *E. chaffeensis* survival [56, 65, 94].

TRP120 is a moonlighting effector which activates Wnt, Notch and Sonic Hedgehog signaling pathways during infection [80, 85, 94]. Two host proteins identified to interact with TRP120 are the Notch metalloprotease, ADAM17, and a Notch antagonist, FBW7 [60]. Notch activation plays significant roles in various other functions, including cellular homeostasis, MHC Class II expansion, B- and T- cell development, and innate immune mechanisms such as autophagy and apoptosis [104-106, 210, 211]. Notch activation has been shown to downregulate PRR expression during *E. chaffeensis* infection; however, downregulation of PRRs may not play a significant role in *E. chaffeensis* infection [105]. Therefore, uncovering the molecular mechanisms utilized by *E. chaffeensis* to subvert innate host defense for infection and survival is critical and will provide a model to study host-pathogen interactions and their roles in repurposing host pathways to modulate innate immune response.

*Ehrlichia chaffeensis* inhibition of apoptosis for intracellular survival has been recently reported [80, 212]. Interestingly, activation of Notch assists in inhibition of apoptosis by stabilizing expression of an anti-apoptotic protein, X-linked inhibitor of apoptosis (XIAP) [204]. Further, colocalization of TRP120 with both the Notch-1 receptor and ADAM17 has been shown [60]. The premise based on these data, support my central hypothesis which is *E. chaffeensis* TRP120 contains a SLiM ligand mimetic that activates Notch signaling to upregulate NICD and inhibit mitochondrial apoptotic signaling and caspase activation. This proposal will investigate TRP120-Notch-1 interaction, and the role of Notch activation in inhibition of host cell apoptosis to promote ehrlichial infection and intracellular survival.

The overall objective of this research project is to identify the SLiM ligand mimetic in *E. chaffeensis* TRP120 and determine the functional implications of TRP120 Notch activation on infection. Two aims were proposed to investigate this hypothesis. **Aim 1** was to investigate the

molecular basis of TRP120 Notch activation. **Aim 2** was to investigate the role of *E. chaffeensis* Notch stabilization of XIAP to inhibit apoptosis. Based on the data collected during my research, I have concluded that a TRP120-TR Notch SLiM mimetic motif directly binds Notch-1 at a region containing the LBD to activate Notch signaling. TRP120 Notch activation results in an anti-apoptotic program involving inhibitor of apoptosis proteins (IAPs) that inhibits caspase activation for intracellular survival.

The proposed study is highly significant by revealing a molecular mechanism whereby obligately intracellular pathogens, with small genomes and limited protein effectors, have evolved moonlighting proteins and molecular mimicry to rewire conserved signaling pathways and cellular functions to ensure persistent infection and survival. Understanding Notch activation during *E. chaffeensis* infection will allow for the development of agents targeting critical steps of Notch signaling to inhibit infection and survival in the macrophage.

## CHAPTER 2. MATERIALS AND METHODS

**Cell culture and *E. chaffeensis* infection.** Human monocytic leukemia cells (THP-1; 415 ATCC TIB-202) were propagated in RPMI media (ATCC) containing 2 mM L-glutamine, 10 mM HEPES, 1 mM sodium pyruvate, 4500 mg/L glucose, 1500 mg/L sodium bicarbonate, supplemented with 10% fetal bovine serum (FBS; Invitrogen) at 37°C in 5% CO<sup>2</sup> atmosphere. *E. chaffeensis* (Arkansas strain) was cultivated in THP-1 cells. Host cell-free *E. chaffeensis* was prepared by rupturing infected THP-1 cells or primary human monocytes with sterile glass beads (1 mm) by vortexing. Infected THP-1 cells were harvested and pelleted by centrifugation at 500 × g for 5 min. The pellet was resuspended in sterile phosphate-buffered saline (PBS) in a 50-ml tube containing glass beads and vortexed at moderate speed for 1 min. The cell debris was pelleted at 1,500 × g for 10 min, and the supernatant was further pelleted by high-speed centrifugation at 12,000 × g for 10 min, 4°C. The purified ehrlichiae were resuspended in fresh RPMI media and utilized as needed.

**Human PBMC and primary monocyte isolation.** Primary human monocytes were isolated from 125ml of human blood obtained from Gulf Coast Regional Blood Center (Houston, TX). Blood was diluted in RPMI media and separated by density gradient separation on Ficoll at 2000rpm for 20 minutes. The plasma was removed from the separated sample and the buffy coat was collected. Buffy coat was diluted with DPBS containing 2% FBS and 1mM EDTA and centrifuged at 1500rpm for 15 minutes. Supernatant was removed and all cells were combined and mixed carefully. Combined cells were then centrifuged at 1500rpm for 10 minutes and supernatant was removed. Cells were resuspended into 1mL of DPBS containing 2% FBS and 1mM EDTA. Cells were then diluted to 5 × 10<sup>7</sup>/mL concentration, and monocytes were separated by the EasySep Human Monocyte Enrichment Kit w/o CD16 depletion (Stemcell 436 #19058) according to the manufacturers protocol. Primary human monocytes were then cultured

in RPMI media (ATCC) containing 2 mM L-glutamine, 10 mM HEPES, 1 mM sodium pyruvate, 4500 mg/L glucose, 1500 mg/L sodium bicarbonate, supplemented with 10% fetal bovine serum (FBS; Invitrogen) at 37°C in 5% CO<sub>2</sub> atmosphere

**Antibodies and reagents.** Primary antibodies used in this study for immunofluorescence microscopy and immunoblot analysis include polyclonal rabbit (2042S, Cell Signaling Technology, Danvers MA) or mouse monoclonal  $\alpha$ -XIAP (sc-55550, Santa Cruz Biotechnology, Dallas TX), rabbit monoclonal  $\alpha$ -Caspase-3 (9662S; Cell Signaling Technology), rabbit monoclonal  $\alpha$ -Caspase-7 (9494S; Cell Signaling Technology), rabbit monoclonal  $\alpha$ -Caspase-8 (4790T; Cell Signaling Technology), rabbit  $\alpha$ -Caspase-9 (9502S; Cell Signaling Technology), polyclonal rabbit  $\alpha$ -TRX (T0803; Sigma-Aldrich, Saint Louis, MO), polyclonal rabbit  $\alpha$ -Notch1, intracellular (07-1231; Millipore Sigma, Billerica, MA), monoclonal rabbit  $\alpha$ -Notch1 (3608S; Cell Signaling Technology, Danvers MA), rabbit  $\alpha$ -TRP120-I1, rabbit monoclonal  $\alpha$ -GAPDH (2118L; Cell Signaling Technology), and human monoclonal  $\alpha$ -OMP-1 [213]. Synthetic peptides used in this study were commercially generated (Genscript, Piscataway, NJ). The pharmacological inhibitors of XIAP, Notch and Caspase-9 in this study were SM-164 (56003S; Cell Signaling Technology), DAPT (GSI-IX) (S2215; Tocris Bioscience, Bristol, UK) and Z-LEHD-FMK TFA (S731303; Tocris Bioscience), respectively. Cell death inducers in this study included rhTNF- $\alpha$  (210-TA/CF; R&D Systems, Minneapolis MN) and Staurosporine (9953S; Cell Signaling Technology). Polyclonal rabbit anti-TRP120 antiserum was commercially generated against a TRP120 epitope inclusive of aa. 290-301 (GenScript, Piscataway, NJ). Synthetic peptides used in this study were commercially generated (Genscript, Piscataway, NJ; Table 1).

**Immunoblot analysis.** Cells were infected or treated as indicated in text and figure legends and subsequently lysed with Triton-X 100 supplemented with protease inhibitor cocktail, Halt phosphatase and Phenylmethylsulfonyl fluoride (PMSF) for 30 min, with lysing by pipetting every 10 min on ice. Lysates were cleared by centrifugation at 14,000 x *g* (4°C) for 20 min.

Protein concentration of cleared lysates were determined by bicinchoninic acid assay (BCA assay). Laemmli buffer was added to lysates then boiled for 5 min at 95°C. Lysates were then subjected to SDS-PAGE and transferred to nitrocellulose membrane. Membranes were blocked using 5% nonfat milk in TBST and then exposed to  $\alpha$ -XIAP,  $\alpha$ -NICD,  $\alpha$ -CASP-3, -7 or -9 or  $\alpha$ -GAPDH antibodies overnight at 4°C. Membranes were washed thrice in Tris-buffered saline containing 1% Triton (TBST) for a total of 30 min followed by 1 h of incubation with horseradish peroxidase-conjugated anti-rabbit or anti-mouse secondary antibodies (SeraCare, Milford, MA) (diluted 1:10,000 in 1% nonfat milk in TBST). Proteins were visualized with ECL via Chemi-doc2 and densitometry was measured with VisionWorks image acquisition and analysis software.

**Quantitative PCR.** Uninfected, *E. chaffeensis*-infected or inhibitor-treated THP-1 cells were collected at 12, 24, 48 and 72 h intervals. RNeasy Mini Kit (QIAGEN, Valencia, CA, USA) was used to purify RNA followed by cDNA synthesis (0.5  $\mu$ g of RNA) using iScript RT kit (Bio-Rad). qPCR using the Brilliant II SYBR® Green QPCR Master Mix (Agilent) was performed. PCR primer sequences included *XIAP* (F: 5'-GAGAAGATGACTTTTAAACAGTTTGA-3'; R: 5'-TTTTTTGCTTGAAAGTAATGACTGTGT-3'), *CASP-3* (F: 5'-TGCAGCAAACCTCAGGGAAA-3'; R: 5'-AGTAACCCCTGCTTAATCGTCA-3'), *CASP-7* (F: 5'-ATTTAGGCTTGCCGAGGGAC-3'; R: 5'-ATGCTTGGCAGACAATGGAC-3'), *CASP-9* (F: 5'-GGCTGCTCCTGTTGGATGTA-3'; R: 5'-CCTTTTACCCTTGGTTTGGGC-3'), *DSB* (F: 5'-GCTGCTCCACCAATAAATGTATCCT-3'; 5'-GTTTCATTAGCCAAGAATTCCGACACT-3') and *GAPDH* (F: 5'-GGAGTCCACTGGCGTCTTCAC-3'; R: 5'-GAGGCATTGCTGATGATCTTGAG-3'). Relative gene expression was calculated by determining the cycle threshold (Ct) value and normalizing to *GAPDH*. Real-time PCR was performed as previously described [81].

**Co-immunoprecipitation.** Magna ChIP™ A/G Chromatin Immunoprecipitation Kit (MilliporeSigma, Burlington, MA) was used to investigate XIAP and NICD interactions during *E. chaffeensis* infection. Briefly, THP-1 cells were infected with *E. chaffeensis* (MOI 100) or left

uninfected (control) for 24 h. Cells were harvested, and Co-IP was performed according to the manufacturer's protocol. XIAP and NICD antibodies (Cell Signaling Technology) were used to determine interactions. IgG purified from normal serum was used as control antibody. Bound antigen was eluted, solubilized in 4X SDS sample loading buffer and processed for immunoblot analysis. The membrane was probed with XIAP or NICD antibody to confirm pulldown. Co-immunoprecipitation was performed in triplicate experiments.

**Transfection.** HeLa cells ( $1 \times 10^6$ ) were seeded in a 60 mm culture dish 24 h prior to transfection. All proteins were expressed in a pcDNA3.1+C-6His vector. TRP120 full-length (pcDNA3.1+TRP120\_FL\_C-6His) and its HECT Ub ligase catalytic inactive mutant (pcDNA3.1+TRP120\_C520S\_C-6His) were cloned into the pcDNA3.1+C-6His vector at NheI/XbaI sites. pcDNA3.1+C-6His empty vector was used as a control. All vectors were added to Opti-MEM and Lipofectamine 3000 mixture and incubated for 20 min at 37°C. Lipofectamine/plasmid mixtures were added to HeLa cells and incubated for 4 h at 37°C. The medium was aspirated 4 h posttransfection and fresh medium was added to each plate and incubated for 24 h.

**Immunofluorescent confocal microscopy.** THP-1 cells ( $1 \times 10^6$ ) were infected with *E. chaffeensis* (MOI 50 or 100) for indicated time intervals at 37°C. Cells were collected and fixed using ice-cold 4% formaldehyde and washed with sterile 1X PBS five times for 5 min. Cell samples were permeabilized and blocked in 0.5% Triton X-100 and 2% bovine serum albumin (BSA) in PBS for 30 min. Cells were washed with sterile 1X PBS three times for 5 min and probed with XIAP, NICD or DSB antibodies for 1 h at room temperature. Cells were washed with sterile 1X PBST (0.1% Tween) three times for 5 min and probed with Alexa Fluor IgG (H+L) or Alexa Fluor IgG (H+L) for 30 min at room temperature, washed three times with sterile 1X PBST, and mounted with ProLong Gold antifade reagent with DAPI (Molecular Probes). Slides were imaged on a Zeiss LSM 880 confocal laser scanning microscopy. Mander's correlation

coefficients were generated by ImageJ software to quantify the degree of colocalization between fluorophores.

**Sequence Homology.** Genome and transcriptome sequences encoding *E. chaffeensis* TRP120 and Homo sapiens Notch ligand proteins were recovered using BLAST searches with the online version at the NCBI website. Sequences were submitted to NCBI Protein BLAST and ClustalW2 sequence databases for sequence alignment.

**Informational Spectrum Method (ISM).** ISM analyzes the primary structure of proteins by assigning a physical parameter which is relevant for the protein's biological function (37, 60). Each amino acid in TRP120 and Notch ligand sequences was given a value corresponding to its electron-ion interaction potential (EIIP), which determines the long-range properties of biological molecules. The value of the amino acids within the protein were Fourier transformed to provide a Fourier spectrum that is representative of the protein, resulting in a series of frequencies and amplitudes. The frequencies correspond to a physico-chemical property involved in the biological activity of the protein. Comparison of proteins is performed by cross-spectra analysis. Proteins with similar spectra were predicted to have a similar biological function. Inverse Fourier Transform was performed to identify the sequence responsible for obtained signals at a given frequency.

**Pull Down Assay.** Recombinant His-tagged TRP120 (10 µg) and Notch-1 (10 µg) (Sino Biological) were incubated with Ni-NTA beads alone, or in combination, for 4 h at 4°C. Supernatants were collected and the Ni-NTA beads were washed 5X with 10 mM imidazole wash buffer. Proteins were eluted off with 200 mM imidazole elution buffer and binding determined by Western blot analysis.

**TRP120 recombinant protein and peptide treatment.** Full length or truncated constructs of rTRP120, or rTRX control were expressed in a pBAD expression vector, which has been

previously optimized by our laboratory (59, 61, 62). Recombinant TRP120 full length, truncated constructs, and rTRX were purified via nickel-nitrilotriacetic acid (Ni-NTA) purification system. All recombinant proteins were dialyzed via PBS and tested for bacterial endotoxins using the Limulus Amebocyte Lysate (LAL) test. rTRP120-TR was dialyzed in 1X PBS and tested for bacterial endotoxins using the Limulus amebocyte lysate (LAL) test. TRP120 synthetic peptides were commercially generated (Genscript, Piscataway, NJ). THP-1 cells or primary monocytes were treated with 2 µg/ml of rTRP120-TR or TRX, or 1 µg/ml of synthetic TRP120 peptides for 0-72 h timepoints. Cells were collected post-treatment and immunoblot and qPCR analysis was performed.

Table 2. TRP120 Synthetic Peptides

TRP120-N1 peptide 1:	DVASHESGVSDQPAQVVTERESEIESHQG
TRP120-N1 peptide 2:	PFVAESEVSKVEQEETNPEVLIKDLQDVAS
TRP120-N1 peptide 3:	RESEIESHQGETEKESGITESHQKEDEIVSQPSSE
TRP120-N1 peptide 4:	RESEIESHQGET
TRP120-N1 peptide 5:	EKESGITESHQK
TRP120-N1 peptide 6:	EDEIVSQPSSE
TRP120 dmut	RESEIESHQGETEKESGITESHQK
TRP120 dmut 2	AAEIVSAASSE
TRP120 dmut 3	AAAIVSQPSSE
TRP120 dmut 4	EDEIVSQAAAA

**Protein-coated fluorescent microsphere assay.** TRP120 and TRX recombinant proteins were desalted using Zeba spin desalting columns (Thermo Fisher Scientific, MA) as indicated by the manufacturer protocol. Protein abundance of desalted recombinant protein was assessed by bicinchoninic acid assay (BCA assay). One-micrometer, yellow-green (505/515), sulfate FluoSpheres (Life Technologies, CA) were first equilibrated with 40 $\mu$ M of MES buffer followed by incubation with 10 $\mu$ g of desalted TRP120 or TRX recombinant protein in 40 $\mu$ M MES (2-(N490 morpholino) ethanesulfonic acid) buffer for 2 h at room temperature on a rotor. TRP120 or TRX coated FluoSpheres were washed twice with 40 $\mu$ M MES buffer at 12,000 x g for 5 mins and then resuspended in RPMI media. To determine TRP120 or TRX protein coating of FluoSpheres, dot blotting of FluoSpheres samples was performed after protein coating using  $\alpha$ TRX or  $\alpha$ -TRP120 antibodies.  $8 \times 10^5$  THP-1 cells/well were plated in a 96-well round bottom plate, and the TRP120 or TRX coated FluoSpheres were added to each well at approximately 5 beads/cell. The cell and protein-coated FluoSpheres were incubated between 5-60 mins at 37°C with 5% CO<sup>2</sup>, collected and unbound beads were washed twice with 1 X PBS, followed by fixation by cytospin for 15 mins. Cell samples were then processed for analysis by immunofluorescent confocal microscopy, as previously mentioned. FluoSpheres are light sensitive, therefore all steps were performed in the dark.

**Surface Plasmon Resonance.** SPR was performed using a BIAcore T100 instrument with nitrilotriacetic acid (NTA) sensor chip. Purified polyhistidine-tagged, full-length, rTRP120-TR, rTRX and human rNotch-1 Fc Chimera Protein, CF (R&D Systems, MN) were dialyzed in running buffer (100 mM sodium phosphate [pH 7.4], 400 mM NaCl, 40  $\mu$ M EDTA, 0.005% [vol/vol]). Briefly, each cycle of running started with charging the NTA chip with 500  $\mu$ M of NiCl<sub>2</sub>. Subsequently, purified polyhistidine-tagged, full-length, truncated rTRP120 proteins, or rTRX (0.1  $\mu$ M) were immobilized on the NTA sensor as ligand on flow cell 2. Immobilization was carried out at 25°C at a constant flow rate of 30  $\mu$ l/min for 100s. Varying concentrations of

Notch1-NECD constructs (0-800 nM) were injected over sensor surfaces as analyte with duplicates along with several blanks of running buffer. Injections of analyte were carried out at a flow rate of 30  $\mu$ l/min with contact time of 360 s and a dissociation time of 300 s. Finally, the NTA surface was regenerated by using 350 mM EDTA. Readout included a sensogram plot of response against time, showing the progress of the interaction. Curve fittings were done with the 1:1 Langmuir binding model with all fitting quality critique requirements met. The binding affinity (KD) was determined for all interactions by extracting the association rate constant and dissociation rate constant from the sensorgram curve ( $KD = K_d/K_a$ ) using the BIAevaluation package software.

**TRP120 Antibody Inhibition of *E. chaffeensis* Notch activation.** Host cell-free *E. chaffeensis* was pre-treated with 5-10  $\mu$ g/ml of polyclonal rabbit anti-TRP120 antibody generated against the TRP120 Notch mimetic SLiM (aa. 284-301), or purified IgG antibody. The cell-free *E. chaffeensis*/antibody mixture was then added to THP-1 cells ( $5 \times 10^5$ ) in a 12-well plate for 2 h. Samples were collected, washed with PBS and prepared for IFA.

**Knockdown experiments.** ON-TARGETplus SMARTpool XIAP siRNA (3  $\mu$ l) (Dharmacon, Lafayette, Co) was transfected into cells ( $1.0 \times 10^6$ ) using lipofectamine 3000 (7.5  $\mu$ l) (Invitrogen, Waltham, MA, USA) according to the manufacturer's instructions. Scrambled siRNA was utilized as a control in both uninfected and *E. chaffeensis*-infected THP-1 cells. siRNA and Lipofectamine mixture were added to 250  $\mu$ l of MEM medium (Invitrogen), incubated for 12 min at room temperature and added in a 6-well plate. Knockdown was assessed by immunoblot analysis as previously described. Cells were knocked down for 24 h and infected with *E. chaffeensis* (MOI 100) for 24 h. Cells were then harvested after 24 h post-infection. Proliferative/cell death analysis was performed on all knockdown cells. Ehrlichial load was determined by qPCR of *dsb* gene as previously described [51]. All siRNA knockdowns were

performed with triplicate technical and biological replicates and significance was determined using a *t*-test analysis.

**Proliferative/Cell Death Analysis.** THP-1 cells were untreated or treated with DMSO, SM-164 (100 nM) alone or in combination with Z-LEHD-FMK TFA (20  $\mu$ M) and incubated at 37°C, 5% CO<sub>2</sub> for 12 h. Z-LEHD-FMK TFA treatment was administered for 2 h prior to SM-164 treatment. Cell death was induced using TNF- $\alpha$  (100 ng/ml). Staurosporine (100 ng/ml) was utilized as a positive apoptosis control. Cells were infected with *E. ch.* (MOI 50) following induction of cell death for 48 h. Apoptosis was analyzed utilizing various cell death assays.

1. *Trypan blue exclusion.* 20  $\mu$ l of cell sample were collected and added to 20  $\mu$ l of trypan blue. Samples were incubated at room temperature for 2 mins and read via the via Nexcelom Cellometer Mini (Nexcelom Bioscience LLC, Lawrence, MA, USA)
2. *Caspase-3/ CPP32 Assay Kit.* Caspase-3/ CPP32 Assay Kit (Colorimetric) [NBP2-54838] was utilized to assess the activity of Caspase-3 according to the manufacturers' protocol.
3. *Hematoxylin and eosin (H&E).* H&E stain was utilized to assess cell morphological changes associated with cell death. Cells were collected and washed with 1X DPBS. Fresh RPMI mediated were added to the cell samples and fixed onto slides by cytospin (800 x *g*, 5 mins). Cells were then fixed by acetone (1 min) and stained with Hematoxylin and eosin (1 min per stain). Slides were rinsed with DI water and dried prior to analysis using light microscopy. Images were taken using the Olympus cellSens software.
4. *Guava® Muse® Cell Analyzer.* Various Muse assays were utilized according to the manufacturers' protocol to determine apoptosis:

- a. The Muse® Count & Viability Kit was used to determine cell count and viability (Part Number MCH100102) Viable cell count (cells/mL) and percentage viability of samples were determined.
- b. The Muse® MultiCaspase Kit (Part Number: MCH100109) was used to determine caspase activation and cellular plasma membrane permeabilization, or cell death. The percentage of live, caspase+, caspase+ and dead, total caspase+, and dead cells was determined.
- c. The Muse® Annexin V & Dead Cell Kit (Part Number: MCH100105) was used to determine live, early, and late apoptosis and cell death. The percentage of live, early apoptotic, late apoptotic, total apoptotic, and dead cells was determined.

**Statistical analysis.** All data are represented as the means  $\pm$  standard deviation (SD) of data obtained from at least three independent experiments done with triplicate biological replicates. Experiments performed with technical replicates are indicated in figure legends and the material and methods section. Analyses were performed using a two-way ANOVA or two-tailed Student's *t* test (GraphPad Prism 6 software, La Jolla, CA).  $P < 0.05$  was considered statistically significant.

## CHAPTER 3. EHRLICHIA SLIM LIGAND MIMETIC ACTIVATES NOTCH SIGNALING IN HUMAN MONOCYTES

### Introduction

*Ehrlichia chaffeensis* is a small, obligately intracellular, Gram-negative tick transmitted bacterium [17] that exhibits tropism for mononuclear phagocytes. *E. chaffeensis* establishes infection through a multitude of cellular reprogramming strategies that involve effector-host interactions resulting in activation and manipulation of cell signaling pathways to suppress and evade innate immune mechanisms [60, 64, 65, 79, 84, 85, 94]. The mechanisms whereby *E. chaffeensis* evades host defenses of the macrophage involves exploitation of Wnt and Notch signaling by the tandem repeat protein (TRP) effector, TRP120 [64, 79, 84, 85, 94].

*E. chaffeensis* TRP120 is a surface-expressed and intracellularly secreted effector that has well-documented moonlighting functions including roles as a nucleomodulin [66, 68], a HECT E3 ubiquitin ligase [64, 65, 69], and as a ligand mimic [50, 79, 84, 94]. Previously, we found that TRP120 is involved in a diverse array of host cell interactions including components of signaling [64] and transcriptional regulation associated with Wnt and Notch signaling pathways [60]. We have recently shown that TRP120 ubiquitinates the Notch negative regulator FBW7 resulting in increased Notch intracellular domain (NICD) levels, as well as other FBW7 regulated oncoproteins during infection [64]. In addition, we have also demonstrated that *E. chaffeensis* [68] Notch activation results in downregulation of toll-like receptor 2 and 4 expression, likely as an immune evasion mechanism [94]. Although we have demonstrated TRP120 activates Notch signaling, the molecular details involved in activation have yet to be defined.

The Notch signaling pathway is evolutionarily conserved and is known to play a critical role in cell proliferation, differentiation, and apoptosis in all metazoan organisms [104, 106, 214]. Notch activation plays significant roles in various other cellular outcomes, including MHC Class II expansion [111], B- and T- cell development [215], and innate immune mechanisms such as autophagy [216] and apoptosis [211, 217]. Canonical Notch activation is driven by direct cell

membrane bound receptor-ligand interactions with four Notch receptors (Notch1-4) and 6 canonical Notch ligands, Delta-like (DLL 1,3,4) and Jagged (Jagged/Serrate-1 and 2). Notch receptor-ligand interactions occur at the Notch extracellular domain (NECD), specifically at epidermal growth factor-like repeats (EGFs) 11-13, the known ligand binding domain (LBD). Module at the N-terminus of Notch ligands (MNNL) and Delta/Serrate/LAG-2 (DSL) domains in canonical Notch ligands interact with the Notch LBD. Although there is evidence demonstrating the requirement of both N-terminal MNNL and DSL Notch ligand domains for Notch receptor binding, there is little information known about ligand regions/motifs that are necessary for Notch activation [119, 124]. During canonical Notch activation, ligands expressed on neighboring cells bind the Notch receptor and create a mechanical force at the negative regulatory region (NRR) which triggers several sequential proteolytic cleavages, releasing the NICD. NICD subsequently translocates to the nucleus and binds to other transcriptional coactivators, including RBPjK and MAML, to activate Notch gene transcription [118]. Notably, secreted noncanonical Notch ligands have also been shown to activate Notch signaling; however, the molecular details of non-canonical Notch ligand-receptor interactions are not well defined [152].

There are three major classes of protein interaction modules which include globular domains, intrinsically disordered domains (IDDs), and short linear motifs (SLiMs), all of which have distinct biophysical attributes [71, 78, 218]. IDDs are 20-50 amino acids in length, are known to be disordered in nature, are located within globular domains or intrinsically disordered protein regions and have transient interactions in the nanomolar range . In comparison, SLiMs are ~3-12 amino acids in length, are known to be disordered in nature, located within globular domains or IDDs, and have low micromolar affinity ranges with transient interactions. SLiMs have been shown to evolve de novo for promiscuous binding to various partners [71, 72]. Ehrlichial TRPs interact with a diverse array of host proteins through several well-known protein-protein interaction mechanisms including post-translational modifications (PTMs), and various protein interaction modules located in IDDs [63, 65, 71, 72].

Microorganisms have developed mechanisms to survive in the host cell which involve hijacking host cell processes. Molecular mimicry has been well-established as an evolutionary survival strategy utilized by pathogens to disrupt or co-opt host function for infection and survival [40, 71, 72, 219]. Studies have determined this occurs through pathogen effectors that mimic eukaryotic host proteins, allowing for pathogens to hijack and manipulate host cellular pathways and functions. SLiMs have been identified as interaction modules whereby eukaryotes and pathogens direct cellular processes through protein-protein interactions [39, 40]. Recently, we have demonstrated TRP120 is a Wnt ligand mimetic that interacts with host Wnt receptors to activate Wnt signaling [79].

In this study, we reveal an *E. chaffeensis* Notch SLiM ligand mimetic whereby TRP120 activates Notch signaling for infection and intracellular survival. Understanding the molecular mechanisms utilized by *E. chaffeensis* to subvert innate host defense for infection and survival is essential for understanding intracellular pathogen infection strategies and provides a model to investigate molecular host-pathogen interactions involved in repurposing host signaling pathways for infection.

## **Results**

### ***E. chaffeensis* TRP120 shares sequence homology and predicted Notch ligand function.**

We have previously shown TRP120 interacts with Notch activating metalloprotease, ADAM17 and Notch antagonist FBW7 using yeast-two hybrid analysis (Y2H) [60]. We have also shown that TRP120 binds to the promoter region of notch1 using chromatin immunoprecipitation sequencing (ChIP-Seq), and that activation of Notch occurs during infection [68, 94]. Notch activation occurs through direct interaction of Notch ligands with the Notch-1 receptor initiating two receptor proteolytic cleavages, resulting in NICD nuclear translocation and subsequent activation of Notch downstream targets. Since TRP120 has been shown to activate the Notch

signaling pathway, we examined TRP120 sequence homology and correlates of biological functionality with Notch ligands.

NCBI Protein Basic Local Alignment Search Tool (BLAST) was used to identify local similarity between TRP120 and canonical/non-canonical Notch ligand sequences. Sequence homology with a TRP120 tandem repeat (TR) IDD motif, TESHQKEDEIVSQPSSE (aa. 284-301), was shown to share sequence homology with several canonical Notch ligands, including Jagged-1, DLL1, DLL4, and non-canonical Notch ligand TSP2 (Fig. 5A). We then used informational spectrum method (ISM) to predict similar functional properties between TRP120 and Notch ligands. ISM is a prediction method that uses the electron ion interaction potential of each amino acid within the primary sequence of proteins to translate the primary sequences into numerical sequences. Translated sequences are then converted into a spectrum using Fourier transform. Cross spectral analysis of the translated sequences is then performed to obtain characteristic frequency peaks that demonstrate if proteins share a similar biological function. TRP120 was predicted to share a similar biological function with canonical Notch ligands, DLL1, 3 and 4, and non-canonical Notch ligand F3 contactin-1, a known adhesion molecule (Figs. S1 A-D). To identify the sequence responsible for the identified frequency peaks, reverse Fourier 142 transform of ISM was performed (Fig. 5B). A 35-mer TRP120-TR IDD motif, IVSQPSSEPFVAESEVSKVEQEETNPEVLIKDLQD (aa. 214-248 and 294-328), was associated with characteristic frequency peaks (Figs. 5B and C). Collectively, these results indicate that the TRP120 sequence and fundamental biophysical properties of the amino acids are consistent with Notch ligands.

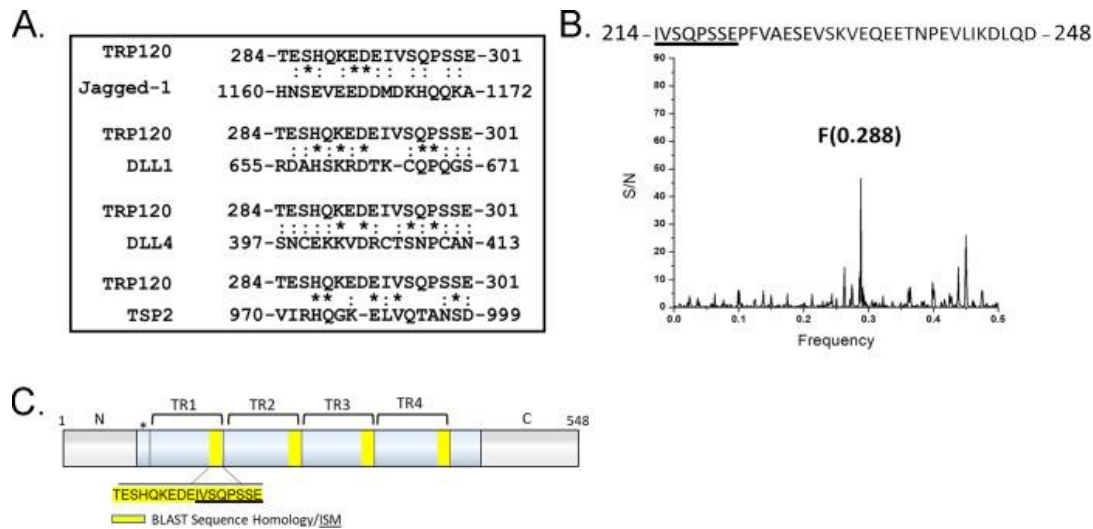


**Figure 5. *E. chaffeensis* TRP120 shares sequence homology and biological function with canonical and noncanonical Notch ligands.**

(A) BLAST analysis of TRP120 with canonical/noncanonical Notch ligands demonstrating amino acid homology. An asterisk (\*) represents identical conserved amino acid residues; a colon (:) represents conservative substitutions. (B) The informational spectrum method (ISM) was used to predict if TRP120 shared a similar biological function with canonical and noncanonical Notch ligands. Primary sequences of TRP120 and Notch ligands were converted into a numerical sequence-based electron-ion interaction potential (EIIIP) of each amino acid. Numerical sequences were converted into a spectrum using Fourier transform. To determine if proteins shared a similar biological function and cross spectra analysis was performed and similar biological function is denoted by a peak at a frequency of  $F(0.288)$ . (C) Schematic of TRP120 N- C- (gray) and TR domains (blue) with four highlighted repetitive TRP120 TR motifs that share sequence homology with Notch ligands. ISM sequence is shown in (B) (underlined). (\*) represents a partial tandem repeat-containing similar (*EDDTVSQPSLE*) but nonidentical sequence to highlighted sequence.

***E. chaffeensis* TRP120 directly interacts with the Notch-1 ligand binding region (LBR).** Canonical activation of the Notch pathway is known to occur through canonical Notch ligands binding to Notch receptor LBD (EGFs 11-13 in the extracellular domain). To investigate if TRP120 interacts with the Notch-1 receptor LBR (EGFs 1-15), we ectopically expressed GFP-9 tagged full length TRP120 (TRP120-FL-GFP) in HeLa cells and probed for endogenous Notch-1 to determine colocalization. Pearson's correlation coefficient (PC) and Mander's coefficient (MC) (correlation range +1 to -1; 0 represents absence of correlation), was used to quantify the degree of colocalization between TRP120-FL-GFP and Notch-1. Ectopically expressed TRP120-FL-GFP was found to strongly colocalize (PC = 0.897 and MC = 0.953) with endogenous Notch-1 (Fig. 6A). In comparison, ectopically expressed AcGFP-vector showed no

colocalization (PC = 0.008 and MC = 0.009) with endogenous Notch-1 (Fig. 6A). Colocalization of TRP120 and Notch-1 demonstrates that these two proteins are in the same spatial location; however, it does not demonstrate direct protein-protein interaction. To confirm a direct interaction, we utilized pull-down assays of recombinant TRP120-FL (rTRP120-FL) and rNotch1 LBR and a direct protein-protein interaction was demonstrated (Figs. 6B and S2A-B). Recombinant thioredoxin (rTRX) is the fusion tag for the pBAD expression vector used to express the rTRP120 constructs; therefore, rTRX was used as a negative recombinant control and no interaction was observed (Fig. 6B). Based on sequence homology and ISM data, a short region of sequence homology within the tandem repeat (TR) domain was identified that could be involved in the TRP120 and Notch-1 LBR. To determine if the TRP120-TR was responsible for the previous TRP120 and Notch-1 LBR interaction, we performed a pull-down assay with rTRP120-TR and rNotch-1 LBR. rTRP120-TR was pulled down with Fc-tagged rNotch-1 LBR demonstrating a direct interaction with the TR domain (Fig. 6C). To further confirm direct interaction of rTRP120-FL or rTRP120-TR and rNotch-1 LBR, surface plasmon resonance was performed. An interaction between both rTRP120-FL (Fig. 6D) and rTRP120-TR (Fig. 6E) with rNotch-1 LBR was detected in a concentration dependent manner. Fitting the concentration response plots for rTRP120-FL and rTRP120-TR yielded a KD (equilibrium dissociation constant) of  $100 \pm 3.5$  nM and  $120 \pm 2.0$  nM, respectively (Figs. 6D-E). No interaction was detected between rTRX and rNotch-1 LBR (Fig. 6F). Additionally, treatment of THP-1 cells with rTRP120-coated sulfate, yellow-green microspheres demonstrated colocalization of rTRP120 and Notch-1 (Figs. 6G). In comparison, rTRX-coated fluorescent microsphere did not colocalize with the Notch-1 receptor (Figs. 6G). rTRP120 and rTRX coating of sulfate, yellow-green microspheres were confirmed using dot blot (Fig. S3) Together, these binding data reveal rTRP120-TR binds the rNotch-1 LBR. *E. chaffeensis* TRP120-TR domain is required for Notch activation. Both the N-terminal MNNL and cysteine-rich DSL domain of Notch ligands are known to be required for receptor binding; however, there is little known regarding ligand motifs required for Notch activation. We have previously demonstrated Notch activation occurs in THP-

1 cells after stimulation with TRP120-coated beads for 15 min [94]. Gene expression levels of *notch1*, *hes1* and *hes5* were upregulated after incubation with TRP120-coated beads. To further delineate the TRP120 domain required for Notch activation THP-1 cells or primary human monocytes were treated with soluble purified truncated constructs of rTRP120 (rTRP120-TR and -C-terminus) (Figs. S2A-B). THP-1 cells infected with *E. chaffeensis* or treated with rJagged-1 were used as positive controls and demonstrated NICD nuclear translocation 2 h post-treatment. In comparison, rTRP120-TR caused NICD nuclear translocation 2 h post-treatment (Figs. 7A-B). NICD nuclear translocation was not observed in untreated cells, cells treated with TRX or rTRP120-C-terminal soluble proteins (Figs. 5A-B). Collectively, these data demonstrate the requirement of TRP120-TR for Notch activation.

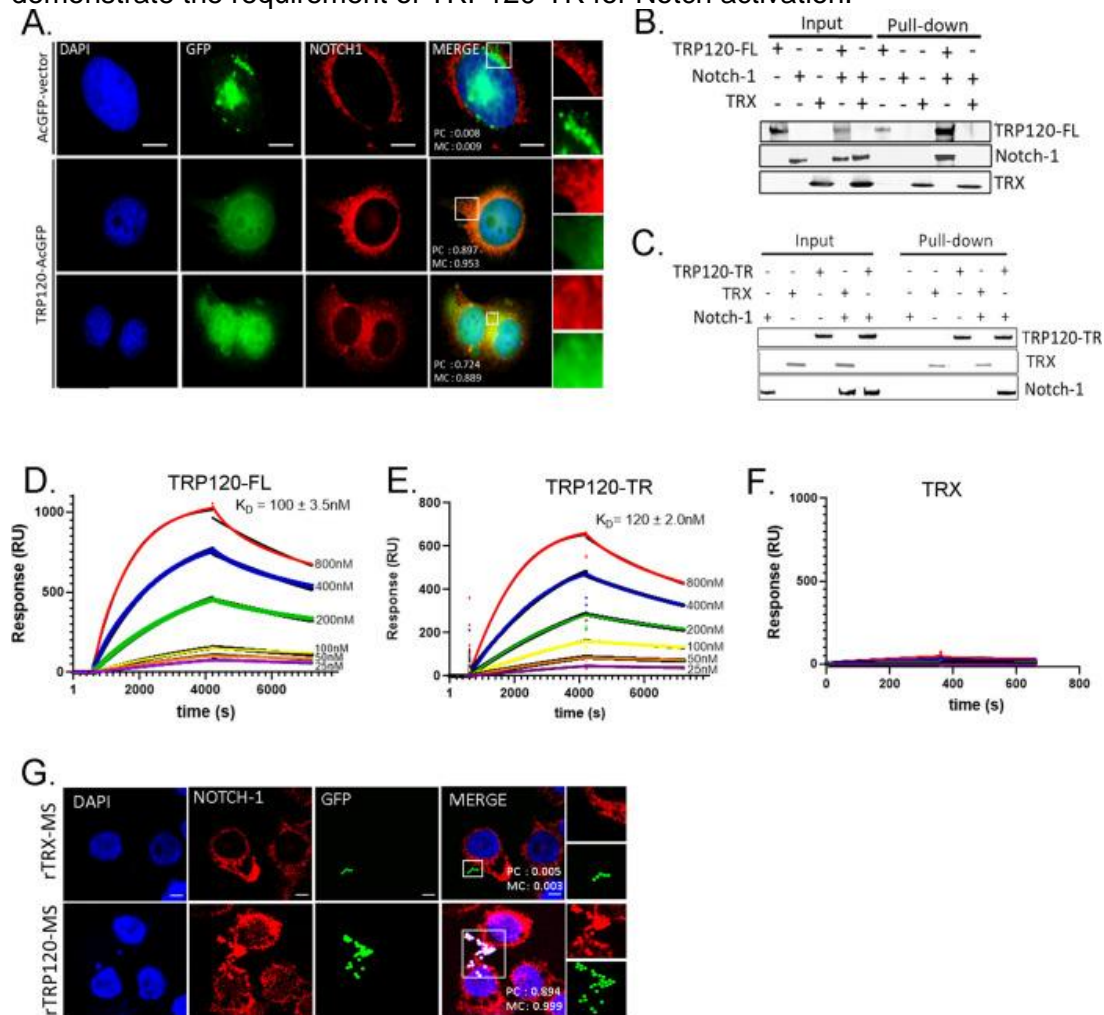


**Figure 6. *E. chaffeensis* TRP120-TR interactions with the Notch receptor ligand-binding region (LBR).**

(A) HeLa cells transfected with TRP120-GFP (green) and probed for endogenous Notch-1 (red) demonstrated colocalization by immunofluorescent microscopy. Colocalization was quantitated by Pearson's and Mander's coefficients (0 no colocalization; +1 strong colocalization). (B and C) His tag pulldown assays demonstrated a direct interaction between TRP120 and Notch-1. rFc-tagged Notch-1 LBR was incubated with (B) TRP120-FL-His, (C) TRP120-TR-His, or TRX-His negative-control on Talon metal affinity resin. Bound Notch-1, TRP120-His,  $\alpha$ -TRP120 against a TR peptide or TRX-His were detected with  $\alpha$ -Notch-1,  $\alpha$ -TRP120, or  $\alpha$ -TRX antibodies. (D-F) Surface plasmon resonance of (D) TRP120-FL-His, (E) TRP120-TR-His, or (F) TRX-His with Fc-tagged Notch-1 LBR on a Biacore T100 with a series S Ni-nitrilotriacetic acid (NTA) sensor chip. TRP120-FL-His, TRP120-TR-His, or TRX-His were immobilized on the NTA chip and 2-fold dilutions (800 nM to 25 nM) of Fc-tagged Notch-1 LBR were used as an analyte to determine binding affinity ( $K_D$ ). Sensograms and  $K_D$  are representative of data from triplicate experiments. (G) THP-1 cells were treated with rTRX- or rTRP120-FL-coated fluorescent microspheres for 1h. Colocalization was visualized by confocal immunofluorescent microscopy. Notch-1 was immunostained with tetramethylrhodamine isothiocyanate (TRITC) and TRP120-coated fluorescein isothiocyanate (FITC) auto-fluorescent microspheres. Nuclei were stained with DAPI (blue). White boxes indicate areas of colocalization measurements. Scale bar = 10  $\mu$ m. (H) Dot blot of PBS, TRX, or TRP120-FL-coated microspheres probed with  $\alpha$ -TRX or  $\alpha$ -TRP120 antibodies, respectively.

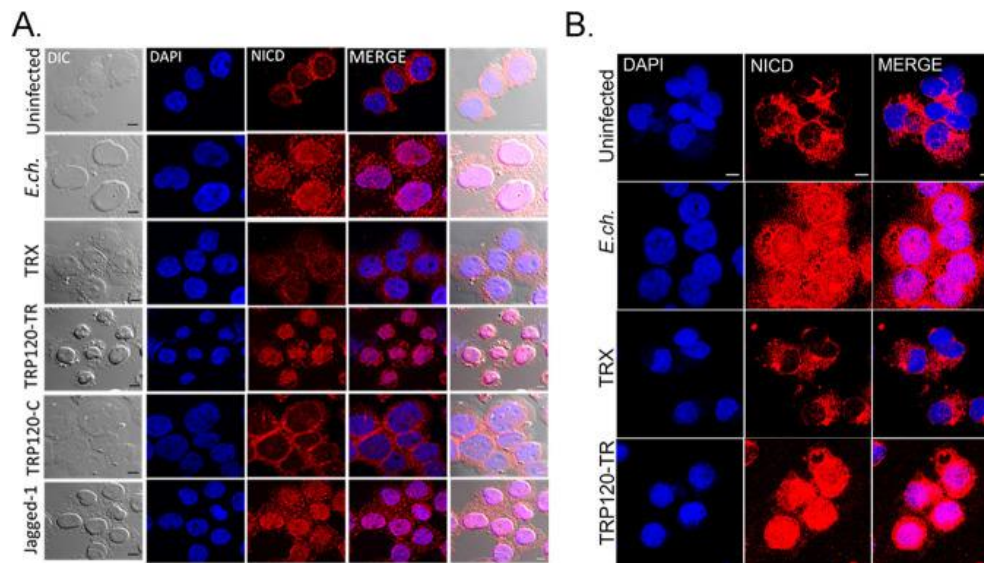


**Figure 7. TRP120-TR activates Notch and NICD nuclear translocation in primary human monocytes.**

(A) Soluble recombinant TRP120-TR or -C-terminal proteins (2  $\mu$ g/mL) were incubated with THP-1 cells for 2 h. Cells were collected and NICD localization was determined by confocal immunofluorescent microscopy. Uninfected/untreated or recombinant TRX-treated THP-1 cells were used as negative controls. *E. chaffeensis*-infected or recombinant Jagged-1 treated THP-1 cells were used as positive controls. NICD nuclear translocation was detected in *E. chaffeensis*-infected, TRP120-TR and Jagged-1 treated cells. (B) Primary human monocytes were treated with soluble TRP120-TR or recombinant TRX as described above and NICD nuclear translocation was detected in *E. chaffeensis*-infected and TRP120-TR-treated cells. Endpoint analysis was performed as described in 3. Experiments were performed in triplicate and representative images are shown.

***E. chaffeensis* TRP120-TR Notch ligand IDD-mimetic activates Notch.** To determine if Notch is activated by a TRP120-TR Notch mimetic IDD motif, several TRP120-TR synthetic peptides were generated (Fig. 8A). THP-1 cells or primary human monocytes were treated with TRP120-TR IDD peptides for 2 h. THP-1 cells infected with *E. chaffeensis* were used as a positive control and scrambled peptide was used as negative control. A 35-aa TRP120-TR IDD motif (TRP120-N1-P3) caused NICD nuclear translocation (Figs. 8B and C), in comparison to scrambled negative control treated cells. Importantly, the TRP120-TR IDD contained a motif identified in both sequence homology and ISM data (Fig. 5C). Inhibition of Notch signaling by DAPT, a  $\gamma$ -secretase inhibitor, abrogated Notch activation with TRP120-N1-P3 treatment, indicating that TRP120-N1-P3 directly binds to the Notch-1 receptor for Notch activation (Fig. 8B). To confirm Notch activation by TRP120-N1-P3, gene expression levels of Notch downstream targets were examined by human Notch signaling pathway array analysis. In comparison to untreated THP-1 cells, a significant increase in Notch downstream targets, including *HES1*, *HES5*, *HEY1* and *HEY2* gene expression levels occurred in TRP120-N1-P3 treated cells (Figs. 9A-B, Table S1A). Interestingly, Notch gene expression by TRP120-N1-P3 treatment was increased in a concentration-dependent manner (Fig. 9B, Table S1A). Importantly, rJagged-1 also demonstrated similar upregulation of Notch genes in a concentration-dependent manner (Fig. S4). These data demonstrate that a TRP120 IDD mimetic motif is responsible for TRP120 Notch activation.

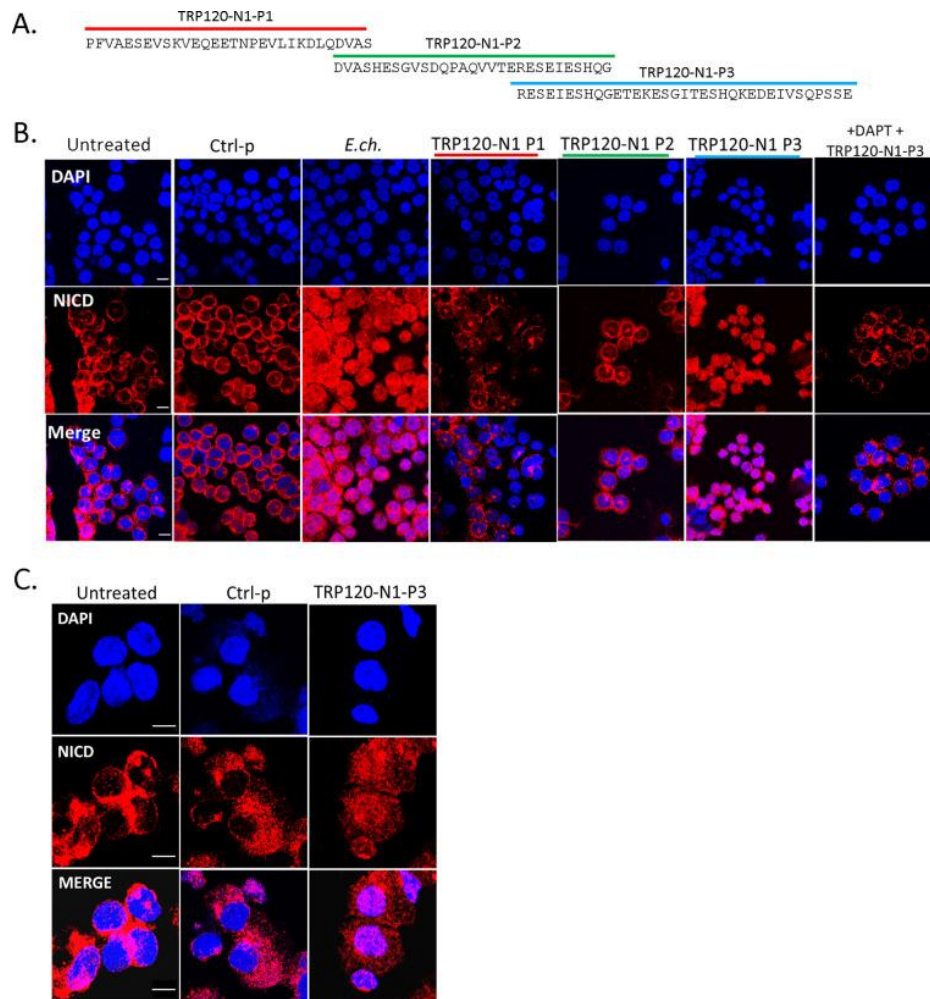


**Figure 8. A TRP120-TR Notch-1 memetic IDD peptide stimulates NICD nuclear translocation.**

(A) Overlapping TRP120-TR IDD peptide sequences (P1-P3) (B) THP-1 cells or (C) Primary human monocytes were incubated with synthetic TRP120-TR IDD peptides to determine the TRP120-TR Notch-1 memetic motif responsible for Notch activation. TRP120-TR peptides were overlapping peptides spanning an entire TR domain. Cells were treated with peptide (1  $\mu\text{g}/\text{mL}$ ) for 2 h and confocal immunofluorescent microscopy was used to visualize NICD localization. NICD nuclear translocation denotes Notch activation. A scrambled peptide (Ctrl-p) was used as negative control and *E. chaffeensis*-infected cells were used as positive control. To determine if direct interaction of the TRP120-N1-P3 peptide and Notch receptor was necessary for Notch activation, THP-1 cells were pretreated with DAPT, a  $\gamma$ -secretase inhibitor, and treated with TRP120-N1-P3 peptide for 2 h.

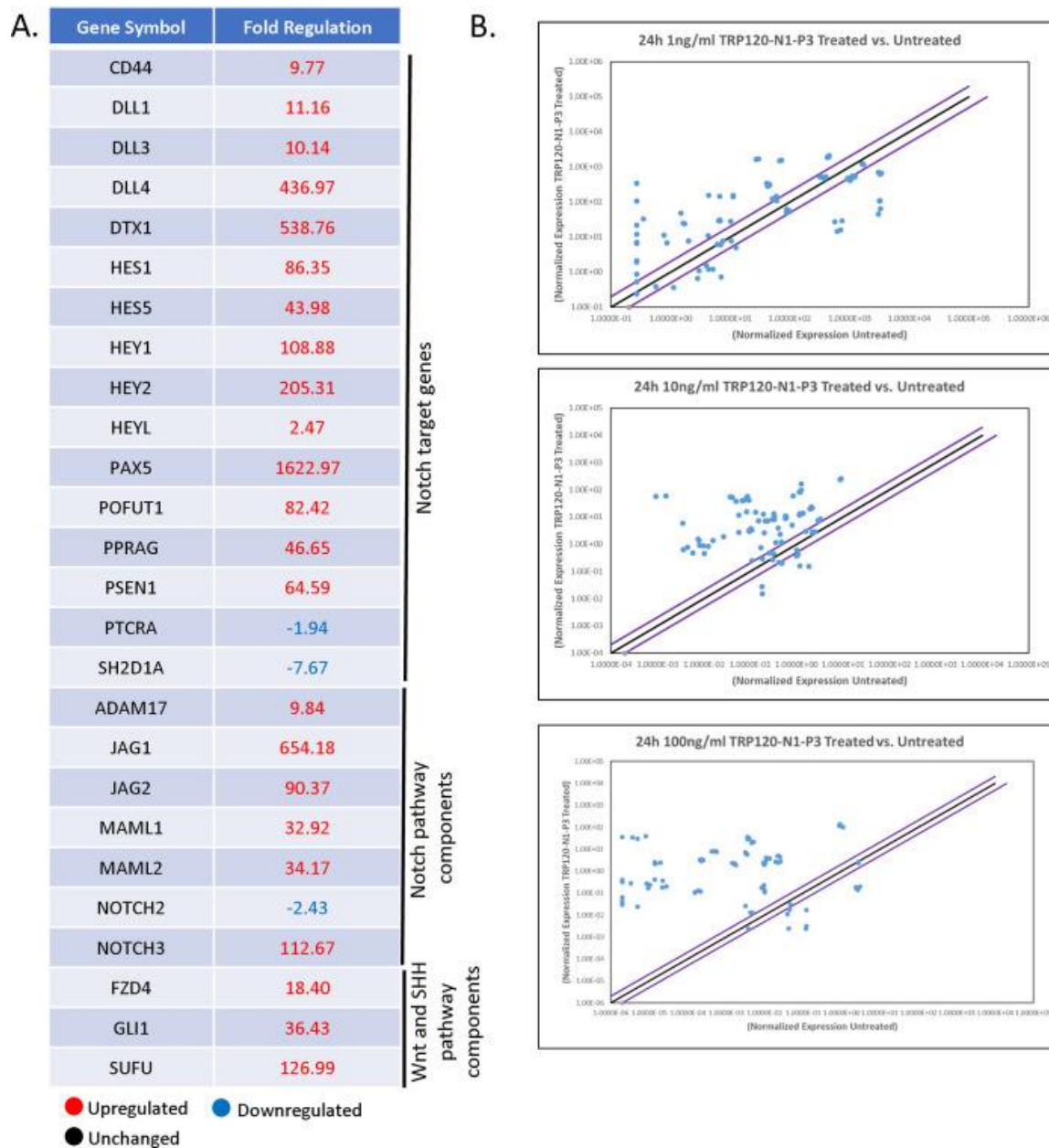


**Figure 9. TRP120-N1-P3 IDD peptide stimulates Notch gene expression.**

(A) Table of Notch pathway genes with corresponding fold change displaying differential expression (up, down or no change) at 24 h pt with 10 ng/mL of TRP120-N1-P3 peptide (B) Scatterplots of expression array analysis of 84 Notch signaling pathway genes to determine Notch gene expression 24 h after stimulation with 1 ng/mL (top), 10 ng/mL (middle) or 100 ng/mL (bottom) of TRP120-N1-P3 peptide. Purple lines denote a 2-fold upregulation or downregulation in comparison to control, and the black line denotes no change. Scatterplots are representative of three independent experiments ( $n = 3$ ).

***E. chaffeensis* TRP120-TR Notch ligand SLiM mimetic activates Notch.** It is well-documented that SLiMs are found in two general groups; posttranslational modification (PTM)

motifs or ligand motifs that mediate binding events. We have previously identified a functional TRP120 HECT E3 ligase catalytic motif located in the C-terminus [64, 65] and have recently identified a TRP120-TR Wnt SLiM mimetic motif [79]. To determine if the TRP120-TR Notch mimetic motif could be a SLiM (3-12 aa), overlapping TRP120-TR synthetic peptides that span the identified 35-aa TRP120-TR IDD motif were synthesized (Fig. 10A). Treatment with P4 or P5 TRP120-TR Notch mimetic SLiM peptides in THP-1 cells did not result in NICD nuclear translocation (Fig. 1B); however, TRP120-TR Notch mimetic SLiM P6 (TRP120-N1-P6) located at the C-terminus resulted in NICD nuclear translocation (Fig. 10B). TRP120-N1-P6 was also shown to cause NICD nuclear translocation in primary human monocytes (Fig. 10C). Furthermore, pre-treatment of DAPT inhibited TRP120-N1-P6 Notch activation (Fig. 10B). Upregulation of Notch downstream targets occurred with TRP120-N1-P6 treatment in a concentration dependent manner (Figs. 11A-B, Table S1B), as previously shown with the TRP120-N1-P3 peptide. In comparison, TRP120-N1-P5 peptide treatment, did not result in significant upregulation of Notch gene expression (Fig. 11B). To confirm that TRP120-N1-P6 is required for Notch activation, a TRP120-N1-P6 deletion mutant peptide (TRP120-N1- $\Delta$ P6) (Fig. 12A) was tested. THP-1 cells stimulated with TRP120-N1- $\Delta$ P6 peptide exhibited abrogated Notch activation as demonstrated by NICD translocation (Fig. 12B). To determine the residues required in the TRP120-TR Notch mimetic SLiM, alanine mutagenesis of mutant peptides dmut-2, -3 and -4 was performed to determine the contribution of specific amino acids to Notch activation (Fig. 12A, blue boxes). Mutated residues were selected based on sequence homology and ISM data. Mutants (TRP120-N1- $\Delta$ P6, dmut-2, -3 and -4) exhibited reduced Notch activation as determined by NICD translocation, but only the TRP120-N1- $\Delta$ P6 peptide resulted in full abrogation of NICD nuclear translocation (Fig. 12A). Collectively, these data demonstrate that the TRP120-N1-P6 SLiM is a Notch mimetic.

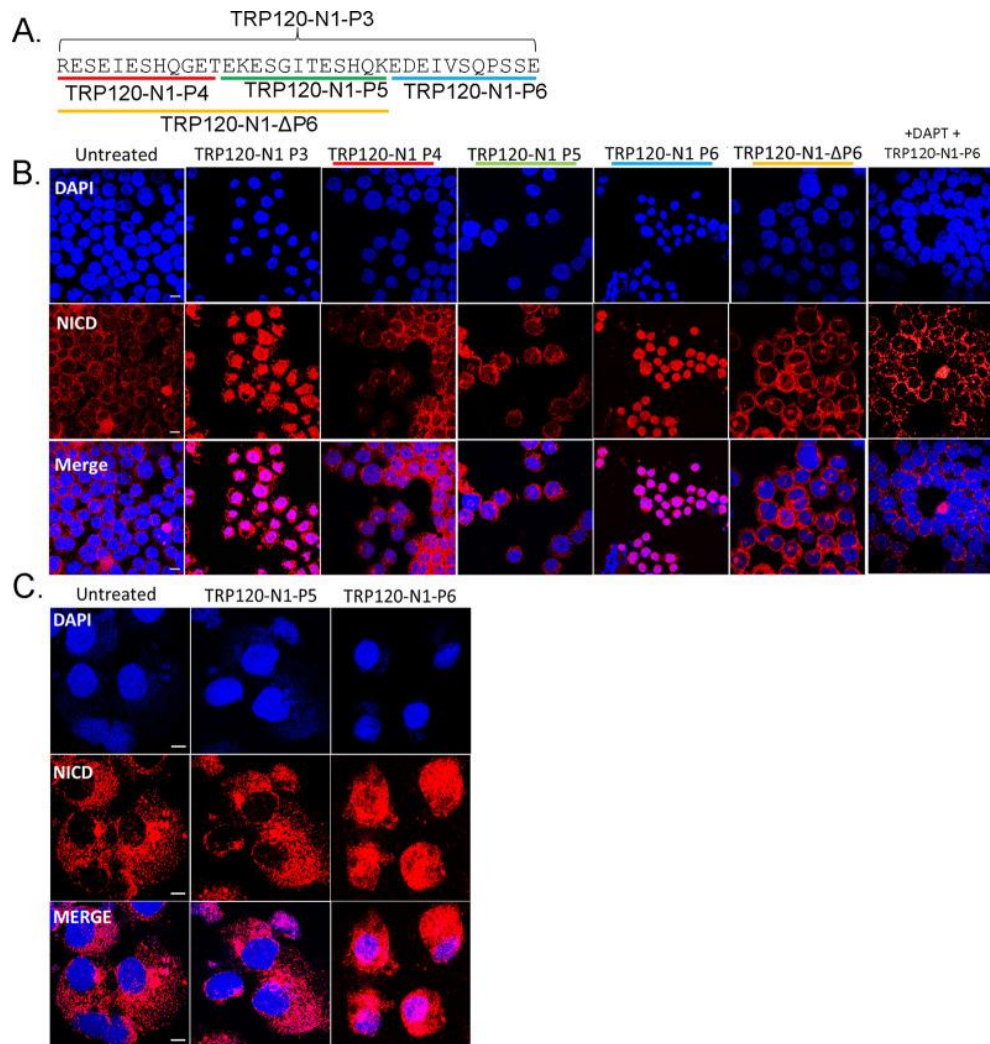


**Figure 10. A TRP120-TR Notch-1 memetic SLiM peptide activates Notch signaling.**

(A) TRP120-N1 SLiM (P4-P6) and TRP120-N1-ΔP6 peptide sequences. (B) THP-1 cells or (C) primary human monocytes were treated with synthetic TRP120-TR SLiM peptides to identify the TRP120-TR Notch-1 SLiM memetic motif. TRP120-TR peptides were SLiM peptides spanning the entire TRP120-N1-P3 peptide sequence. TRP120-N1-P6 deletion mutant peptide has a deletion of the TRP120-N1-P6 amino acids. Cells were treated with peptide (1 μg/mL) for 2 h and NICD localization visualized by confocal microscopy. TRP120-N1-P3 peptide was used as a positive control. To determine if direct interaction of the TRP120-N1-P6 peptide and Notch receptor was necessary for Notch activation, THP-1 cells were pretreated with DAPT, a γ-secretase inhibitor, and treated with TRP120-N1-P6 peptide for 2 h. Representative data of all experiments are shown ( $n=3$ ).

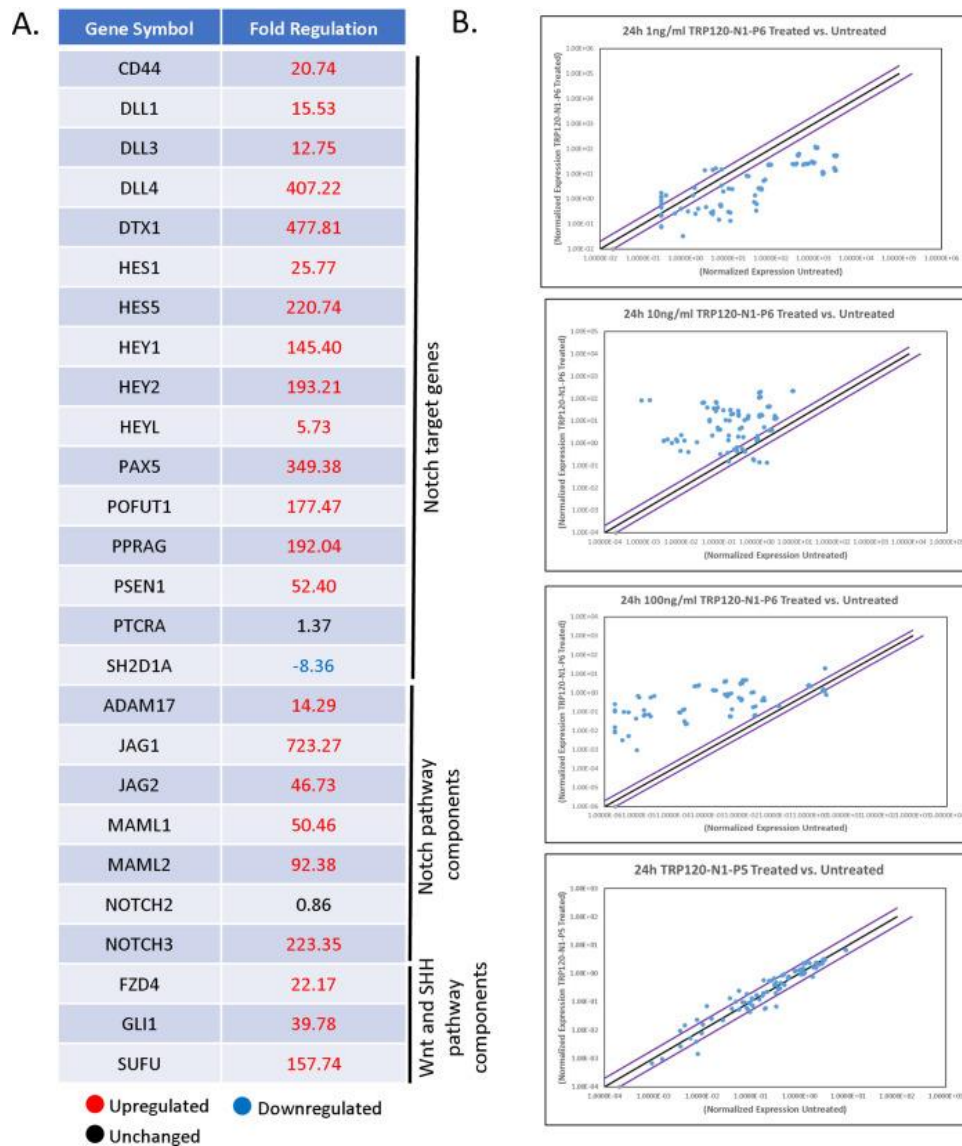


**Figure. 11 TRP120-N1-P6 SLiM Notch memetic peptide stimulates Notch gene expression.**

(A) Selected Notch pathway genes with corresponding fold change displaying differential expression (upregulation and downregulation) at 24 h pt with 10 ng/mL of TRP120-N1-P6 peptide. (B) Scatterplots of expression array analysis of 84 Notch signaling pathway genes to determine Notch gene expression with 1 ng/mL, 10 ng/mL, 100 ng/mL of TRP120-N1-P6 peptide or TRP120-N1-P5 treatment (10 ng/mL) compared to untreated cells (bottom) at 24 pt. Purple lines denote a 2-fold upregulation or downregulation in comparison to control, and the black lines denote no change. Scatterplots are representative of three independent experiments ( $n = 3$ ).

**TRP120 Notch SLiM antibody blocks *E. chaffeensis* Notch activation.** To investigate whether the TRP120 Notch mimetic is solely responsible for Notch activation by *E. chaffeensis*,

THP-1 cells were pre-treated with a purified rabbit polyclonal antibody generated against the TRP120-N1-P6 SLiM and subsequently infected with *E. chaffeensis* for 2 h. Negative pre immune serum was used as a negative control. NICD nuclear translocation was determined in  $\alpha$ -TRP120-N1-P6 SLiM or negative pre-immune serum treated cells. THP-1 cells treated with  $\alpha$ -TRP120-N1-P6 SLiM did not display NICD nuclear translocation, in comparison to the negative pre-immune serum control (Fig. 10B). These data suggests that TRP120-N1-P6 SLiM is the only Notch mimic involved in Notch activation by *E. chaffeensis*.

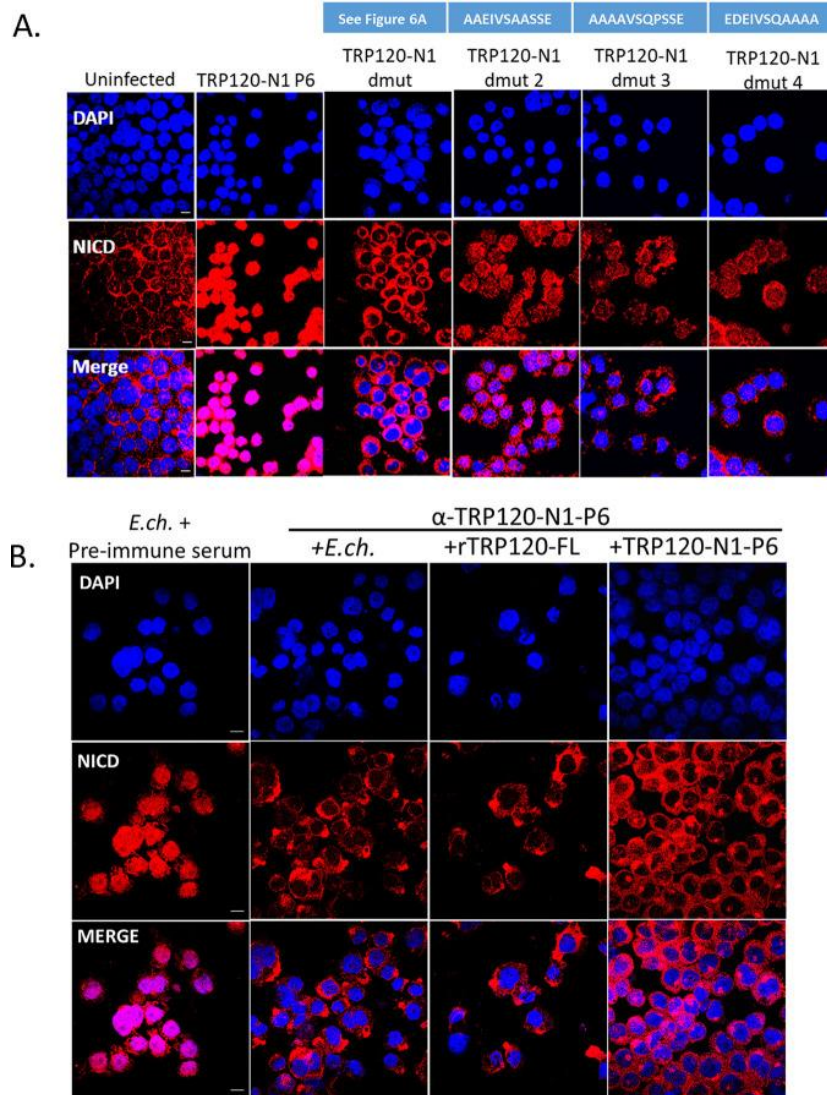


**Figure 12. Amino acids critical to TRP120-N1-P6 memetic SLiM activity and anti-SLiM antibody blocks Notch activation.**

(A) Critical amino acids of the TRP120-N1-P6 memetic SLiM determined by alanine mutagenesis (mutant peptide sequences are shown above the corresponding panel). THP-1 cells were treated with mutant peptides (dmut2, -3, and -4; 1 µg/mL) for 2 h and confocal immunofluorescent microscopy was used to visualize NICD localization. NICD nuclear translocation denotes Notch activation. Peptide TRP120-N1-ΔP6 peptide was used as a negative-control and TRP120-N1-P6 was used as a positive control. (B) Cell-free *E. chaffeensis*, rTRP120-FL, or TRP120-N1-P6 were incubated with α-TRP120-N1-P6 rabbit polyclonal antibody (5 µg/mL) for 30 min. Preimmune serum was used as a control antibody. THP-1 cells were subsequently inoculated with the cell-free *E. chaffeensis*/α-TRP120-N1-P6 mixture for 2 h and confocal immunofluorescent microscopy was used to visualize NICD nuclear localization. Representative data of all experiments are shown ( $n = 3$ ).

## Discussion

We have previously demonstrated TRP120-host interactions to occur with a diverse array of host cell proteins associated with conserved signaling pathways, including Wnt and Notch [60]. Two proteins shown to interact with TRP120 were the Notch metalloprotease, a disintegrin and metalloprotease domain (ADAM17), and a Notch antagonist, F-box and WD repeat domain-containing 7 (FBW7). In addition, we have demonstrated that *E. chaffeensis* and rTRP120 activates Notch signaling to downregulate TLR2/4 expression for intracellular survival; however, the molecular mechanisms utilized for TRP120 Notch activation have not been previously studied [94]. Moreover, Keewan et al, demonstrated activation of Notch signaling during *Mycobacterium avium paratuberculosis* (MAP) infection. Notch-1 signaling was shown to modulate macrophage polarization and immune defenses against during infection, but the molecular mechanisms were not defined [210]. In this study, we investigated the molecular interactions involved in TRP120 Notch activation and have defined a TRP120 Notch SLiM mimetic responsible for Notch activation.

Molecular mimicry has been well-established as an evolutionary survival strategy utilized by pathogens to disrupt or co-opt host function as a protective mechanism to avoid elimination by the host immune system [39, 220-222]. More specifically, SLiMs are a distinct, intrinsically

disordered class of protein interaction motifs that have been shown to evolve de novo for promiscuous binding to various partners and have been documented as a host hijacking mechanism for pathogens [39, 40, 71, 75]. Although SLiM mimicry has been established as a mechanism utilized by pathogens to repurpose host cell functions for survival, a Notch ligand mimic has never been defined.

TRP120 is a type 1 secretion system (T1SS) effector that is found on the surface of infectious dense-cored *E. chaffeensis* and is also secreted into the host cell after entry where it translocates to the host cell nucleus. TRP120 contains four intrinsically disordered tandem repeat (TR) domains that have been previously described as important for TRP120's moonlighting capabilities [50, 66]. Within these intrinsically disordered domains are various SLiMs responsible for TRP120 multi-functionality. We have recently defined a novel TRP120 repetitive SLiM that activates Wnt signaling to promote *E. chaffeensis* infection [79]. In the current study, we have also determined TRP120-TR as the domain also responsible for Notch activation. Sequence homology studies and Information Spectrum Method (ISM) have shown sequence similarity and similar biological function between TRP120 and endogenous Notch ligands. ISM is a virtual spectroscopy method utilized to predict if proteins share a similar biological function based on the electron-ion interaction potential of amino acids, and only requires the nucleotide sequence of each protein. It was recently used to determine prediction of potential receptor, natural reservoir, tropism and therapeutic/vaccine target of SARS-CoV-2 [223]. Our results demonstrate a shared sequence similarity and biological function with both canonical and non-canonical Notch ligands that occurs within the tandem repeat domain of TRP120 (TRP120-TR). Both sequence homology and ISM studies identified specific tandem repeat sequences that are functionally associated with endogenous Notch ligands and range between 20-35 amino acids in size. This data suggested that intrinsically disordered regions found within the TRP120-TR domain are responsible for Notch ligand mimic function and direct effector-host protein interaction with the Notch receptor.

Notch ligand binding occurs specifically with EGFs 11-13 within the LBR of the Notch receptor [224]. Canonical Notch ligands are known to contain a DSL domain that is important for Notch binding and activation, but a conserved activation motif has not been defined. Colocalization of TRP120 with Notch-1 was previously shown to occur during *E. chaffeensis* infection [94]; however, a direct interaction was not previously shown using yeast-two hybrid [60], possibly due to limitations of this technique with protein interactions involving membrane proteins [225]. Using pull down, SPR and protein-coated fluorescent microsphere approaches, we further studied TRP120-Notch-1 interaction and found direct binding occurs through TRP120-TR at a Notch-1 LBR (EGFs 1-15). TRP120-TR and Notch-1 LBR interaction occurred at an affinity of  $120 \pm 2.0$  nM, indicating a strong protein-protein interaction. Numerous structural studies of interactions of Notch with endogenous ligands have shown low affinity interactions between Notch Jag or DLL ECDs [128, 165, 166, 224]. One study demonstrated weak affinities between Notch-1 with an engineered high affinity Jag-1 variant ( $K_D = 5.4$   $\mu$ M) and DLL4 (12.8  $\mu$ M) [224]. The higher binding affinity of TRP120-TR in comparison to canonical Notch ligands suggests that the four tandemly repeated motifs folds in a structure that potentiates binding between TRP120 and Notch-1. In addition, stimulating THP-1 cells and primary monocytes with TRP120-TR resulted in NICD nuclear translocation, indicating that TRP120-TR is the TRP120 domain responsible for Notch activation. Interestingly, TRP120-Fzd5 interaction also occurred through the tandem repeat domain and supports our current findings that TRP120-host protein interactions occur within regions of the tandem repeat domain, likely due to its disordered nature [79].

Secreted and membrane-bound proteins have been shown to activate Notch signaling. These non-canonical Notch ligands lack the DSL domain but still have the ability to modify Notch signaling. Some of the non-canonical Notch proteins contain EGF-like domains; however, others share very little sequence similarity to endogenous Notch ligands [119, 175]. TSP2 is a secreted mammalian protein containing EGF-like domains. TSP2 was found to potentiate Notch signaling by direct Notch-3/Jagged1 binding [175]. Furthermore, TSP2 binds directly to purified

Notch-3 protein containing EGF-like domains 1–11, suggesting a direct interaction. Noncanonical Notch ligand TSP2 was found to share significant sequence homology within the TRP120-TR sequence. Homologous regions included the identified TRP120-TR Notch SLiM mimetic. Although TSP2 has been identified as a secreted, non-canonical Notch ligand, there has been no activating motif identified to date. F3/contactin1, another identified secreted noncanonical Notch ligand, does not contain DSL or EGF-like domains; however, it activates the Notch signaling pathway through the Notch-1 receptor [168]. TRP120 was found to share biological function with F3/contactin1 by ISM. F3/contactin1 has been demonstrated to bind to Notch-1 at two different locations within the NECD and activates Notch signaling when presented as purified soluble protein [168]. Therefore, Notch activation by secreted, noncanonical Notch ligands has been demonstrated; however, more insight into the molecular details of those interactions needs to be elucidated. TRP120 is found on the surface of infectious dense-cored ehrlichiae [59] and contributes to internalization of *E. chaffeensis* by activation of the Wnt pathway [85]. Thus, during infection, TRP120 likely activates Notch signaling as a surface bound protein when *E. chaffeensis* encounters the host cell as was demonstrated with whole *E. chaffeensis*. In addition, we also demonstrated that soluble TRP120 and peptide can activate Notch signaling. This is a significant finding that could have implications with regard systemic effects of TRP120 that may be released during infection. Moreover, these finding provide new information regarding activation of Notch signaling by soluble ligands, which were previously thought to require cell to cell interactions. This study provides new insight regarding non-canonical Notch ligand activation of the Notch signaling pathway.

SLiMs have been identified in secreted effector proteins of intracellular bacterial pathogens, including *Ehrlichia*, *Anaplasma phagocytophilum* [76], *Legionella pneumophila* [226-229] and *Mycobacterium tuberculosis* [230]. This investigation identifies a novel Notch SLiM (11 aa) that can activate Notch signaling as a soluble ligand. Complete NICD nuclear translocation was previously shown to occur at 2 h post-infection [94], indicating that NICD nuclear

translocation during *E. chaffeensis* infection is a result of TRP120-TR Notch ligand SLiM mimetic interaction with the Notch-1 receptor. In addition, Notch signaling pathway genes were upregulated at 24 h in TRP120-TR Notch mimetic SLiM-treated THP-1 cells. These data are consistent with our previous findings where we detected upregulation of Notch signaling pathway components and target genes during *E. chaffeensis* infection at 12, 24, 48, and 72 h.p.i., with maximum changes in Notch gene expression occurring at 24 h.p.i [94]. Furthermore, during *E. chaffeensis* infection, TRP120 mediated ubiquitination and proteasomal degradation of Notch negative regulator, FBW7 begins at 24 h.p.i. and gradually decreases during late stages of infection [64]. Both TRP120 and FBW7 are localized to the nucleus beginning at 24 h.p.i., suggesting that TRP120-degradation of FBW7 assists in upregulation of Notch downstream targets at this timepoint [64].

Interestingly, both the TRP120 Notch mimetic IDD (TRP120-N1-P3) and SLiM (TRP120-N1-P6) resulted in concentration-dependent upregulation of Notch downstream targets. Similar to our findings, studies have shown that the Notch pathway can induce heterogeneous phenotypic responses in a Notch ligand or NICD dose dependent manner. Klein et al. demonstrated that high levels of Notch ligands can induce a ligand inhibitory effect, while lower levels of Notch ligand activate Notch signaling activity [122]. Similarly, Semenova D et al. has shown that NICD and Jag1 transduction increases osteogenic differentiation in a dose-dependent manner; however high dosage of NICD and Jag1 decreases osteogenic differentiation efficiency [231]. Furthermore, Gomez-Lamarca et al. has shown that NICD dosage can influence CSL-DNA binding kinetics, NICD dimerization, and chromatin opening to strengthen transcriptional activation [122]. Therefore, an increase in Notch ligand-receptor interaction may lead to increased NICD release and Notch signaling strength.

Alanine mutagenesis demonstrated the entire 11-aa TRP120-TR Notch ligand SLiM mimetic is required for Notch activation. Importantly, SLiMs are known to have low-affinity, transient protein-protein interactions within the low-micromolar range [71]. In this case, the repeated TRP120-TR Notch ligand SLiM mimetic motif may cause TRP120 to fold in a tertiary

structure upon binding to the Notch-1 receptor that stabilizes the TRP120-Notch-1 interaction. Based on this data, *E. chaffeensis* TRP120 could be used as a model to study SLiMs within intrinsically disordered effector proteins that are utilized for host exploitation by other intracellular bacterial pathogens.

To demonstrate that TRP120-TR Notch ligand SLiM mimetic motif is solely responsible for *E. chaffeensis* activation of Notch, we generated an antibody against the mimetic epitope to block *E. chaffeensis* TRP120-Notch-1 binding. Our results demonstrated antibody blockade of Notch activation by *E. chaffeensis*, rTRP120 and the TRP120-TR Notch ligand SLiM peptide. This data strongly supports the conclusion that the TRP120-TR Notch ligand SLiM mimetic is responsible for *E. chaffeensis* Notch activation and may provide a new *E. chaffeensis* therapeutic target. Hence, this study serves to provide insight into the molecular details of how Notch signaling is modulated during *E. chaffeensis* infection and may serve as a model for other pathogens.

Further outstanding questions regarding regulation of the Notch signaling pathway during *E. chaffeensis* remain. We have recently demonstrated maintenance of Notch activation is linked to TRP120-mediated ubiquitination and proteasomal degradation of tumor suppressor FBW7, a Notch negative regulator [64]. However, other potential Notch regulators may serve as a target for TRP120-mediated ubiquitination for constitutive Notch activation during infection. Suppressor of Deltex [Su(dx)] is an E3 ubiquitin ligase that serves as another negative regulator of Notch signaling by degrading Deltex, a positive regulator of Notch signaling [138]. Su(dx) may serve as another target of TRP120-mediated ubiquitination to maintain Notch activity during *E. chaffeensis* infection. Furthermore, how secreted non-canonical Notch ligands are able to cause separation between the NICD and NECD remains unknown. TRP120 causes Notch activation, resulting in upregulation of Notch downstream targets; however, the mechanism of how the S2 exposure for ADAM cleavage is not understood. Future crystallography studies on TRP120 and Notch-1 interaction may provide more insight into these structural details required for TRP120-N1-P6 SLiM Notch activation [128, 232].

In conclusion, we have demonstrated *E. chaffeensis* Notch activation is initiated by a TRP120 Notch SLiM mimetic. Our findings have identified a pathogen protein host mimic to repurpose the evolutionarily conserved Notch signaling pathway for intracellular survival (Fig. 13). This study gives more insight into how obligate intracellular pathogens, with small genomes have evolved host mimicry modules de novo to exploit conserved signaling pathways to suppress innate defenses to promote infection.

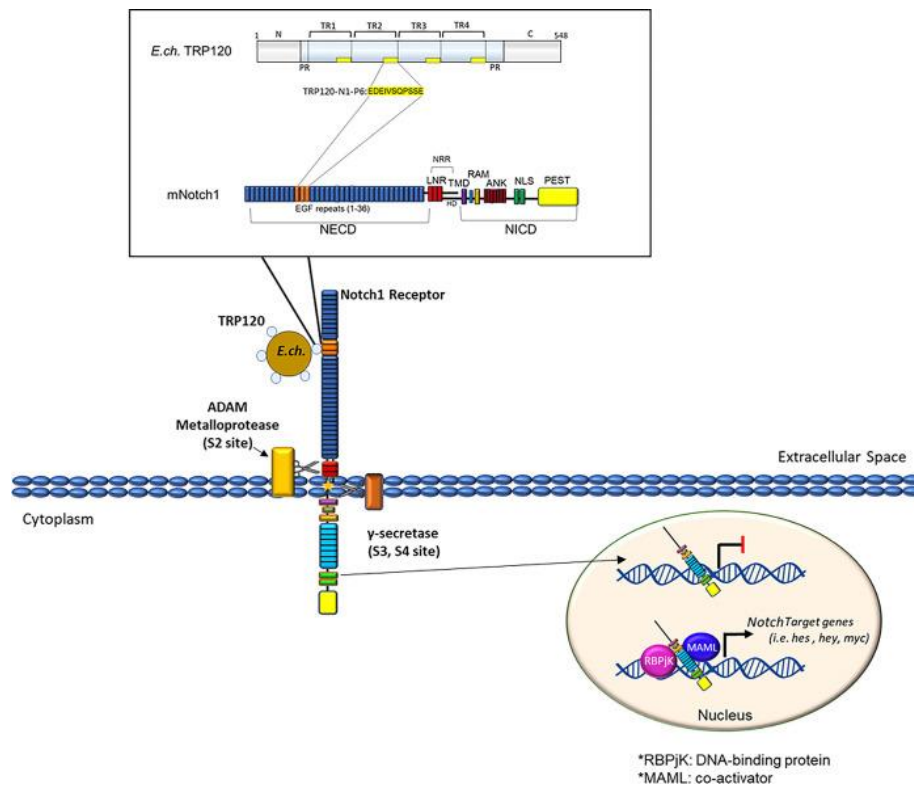


**Figure 13. Proposed model of *E. chaffeensis* TRP120 Notch activation.**

A TRP120-TR Notch SLiM mimetic motif (TRP120-N1-P6; yellow highlight) binds the Notch-1 extracellular domain at a region containing the confirmed Notch ligand-binding domain (LBD) to activate Notch signaling. TRP120-N1-P6 binding leads to NICD nuclear translocation and upregulation of Notch gene targets. Image created by L. Patterson using Microsoft Powerpoint.

## CHAPTER 4. *EHRlichia* NOTCH SIGNALING INDUCTION PROMOTES XIAP STABILITY AND INHIBITS

### APOPTOSIS

#### Introduction

*Ehrlichia chaffeensis* is an obligately intracellular Gram-negative bacterium, and the etiologic agent of human monocytotropic ehrlichiosis (HME), a life-threatening emerging tick-borne zoonosis [17]. *E. chaffeensis* preferentially infects mononuclear phagocytes and has evolved sophisticated molecular-based strategies to evade host defense mechanisms for survival [50, 51, 56, 60, 61, 64-66, 68, 69, 79-81, 84, 85, 94, 233]. *E. chaffeensis* immune evasion strategies are mediated, in part, by tandem repeat proteins (TRPs). TRPs are type 1 secretion system (T1SS) effectors that also elicit strong host antibody responses during infection [234-237]. Notably, TRP120 decorates the surface of dense-cored ehrlichiae and has multiple moonlighting functions including as a transcription factor, HECT E3 ubiquitin ligase, and cellular signaling ligand mimetic to repurpose host cell signaling [59, 60, 64, 65, 68, 79-81]. These TRP120 functions directly impact host gene expression and chromatin epigenetics, pathogen-host interactions, and cellular signaling [60, 63, 66, 68, 69, 79-81, 84, 85, 94, 190].

Two apoptosis pathways, extrinsic and intrinsic, have been defined and are well characterized. The extrinsic pathway is activated through a death ligand receptor resulting in the activation of Caspase-8 and induction of the execution pathway leading to apoptosis [182-184]. By comparison, the intrinsic pathway is initiated by various non-receptor mediated stimuli that result in mitochondrial changes, specifically mitochondrial permeability transition (MPT). MPT results in cytochrome c release, triggering formation of a complex known as an apoptosome and subsequent Caspase-9 activation resulting in apoptosis [187, 238]. Execution of apoptosis occurs when Caspase-8 and/or -9 cleave inactivated executioner Caspase-3/7 into their active forms, leading to the cleavage of various downstream targets important for cell survival [187,

239, 240]. Modulation of several proteins that control and regulate apoptotic mitochondrial events (intrinsic apoptosis) occur during *E. chaffeensis* infection including Bcl-2 and BirC3, and others have demonstrated downregulation of apoptotic inducers, such as Bik, BNIP3L, and hematopoietic cell kinase (HCK) [180]. The *E. chaffeensis* type 4 secretion system (T4SS) effector, ECH0825, is also known to suppress apoptosis by inhibiting Bax-induced apoptosis by increasing mitochondrial manganese superoxide dismutase (MnSOD) to reduce reactive oxygen species-mediated damage [190]. Although the manipulation of intrinsic apoptosis as a survival mechanism for *E. chaffeensis* has been previously reported, there remain significant unanswered questions about the mechanisms involved.

We have recently reported that *E. chaffeensis* evasion of macrophage host defenses involve activation of conserved host signaling pathways, including Wnt, Notch and Hedgehog [79-81]. Notably, TRP120 has been demonstrated to activate the evolutionarily conserved Notch signaling pathway using a novel molecularly defined pathogen encoded Notch SLiM ligand mimetic found within the tandem repeat (TR) domain [81]. Notch signaling plays significant roles in cellular homeostasis, MHC Class II expansion, B- and T- cell development, and by modulating innate immune mechanisms such as autophagy and apoptosis [105, 110, 211, 217, 241, 242]. Recently, we have shown that *E. chaffeensis* TRP120-induced Notch signaling results in downregulation of TLR2/4 expression [94]. Moreover, we have also shown that TRP120 degrades the Notch negative regulator, FBW7, resulting in increased levels of several oncoproteins, including the Notch intracellular domain (NICD), which regulates cell survival and apoptosis [64]. Therefore, *E. chaffeensis* induced Notch signaling and increased levels of NICD during *E. chaffeensis* infection may play an important role in inhibiting apoptosis.

Caspases are the enzymes primarily responsible for mediating apoptosis [184, 187, 243], and apoptosis can be blocked by inhibiting caspase activity. The X-linked inhibitor of apoptosis protein (XIAP) is the most potent inhibitor of apoptosis (IAP) [198, 244]. XIAP directly

binds and inhibits initiator and executioner caspases, including Caspases-9 and -3, respectively [194, 199, 203, 244, 245]. Interestingly, Lui, et al demonstrated that NICD suppresses host cell apoptosis by increasing XIAP stability [204]. Interaction between the Notch intracellular domain (NICD) and XIAP prevents ubiquitination and degradation of XIAP, thereby inhibiting apoptosis. Moreover, Caspases -3 and -8 are known to cleave XIAP into two fragments (BIR1-2 and BIR3-RING), leading to differential inhibition of extrinsic and intrinsic apoptotic pathways [196]. BIR3-RING fragments are potent inhibitors of Caspase-9, resulting in inhibition of Bax-mediated (intrinsic) apoptosis. Therefore, Notch activation and FBW7 degradation during *E. chaffeensis* infection may stabilize XIAP as a mechanism to inhibit intrinsic, caspase-dependent apoptosis.

In this study, we reveal a novel mechanism whereby *E. chaffeensis* inhibits intrinsic apoptosis through Notch activation and NICD stabilization of XIAP. Inhibition of apoptosis through modulation of Notch signaling provides further evidence that *E. chaffeensis* hijacks evolutionarily conserved signaling pathways primarily to evade innate host defense mechanisms.

## Results

***E. chaffeensis* infection and TRP120 increases XIAP levels.** We recently demonstrated that NICD levels temporally increase during *E. chaffeensis* infection [64]. Increased levels of NICD were associated with TRP120 ubiquitination and degradation of a Notch negative regulator, FBW7. NICD is known to directly bind to the XIAP BIR-RING domain prevent XIAP autoubiquitination and degradation [204], thereby inhibiting apoptosis. To investigate if XIAP was upregulated during infection, THP-1 cells were incubated with *E. chaffeensis* (MOI 50), and XIAP protein and gene expression levels were analyzed by immunoblot and qPCR. Uninfected THP-1 cells had no change in XIAP expression levels (Fig. 14A). In comparison, increases in both NICD and XIAP protein levels were demonstrated over the course of infection, with

significant increases detected at 24, 48 and 72 hpi (Fig. 14A). Interestingly, additional cleaved fragment was observed at 48 and 72 hpi that was identified as the BIR3-RING domain of XIAP (Fig. 14A). When cleaved, BIR3-RING also acts as a potent inhibitor of the intrinsic apoptotic pathway by binding the Caspase-9 monomer preventing its cleavage and heterodimerization. Moreover, transcriptional levels of XIAP were also shown to be significantly upregulated in a temporal manner (Fig. 12B). XIAP expression was determined in THP-1 cells treated with recombinant TRP120 tandem repeat domain (rTRP120-TR), or the recently described TRP120 Notch ligand memetic SLiM (TRP120-TR-P6) peptide. Significant temporal increase in XIAP levels were detected in cells treated with rTRP120-TR (Fig. 14C) or TRP120-TR-P6 peptide (Fig. 14D), demonstrating *E. chaffeensis* TRP120 promotes increased XIAP levels.

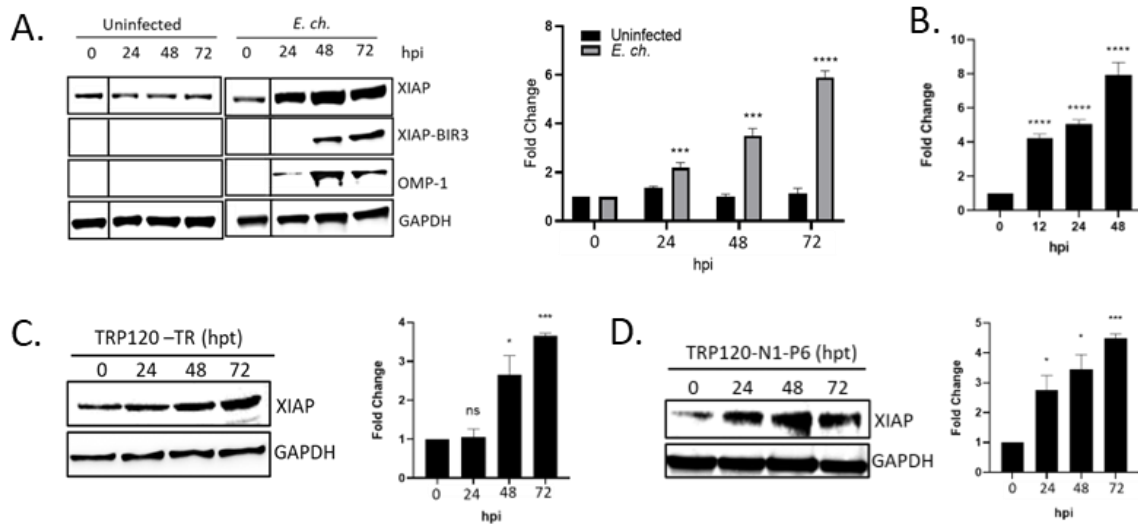


**Figure 14: XIAP is increased during *E. chaffeensis* infection.**

(A) Immunoblot of XIAP, cleaved XIAP-Bir3 and OMP-1 expression in uninfected and *E. ch.* infected THP-1 cells at 0-72 hpi (MOI 50). Outer Membrane Protein 1 (OMP-1) is a major immunodominant protein of *E. ch.* Infection used to confirm the presence of infection. GAPDH was utilized as a loading control. Fold differences in XIAP protein levels in *E. ch.* infected and uninfected THP-1 cells. (B) Changes in XIAP transcript levels in *E. ch.* infected and uninfected THP-1 cells (0 hpi), as measured by RT-qPCR analysis. (C) Immunoblot and quantification of XIAP in TRP120-TR treated THP-1 cells. (D) Immunoblot and quantification of XIAP in TRP120-N1-P6 memetic peptide treated THP-1 cells. Bar graphs represent means  $\pm$  SD. \*\*\*\*,  $P < 0.0001$ . Experiments were performed in triplicate ( $n=3$ ) and representative images are shown.

**NICD interacts with XIAP during infection.** To determine if NICD was directly binding XIAP, confocal microscopy was performed to visualize XIAP/NICD colocalization. Interestingly, strong NICD and XIAP colocalization according to Mander's coefficient (MC) was observed in *E. chaffeensis*-infected cells at 24 (MC = 0.9), 48 (MC = 0.9) and 72 (MC = 0.8) hpi (Fig. 15A). XIAP levels were also temporally increased at 24, 48 and 72 hpi based on mean fluorescence intensity (Fig. 15B). By immunoblot, significant temporal increases in XIAP and NICD were detected (Fig. 15C). Co-immunoprecipitation of XIAP and NICD from uninfected and *E. chaffeensis*-infected lysates (24 hpi) demonstrated direct interaction and increased XIAP and NICD levels (Fig. 15D).

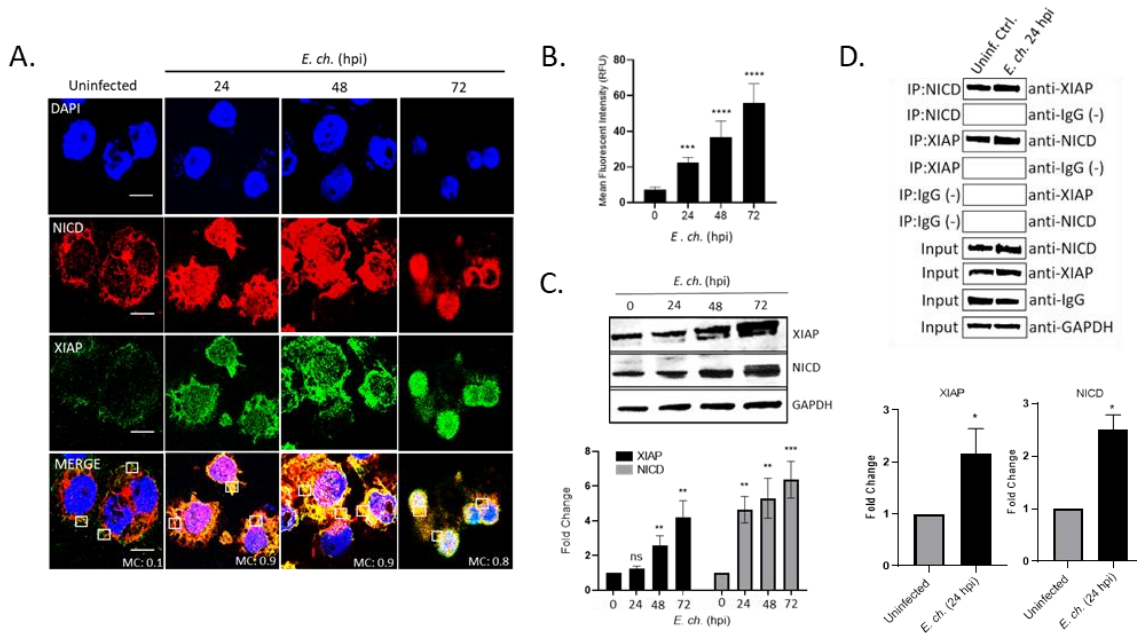


**Figure 15: NICD interaction of XIAP during *E. chaffeensis* infection.**

(A) Uninfected or *E.ch.-infected* THP-1 cells at 24, 48 and 72 hpi (MOI 50) probed for endogenous NICD (red) or endogenous XIAP (green) demonstrate colocalization by immunofluorescent confocal microscopy (Scale bar = 10  $\mu$ m). Colocalization was quantitated by Mander's coefficient (0 no colocalization; +1 strong colocalization). Mean fluorescence intensity of the XIAP protein expression in 20 THP-1 cells. Mean pixel values were obtained using the ImageJ Measure Analysis tool. Background intensity was determined and subtracted from the fluorescence intensity value of the cells. The mean value from each group was an average of 20 cells. (C) Immunoblot and fold differences of XIAP or NICD in *E.ch.-infected* THP-1 cells at 0-72 hpi (MOI 50). GAPDH was utilized as a loading control. (D) Co-IP and reverse Co-IP demonstrate the direct interaction between XIAP and NICD at 24 hpi compared to the IgG negative control. Western blot analysis was normalized to GAPDH expression. Quantification of NICD or XIAP levels from one

representative CO-IP experiment are shown. Experiments were performed in triplicate (n=3) and representative images are shown.

**Notch activation and XIAP stabilization by NICD.** To confirm that the increase in XIAP levels was a direct result of Notch activation, THP-1 cells were pre-treated with DAPT, a Notch  $\gamma$ -secretase inhibitor. Cells pre-treated with DAPT inhibitor and infected with *E. chaffeensis* (MOI 50) exhibited decreased XIAP levels 24 and 48 hpi (Fig. 16A). To further determine the direct relationship between NICD and XIAP levels during *E. chaffeensis* infection, uninfected and *E. chaffeensis*-infected THP-1 cells were treated at 1 hpi with DAPT and SM-164, a Smac/DIABLO mimetic compound that antagonizes inhibitor of apoptosis proteins (IAPs) that promotes activation of caspases and apoptosis [203]. Cell death was induced by TNF- $\alpha$ , followed by subsequent infection with *E. chaffeensis* (MOI 50). H&E staining of THP-1 cells treated with DAPT/SM-164 did not contain morulae, displayed significant cell death, and had significantly decreased ehrlichial load compared to uninfected, *E. chaffeensis*-infected, DMSO alone, or with DAPT or SM-164 alone treated cells (Figs. 16B and C).

To further confirm Notch signaling promotes cell survival and ehrlichial infection, Caspase-3/ CPP32 activity was determined by measuring the absorbance of DEVD-pNA, a Caspase-3 substrate [246]. An approximately 2-fold increase in Caspase 3/ CPP32 levels were detected in THP-1 cells treated with both DAPT and SM-164 compared to uninfected, DMSO treated, or *E. chaffeensis* infected treated with either DAPT or SM-164 (Fig 16D). Significant upregulation of Caspase-3/ CPP32 activity was also demonstrated in the SM-164 treated compared to untreated cells; however, DAPT/SM-164 combination treatment demonstrated significantly higher Caspase-3/ CPP32 levels (Fig 16D). Collectively, these data suggest that XIAP is stabilized by NICD during *E. chaffeensis* infection.

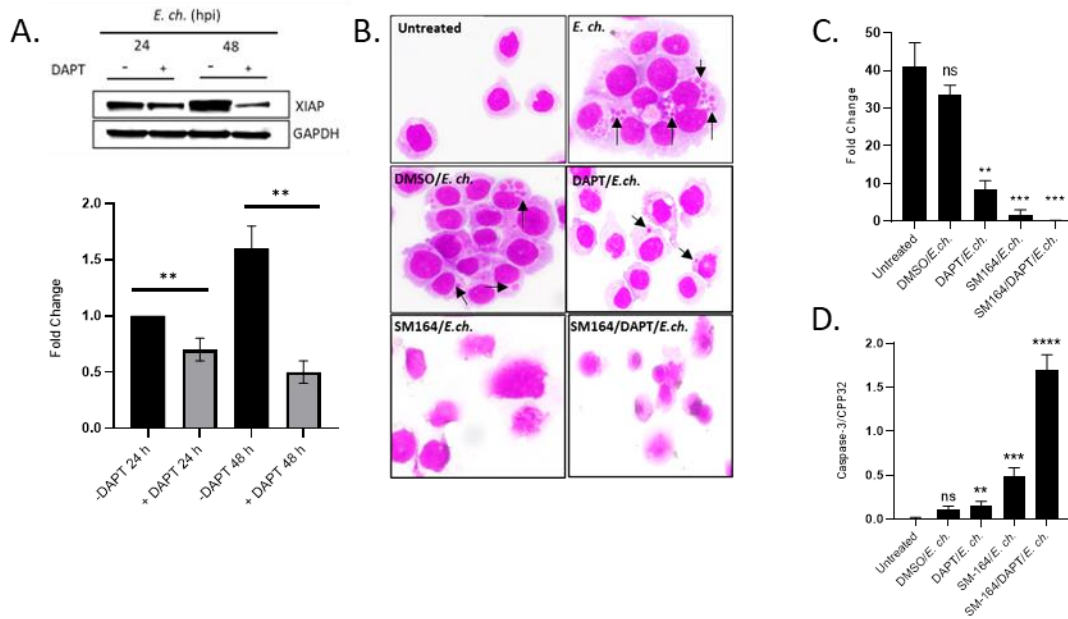


**Figure 16: Notch activation stabilizes XIAP during *E. chaffeensis* Infection.**

(A) Immunoblot and fold differences of XIAP expression in *E. ch.*-infected THP-1 cells with or without DAPT pre-treatment at 24 or 48 hpi. (B) H&E stained uninfected or *E.ch.*-infected THP-1 cells untreated or pre-treated with DMSO or SM164 (12h) alone or in combination with DAPT (1h). Cell death was stimulated by TNF- $\alpha$  prior to the addition of *E.ch.* (MOI 50). Black arrows identify *E.ch.* Inclusions (morulae). (C) Fold change difference of dsb transcript levels in cell samples previously mentioned in Fig. 3C description. (D) Quantification of Caspase-3/ CPP32 activity read at an absorbance of 405 nm. Bar graphs represent means  $\pm$  SD. \*\*\*\*,  $P < 0.0001$ ; ns = no significance. Experiments were performed in triplicate ( $n=3$ ) and representative images are shown.

**NICD stabilization of XIAP results in antiapoptotic activity and increased infection.** The effect of XIAP on *E. chaffeensis* infection was examined using siRNA knockdown (KD) of XIAP in THP-1 cells. siRNA KD of XIAP resulted in a 77% KD efficiency (Fig. 17A). *E. chaffeensis* infection was significantly decreased 24 hpi in XIAP-KD cells compared to scrambled control siRNA-treated cells (Figs. 17B and C). To determine if the decrease in ehrlichial load was caused by the induction of apoptosis due to XIAP destabilization, cell viability was determined by flow cytometry with the Muse Count & Viability Kit. XIAP-KD cells exhibited a viability of ~8% compared to 81% in scr-KD cells (Fig. 17D). Furthermore, XIAP-KD cells displayed

morphological changes associated with apoptosis including shrinkage of the cell, fragmentation into membrane-bound apoptotic bodies and nuclear fragmentation (Fig. 17D).

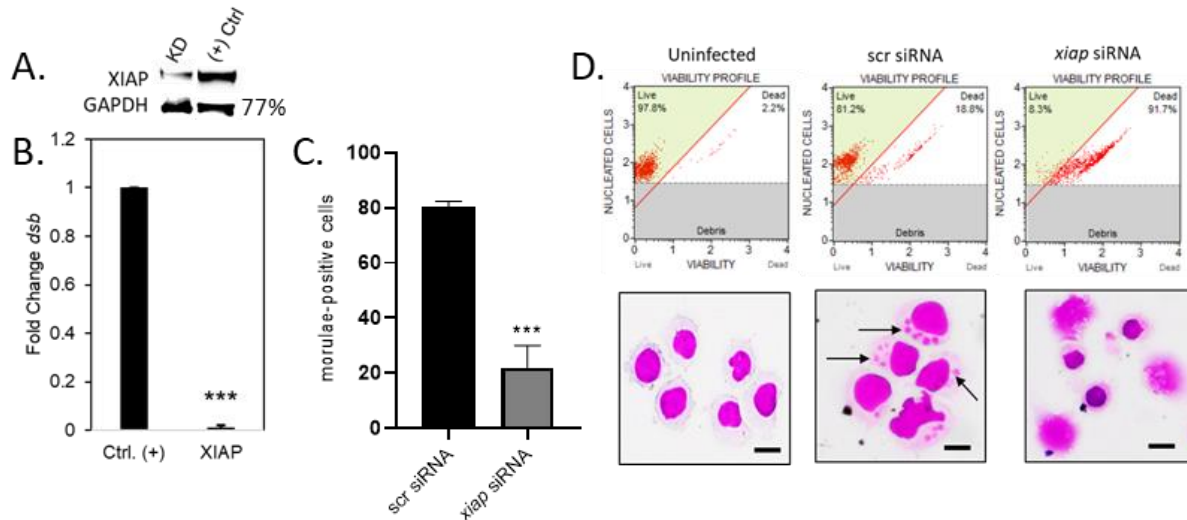


**Figure 17: XIAP enhances cell viability to promote *E. chaffeensis* infection.**

(A) Immunoblot depicting knockdown efficiency of *xiap* in siRNA knockdown cells compared to positive control from *E.ch.* THP-1 cells harvested at 24 hpi. Percent knockdown of XIAP relative to positive control is shown to the right of the immunoblot. GAPDH is utilized as a loading control. (B) Small interfering RNA-transfected (siRNA) THP-1 cells were infected with *E. ch.* (MOI 100, 24 hpt). Scrambled siRNA (scrRNA) was transfected as an infected positive control. *E. ch.* infection was quantified as fold change at 24 hpi and was determined by qPCR amplification of the *dsb* gene. Knockdowns were performed with at least three biological and technical replicates for t-test analysis. (C) Quantification of *xiap* or scr siRNA treated THP-1 cells containing *E.ch.* inclusions (morulae). Morulae were visualized by H&E staining. (D) Representative image of uninfected or *E. ch.*-infected scr or *xiap* siRNA treated cells by H&E staining. Black arrows identify *E.ch.* Inclusions (morulae). Quantitative analysis of cell viability by the Muse® Count & Viability Kit for uninfected or *E. ch.*-infected scr or *xiap* siRNA treated cells is represented. Bar graphs represent means  $\pm$  SD. \*\*\*\*,  $P < 0.001$ . Experiments were performed in triplicate ( $n=3$ ) and representative images are shown.

**XIAP stabilizes pro-caspase levels to inhibit apoptosis.** Smac/DIABLO is a cytosolic antagonist to IAPs [247]. To determine the significance of IAPs during *E. chaffeensis* infection, THP-1 cells were treated with SM-164, a Smac/DIABLO mimetic compound. Cell death was induced by TNF- $\alpha$ , followed by subsequent infection with *E. chaffeensis*. Treatment with SM-164

resulted in a significant reduction in ehrlichial infection as determined by confocal microscopy and qPCR of the *dsb* gene (Figs. 18A and B). Importantly, cells treated with SM-164/TNF- $\alpha$  had 10-20% viability and exhibited morphological changes of apoptosis including membrane blebbing, nuclear fragmentation and cell shrinkage (Figs. 18A and C, S4A). In comparison, untreated or DMSO-treated cells had cell viabilities ranging from 82-92% and 63-70%, respectively (Figs. 18C, S4A). Additionally, there were unremarkable morphological changes associated with untreated or DMSO-treated cells (Fig. 18A). These data further suggests that NICD stabilization of XIAP results in antiapoptotic activity during *E. chaffeensis* infection. In addition, an increase in early and late apoptotic cells were shown in SM-164/TNF- $\alpha$ -treated cells compared to untreated, DMSO or either SM-164 or DMSO/TNF- $\alpha$  treated cells. Importantly, pre-incubation of THP-1 cells with Caspase-9 inhibitor, Z-LEHD-FMK TFA, prior to SM-164/TNF- $\alpha$  treatment reversed apoptotic effects demonstrated with SM-164/TNF- $\alpha$  (Figs. 18A-C, S4A-B). Collectively, these data demonstrate increases in XIAP levels inhibit intrinsic apoptosis during *E. chaffeensis* infection.

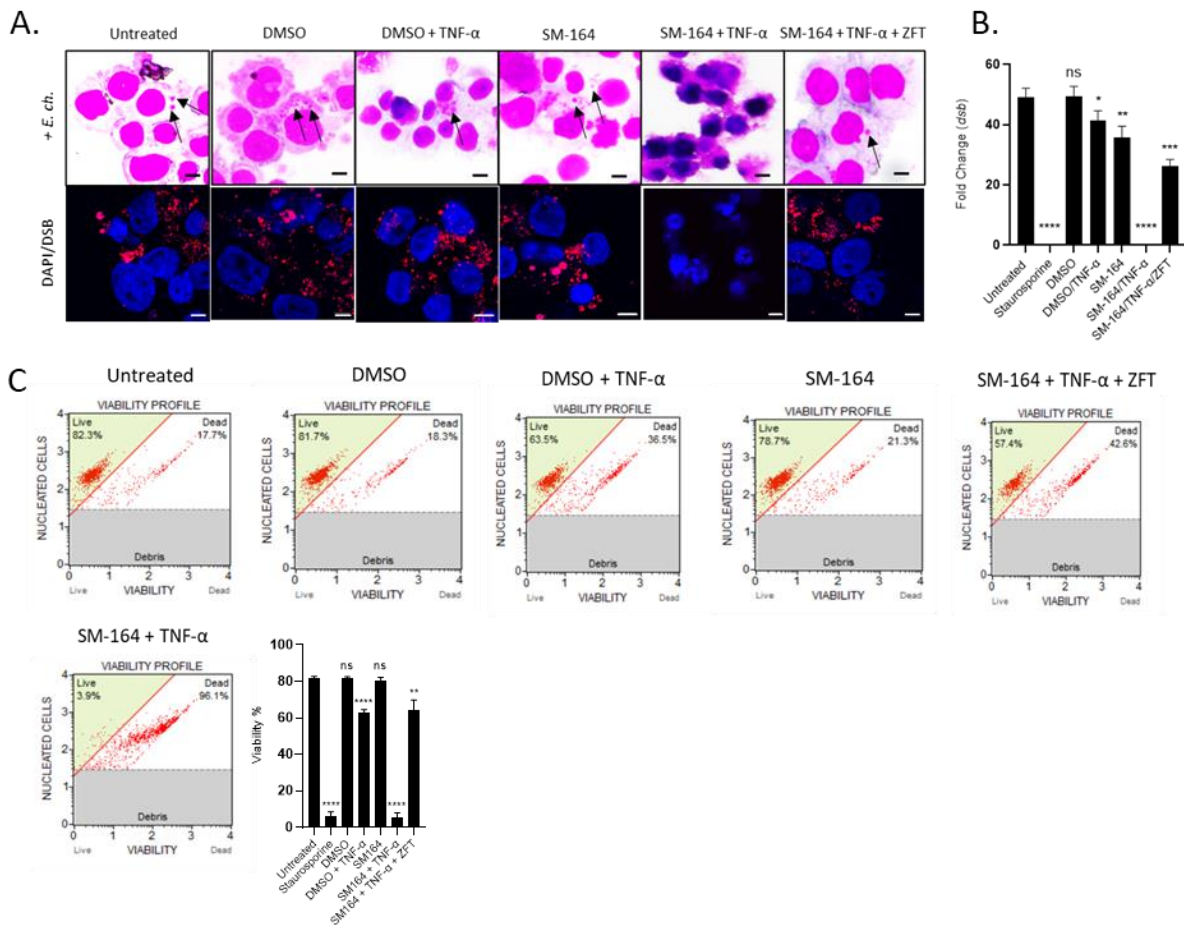


**Figure 18: XIAP stabilizes pro-caspase levels to inhibit apoptosis.**

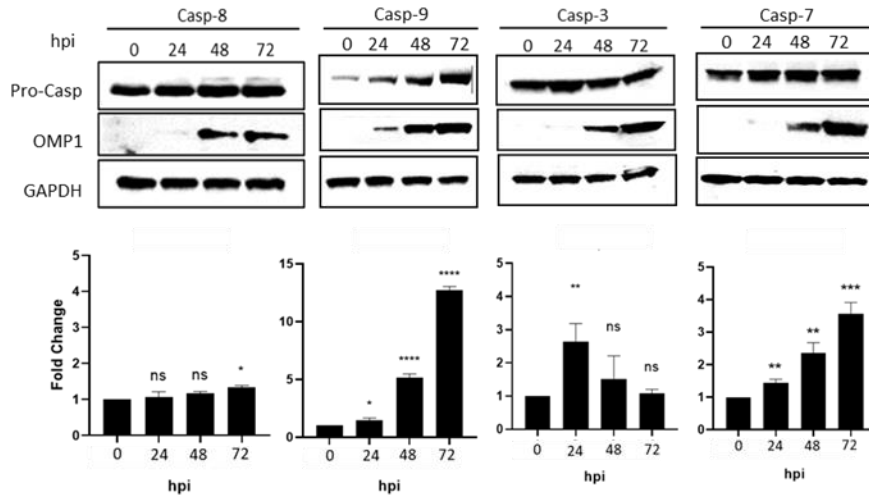
*E. ch.*-infected THP-1 cells (MOI 50) were pre-treated with DMSO or SM-164 alone (100nM, 12h) or SM-164 (100nM, 12h) in combination with caspase-9 inhibitor, Z-LEHD-FMK TFA (20 $\mu$ M, 2h). Cell death was stimulated with TNF- $\alpha$  (100 ng/ml) or staurosporine (100 ng/ml, positive apoptosis control) in the indicated samples. (A) The presence of *E.ch.* was determined by H&E and immunofluorescent confocal microscopy. Black arrows identify *E.ch.* inclusions (morulae) in H&E-stained cells. THP-1 cells were probed for DSB (red) to determine the presence of morulae by immunofluorescent confocal microscopy. DSB was immunostained with tetramethylrhodamine isothiocyanate (TRITC). Nuclei were stained with 4',6'-diamidino-2-phenylindole DAPI (blue). Apoptotic cells were identified by visualization of nuclear morphology by DAPI (Scale bar = 10  $\mu$ m). (B) Fold change difference of *dsb* transcript levels in the indicated cell samples. (C) Cell viability was determined by the Muse® Count & Viability Kit and quantification of cell viability percentage in the previously mentioned treatment groups is shown. Bar graphs represent means  $\pm$  SD. \*\*\*\*,  $P < 0.0001$ ; ns = no significance. Experiments were performed in triplicate (n=3) and representative images are shown.

**Pro-Caspase levels during *E. chaffeensis* infection.** Studies have demonstrated that XIAP differentially inhibits caspases through its baculovirus IAP repeat (BIR) domains [196]. The BIR2 domain directly binds apoptotic executioner Caspases-3 and -7 using a two-site interaction

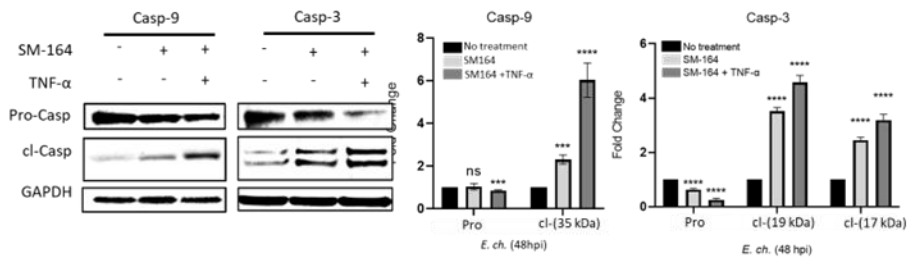
mechanism for inhibition of apoptosis [197]. XIAP also sequesters Caspase-9 in a monomeric state using the BIR3 domain, preventing the catalytic activity of Caspase-9 [203]. Therefore, XIAP is directly associated with inhibition of downstream caspases. During *E. chaffeensis* infection, temporal levels of Caspases-3, -7 and -9 increased during infection (Fig. 19A). Temporal increases in Caspases-3, -7 and -9 gene transcription was also detected during *E. chaffeensis* infection (Fig. S5).

To demonstrate that XIAP was directly associated with downstream caspase inhibition, THP-1 cells were treated with SM-164 and TNF- $\alpha$ , infected with *E. chaffeensis* infection (MOI 50) and Caspase-9 and -3 levels were determined. The SM-164/TNF- $\alpha$  treated cells had significantly lower levels of pro-Caspases-9 and -3, and significantly increased levels of cleaved (active) Caspases-9 and -3 (Fig. 19B). To demonstrate that XIAP was directly associated with downstream caspase inhibition, THP-1 cells were treated with SM-164 in combination with TNF- $\alpha$ , infected with *E. chaffeensis* infection (MOI 50) and multi-caspase levels were determined by flow cytometry. A significant increase in the percentage of caspase+/dead cells with SM-164/TNF- $\alpha$  treatment was detected (Fig. 19C). These data demonstrate increased XIAP levels inhibit caspase activation and apoptosis during *E. chaffeensis* infection.

A.



B.



C.

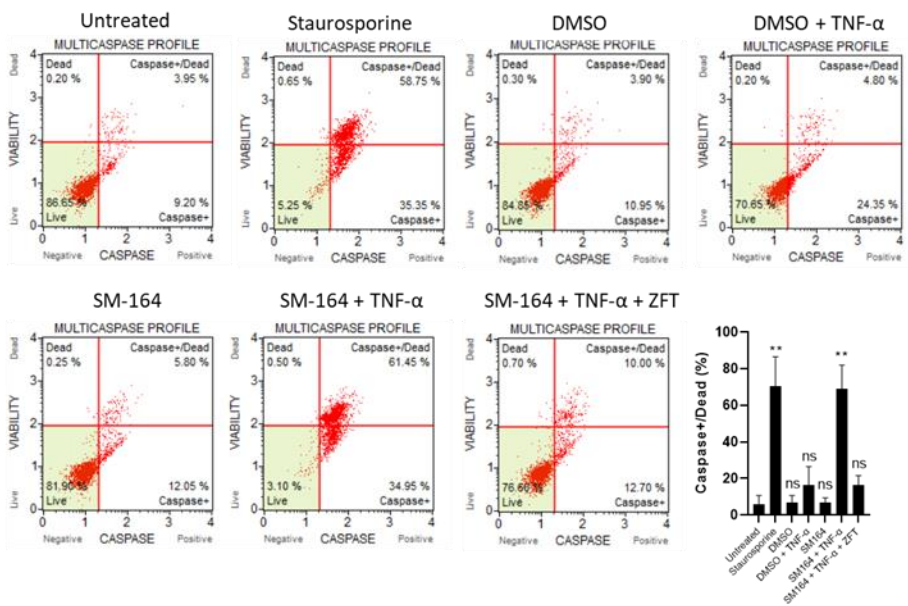


**Figure 19: XIAP stabilizes pro-caspase levels -3, -7 and -9 to inhibit apoptosis during *E. chaffeensis* infection.**

(A) Immunoblots and fold differences of Pro-Casp-8, -9, -3 and -7 in *E. ch.*-infected cells at 0, 24, 48 and 72 hpi. Outer Membrane Protein 1 (OMP-1) is a major immunodominant protein of *E.ch.* Infection used to confirm the presence of infection. GAPDH is utilized as a loading control. (B) Immunoblot and quantification of the fold change of *E.ch.*-infected cells untreated or pre-treated with SM-164 alone or in combination with TNF- $\alpha$ . Cells were probed for total Caspase and cleaved caspase-3 or 9 and fold change difference of pro-caspase and cleaved caspase-3 and -9 levels were determined. (C) *E. ch.*-infected THP-1 cells were pre-treated with DMSO or SM-164 alone (100nM, 12h) or SM-164 (100nM, 12h) in combination with caspase-9 inhibitor, Z-LEHD-FMK TFA (20 $\mu$ M, 2h). Cell death was stimulated with TNF- $\alpha$  (100 ng/ml) or staurosporine (100 ng/ml, positive apoptosis control) in the indicated samples. Percentages of live, caspase+, caspase+ and dead, total caspase+, and dead cells determined by the Muse® MultiCaspase Kit. Quantification of Caspase+/Dead percentage is shown. Bar graphs represent means  $\pm$  SD. \*\*, P < 0.01; ns = no significance. Experiments were performed in triplicate (n=3) and representative images are shown.

***Ehrlichia chaffeensis* TRP120-mediated FBW7 ubiquitination and proteasomal degradation stabilizes XIAP.** We have recently demonstrated FBW7 degradation during *E. chaffeensis* infection results in increased levels of FBW7 regulated oncoproteins including NICD, phosphorylated c-Jun, MCL-1 and cMYC [64]. Data demonstrated that TRP120 ubiquitination of FBW7 results in FBW7 degradation, enhancing infection. To determine the effect of FBW7 and NICD on XIAP and Caspase-3 and -9 activation, HeLa cells were transfected with catalytic-inactive TRP120 (TRP120-C520S) and treated with TRP120-N1-P6 Notch memetic peptide for 2 h to activate Notch signaling followed by induction of cell death by TNF- $\alpha$ . HeLa cells ectopically expressing TRP120-C520S displayed increased cleaved Caspases-3 and -9 compared to uninfected or TRP120-WT transfected cells (Fig. 20). Collectively, these data demonstrate that TRP120 FBW7 degradation stabilizes XIAP for subsequent increased XIAP expression and inhibition of caspase activation during *E. chaffeensis* infection.

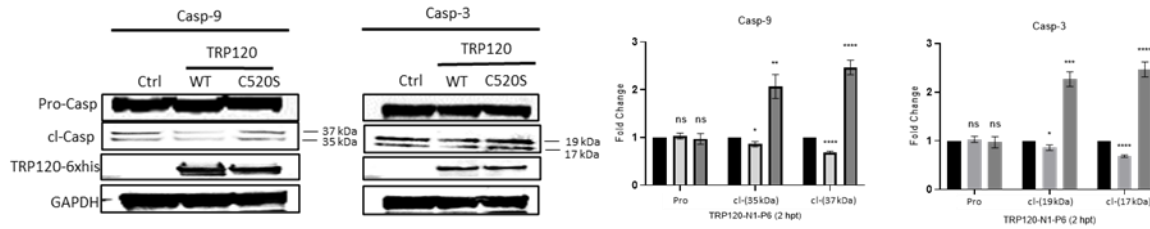


**Figure 20: FBW7 degradation during *E.ch.* Infection enhances XIAP stability and caspase-3 and -9 activation.**

Hela cells were transfected with empty vector, TRP120-WT or catalytic-inactive TRP120 (TRP120-C520S) for 24h, stimulated with TRP120-N1-P6 memetic peptide to activate Notch signaling (2h) and cell death was induced by TNF- $\alpha$  (100 ng/ml, 48h). (A) Immunoblot of Pro- and cleaved caspase-3 or -9 in vector, TRP120-WT or catalytic-inactive TRP120 (TRP120-C520S) treated cells. Fold differences in Pro- and cleaved caspase-3 or -9 protein levels in TRP120-WT or catalytic-inactive TRP120 (TRP120-C520S) treated cells compared with empty vector cells are shown. Bar graphs represent means  $\pm$  SD. \*\*\*\*,  $P < 0.0001$ . Experiments were performed in triplicate ( $n=3$ ) and representative images are shown.

## Discussion

Inhibition of host cell apoptosis is an important survival strategy utilized by *E. chaffeensis* [180, 189, 248]. Previous studies have demonstrated the T4SS effector protein, ECH0825 inhibits host cell apoptosis in human monocytes [249]. ECH0825 localizes to mitochondria and inhibits Bax-induced apoptosis by increasing mitochondrial manganese superoxide dismutase (MnSOD) and reducing reactive oxygen species-mediated damage [249]. Further, upregulation of apoptotic inhibitor genes during *E. chaffeensis* infection, including BCL-2 and BIRC3, and downregulation of apoptotic inducers, such as BIK, BNIP3L, and hematopoietic cell kinase have also been reported [180]. However, there is little information related to *E. chaffeensis* modulation of caspase activation. In this study, we have identified a mechanism by which *E. chaffeensis* TRP120 effector activates the Notch signaling pathway to inhibit caspase-dependent apoptosis through NICD and XIAP interaction.

We recently identified a TRP120 Notch SLIM ligand memetic motif responsible for Notch activation during *E. chaffeensis* infection [81]. Additionally, we demonstrated that *E. chaffeensis*

and rTRP120 activate Notch signaling to downregulate TLR2/4 expression for intracellular survival [94]. TRP120 Notch activation was recently confirmed to occur through a TRP120 tandem repeat (TRP120-TR) Notch SLiM ligand mimetic that directly binds to the Notch receptor in a region containing the known ligand binding region [81]. Although a Notch SLiM mimetic has been recently identified, its role in *E. chaffeensis* survival has not been fully elucidated. In this study, we investigated the functional implications of TRP120 Notch SLiM mimetic activation during *E. chaffeensis* infection and defined a novel antiapoptotic mechanism involving inhibitor of apoptosis (IAP) proteins potentially inhibiting the catalytic activity of caspases through regulation of Notch signaling as modeled in Fig. 8.

Pathogens have evolved various means of subverting innate immune defense of the host for survival [80, 245, 250-255]. One of the most well-studied mechanisms of bacterial pathogens is targeting intracellular signal transduction cascades. Pathways such as MAPK and NF- $\kappa$ B are manipulated by various pathogens [242, 256-258]. Manipulation of these innate immune and inflammatory pathways are regulated through bacterial effector proteins and host-pathogen interactions [50, 259]. In addition, inhibition of apoptosis is well-documented as a bacterial and viral mechanism to subvert innate immune defense [80, 251, 257, 260, 261]. Although intracellular bacterial pathogens manipulate apoptosis by various mechanisms, modulation of the Notch signaling pathway is a strategy that has not been reported.

The Notch signaling pathway is an evolutionary, highly conserved cell signaling pathway that is utilized across metazoan species [101, 262]. The Notch pathway is known to play critical roles in cellular homeostasis, differentiation and cell proliferation [101]. Recently, evidence has demonstrated Notch signaling to also play roles in innate immunity and inflammation, including regulation of Toll-like receptor expression, inflammatory cytokines, macrophage activation, MHC class II expression, B- and T- cell development, autophagy and apoptosis [104, 110, 112, 263-265]. Interestingly, Notch signaling is activated in macrophages by LPS [96], *Mycobacterium*

*bovis* BCG [98], and as we recently reported, *E. chaffeensis* [94]. Activation of Notch by LPS and by *M. bovis* BCG was associated with the regulation of cytokine signaling through different mechanisms. The expression of canonical Notch ligand, Jagged-1, was induced by LPS in a JNK-dependent manner [96]. In comparison, *M. bovis* BCG was shown to upregulate Notch-1 and activate the Notch-1 signaling pathway, leading to the expression of SOCS3, a negative regulator of cytokine signaling [98]. In comparison, *E. chaffeensis* has been demonstrated to activate Notch signaling through a Notch SLiM memetic motif found within the TR domain of the TRP120 effector [81, 94].

Interestingly, Notch has been shown to inhibit apoptosis by directly interfering with the ubiquitination of the most potent inhibitor of apoptosis, XIAP [204]. NICD directly binds the BIR3-RING domain of XIAP to inhibit autoubiquitination. Inhibition of XIAP autoubiquitination results in stabilization of XIAP levels, leading to inhibition of apoptosis [204]. In this study we demonstrated increases in XIAP expression over the course of *E. chaffeensis* infection. A cleavage product was observed at later time points which correlated with the XIAP BIR3-RING domain. Studies have demonstrated this domain to be a potent inhibitor of the intrinsic apoptotic pathway through direct binding to Caspase-9 [196]. XIAP has been shown to sequester Caspase-9 in a monomeric state, which serves to prevent catalytic activity [200]. Previous studies have demonstrated that *E. chaffeensis* inhibits apoptosis through the intrinsic apoptotic pathway by blocking the BCL-2 pathway [180]. In addition, we have recently demonstrated that engagement of the BCL-2 anti-apoptotic cellular programming during *E. chaffeensis* infection is caused by activation of the Hedgehog signaling pathway [80]. Induction of BCL-2 resulted in inhibition of Caspases-9 and -3, preventing activation of intrinsic apoptosis [80]. Therefore, evidence is cumulatively confirming inhibition of intrinsic apoptosis as a survival mechanism for *E. chaffeensis*. Importantly, both rTRP120 and the TRP120 Notch SLiM ligand memetic peptide upregulated XIAP expression in a time-dependent manner, with significant upregulation

occurring at later time-points, as demonstrated with *E. chaffeensis* infected cells. These data support the role of the TRP120 induced Notch signaling activation leading to increased XIAP levels.

Increases in NICD and XIAP levels occurred simultaneously and temporally. We have previously determined that NICD expression increases during infection, attributed in part to *E. chaffeensis* TRP120 ubiquitinating and degrading the Notch negative regulator, FBW7 [64]. Here, we demonstrate NICD to both colocalize and directly bind with XIAP at later time points of *E. chaffeensis* infection. Interestingly, colocalization of NICD and XIAP occurred in both the cytoplasm and the nucleus during *E. chaffeensis* infection. Selective localization of pro-caspases in different subcellular compartments have been previously demonstrated [266]. Pro-Caspase and active caspases -9, -3 and -7 are mainly found in the cytosolic fraction, however Caspases-3 and -9 were also found in the mitochondrial fraction, while caspase-7 in the microsomal fraction in untreated Jurkat T lymphocytes [266]. Caspase-3 was the only major Caspase found in the nucleus [266]. XIAP expression has been found to be mainly cytoplasmic; however, is also present in the nucleus in specific cell types. XIAP nuclear translocation have been previously associated with aberrant cell division and anchorage-independent growth [267, 268]. Previous data has demonstrated increases in XIAP are not associated with stimulation of XIAP transcription by NICD, therefore further investigation is needed to determine the functional implications of NICD/XIAP colocalization in the nucleus during *E. chaffeensis* infection [204]. Inhibition of Notch activation by DAPT, a  $\gamma$ -secretase inhibitor, reversed increases in XIAP levels during *E. chaffeensis* infection. DAPT inhibits Notch receptor enzymatic hydrolysis, NICD release and downstream transcriptional activation by inhibiting  $\gamma$ -secretase activity. Hence, inhibition of NICD is directly associated with decreases in XIAP levels.

Apoptosis is an important innate defense mechanism against microbial infection; however, various intracellular pathogens hijack apoptosis by inhibiting either extrinsic or intrinsic

apoptosis through different mechanisms [80, 269-271]. We demonstrated the importance of XIAP expression in inhibition of apoptosis during *E. chaffeensis* infection. siRNA knockdown of XIAP significantly reduced ehlichial infection. This finding was related to apoptosis, as demonstrated by Muse Count & Viability Assays and microscopy demonstrating cellular morphological hallmarks of apoptosis. siRNA treated cells showed significant cell blebbing, shrinkage of the cell and nuclear fragmentation. XIAP siRNA treated cells contained a significant reduction in morulae compared to scrambled siRNA cells. Interestingly, *A. phagocytophilum* also appears to inhibit apoptosis by preventing XIAP degradation [245]. Moreover, cleaved fragments of XIAP were not detected in *A. phagocytophilum*-infected neutrophils [245], suggesting that XIAP degradation is blocked during *A. phagocytophilum* infection. In contrast, we detected an increase in XIAP cleavage product at 30 kDa, which we identified as XIAP BIR3-RING. As previously stated, the XIAP BIR3-RING cleavage product has been shown to strongly inhibit intrinsic apoptosis. Differences in the presence of the cleavage product observed between *E. chaffeensis* and *A. phagocytophilum* are not well understood and need further investigation. These findings indicate that modulating IAP to inhibit apoptosis may be a conserved mechanism utilized by various intracellular bacterial pathogens for survival.

Various studies have demonstrated XIAP as the most potent endogenous inhibitor of caspases due to weaker binding and inhibition of caspases by other IAP proteins. Interestingly, XIAP has been shown to inhibit both the executioner and intrinsic apoptotic pathways using various domains found within its structure. XIAP inhibits the executioner pathway by directly binding to Caspases-3 and -7 through the linker region between the BIR1 and BIR2 domains [197]. As previously mentioned, XIAP also directly binds to Caspase-9 through its BIR3 domain [199, 200, 203]. We have demonstrated pro-Caspase -3, -7 and -9 levels temporally increase during *E. chaffeensis* infection. However, there were only minor changes in Caspase-8 levels during infection, demonstrating that mitochondrial-mediated apoptosis is the predominantly

targeted for inhibition. By comparison, inhibition of Caspase-8 activation and Bid cleavage has been demonstrated in *A. phagocytophilum*-infected human neutrophils [245].

Previous data has shown that transcriptional levels of caspases do not change at earlier timepoints during *E. chaffeensis* infection [272]. Our data correlates with these observations in that significant upregulation is not shown until 48 hpi. Pro-Caspase-3 protein levels increased at 24 hpi but decreased at 48 and 72 hpi. Cleavage of pro-Caspase-3 levels coincides with BIR3-RING cleavage products observed at 48 and 72 hpi. Activated Caspase-3 has previously been demonstrated to cleave XIAP [196]. The resulting cleavage products are the BIR1-2 and BIR3-RING fragments. The BIR1-2 fragment inhibits Caspases-3 and -7; however, BIR1-2 is a less potent inhibitor of apoptosis than full-length XIAP and may also be susceptible to further degradation [201]. In comparison, the BIR3-RING fragment blocks activation of Caspase-9 by directly binding to and inhibiting activity [199, 200, 203]. Therefore, activation of Caspase-3 may lead to XIAP BIR3-RING fragments that inhibit intrinsic apoptosis through direct Caspase-9 binding. Interestingly, similar evidence of inhibition of Caspases-3 and -9 activation during *A. phagocytophilum* infection has been reported where activation of Caspases-3 and -9 were linked to blockage of XIAP degradation [245].

Caspase inhibition by XIAP is blocked by an endogenous IAP inhibitor, second mitochondrial activator of caspases (SMAC)/Diablo. During induction of apoptosis, SMAC/Diablo is processed and released from the mitochondria where it binds to the BIR2 and BIR3 domains of XIAP to antagonize XIAP activity [203, 247]. SM-164 is a bivalent, SMAC mimetic that induces apoptosis [273]. Treatment with SM-164 in the presence of TNF- $\alpha$  significantly reduced cell viability and ehrlichial load. An increase in caspase-positive apoptotic cells was shown with SM164/TNF- $\alpha$  treatment. Importantly, SM-164/TNF- $\alpha$  treated cells pre-treated with Caspase-9 inhibitor, Z-LEHD-FMK TFA, blocked full induction of apoptosis during *E. chaffeensis* infection. TNF- $\alpha$  has been demonstrated to inhibit apoptosis through both the

extrinsic and intrinsic apoptotic pathways. Activation of the extrinsic pathway results in the cleavage of cytosolic BID to truncated p15 BID (tBID), which translocates to mitochondria and triggers cytochrome c release [274]. Therefore, reversal of cell death by Caspase-9 inhibitor, Z-LEHD-FMK TFA, may occur through Bid activation. In addition, SM-164 treatment resulted in decreased pro-caspase and increased levels of cleaved Caspases-9 and -3 during infection. These results demonstrate direct correlation of XIAP activity and caspase inhibition during *E. chaffeensis* infection.

During *E. chaffeensis* infection, TRP120 ubiquitinates Notch negative regulator, FBW7, resulting in degradation. [64]. Degradation of FBW7 is known to result in increased NICD levels [142]. HeLa cells transfected with TRP120-C520S catalytic mutant displayed an increase in cleaved levels of Caspases-3 and -9, demonstrating a direct relationship between FBW7 stabilization of NICD levels and subsequent increased XIAP expression and caspase inhibition. Collectively, this study serves to provide insight into the molecular details of how TRP120 Notch signaling leads to increased XIAP expression through direct interaction with NICD, leading to inhibition of caspase activation and apoptosis for *E. chaffeensis* survival.

There are multiple questions that remain to be answered regarding *E. chaffeensis* regulation of apoptosis. IAP proteins have been previously shown to interact with one another to form IAP-IAP complexes that inhibit apoptosis [195]. Many of the IAP-IAP complexes consist of one or more of four key IAPs: c-IAP1, c-IAP2, XIAP and survivin. Whether XIAP functions in a complex with other IAPs to inhibit apoptosis during *E. chaffeensis* infection remains unknown. Evolutionarily conserved signaling pathways such as Notch and Hedgehog play key roles in regulation of apoptosis [103, 211, 275]. TRP120 has been demonstrated to inhibit apoptosis activation of Hedgehog signaling [80]. Further investigation is needed to understand potential crosstalk between Notch, Hedgehog and potentially other signaling pathways that are activated during *E. chaffeensis* infection and associated with apoptosis regulation.

In conclusion, we demonstrated *E. chaffeensis* Notch activation results in an XIAP-mediated anti-apoptotic program. Our findings reveal an *E. chaffeensis* initiated, Notch signaling regulated, antiapoptotic mechanism involving inhibitor of apoptosis proteins (IAPs) that inhibits caspase activation (Fig 21). This study gives further insight into the molecular mechanisms of how obligate intracellular pathogens utilize secreted effector proteins mimicking host ligands to exploit conserved signaling pathways to suppress innate defenses and promote infection.

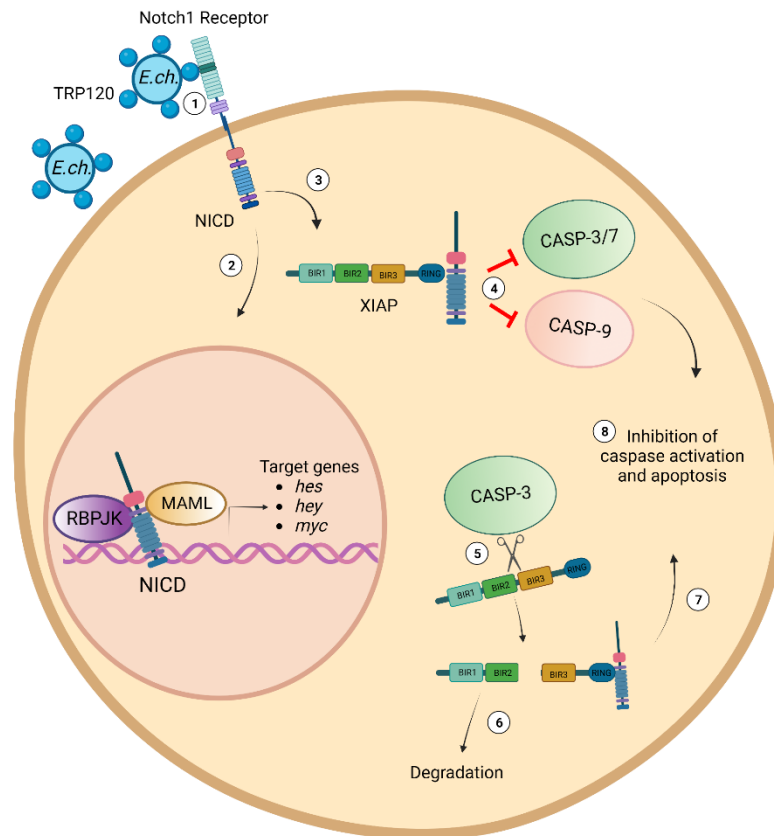


**Figure 21. Model of *E. chaffeensis* TRP120 Notch-mediated apoptosis inhibition.**

Infectious dense-cored *E. chaffeensis* with T1SS TRP120 effector on the surface. (1) *E. ch.* TRP120 binding to the ligand binding region (LBR) of the Notch-1 receptor via the Notch ligand memetic motif (Patterson, Velayutham et al. 2022) activates Notch signaling. (2) Notch intracellular domain (NICD) translocates to the nucleus and activates Notch gene transcription and (3) binds directly to XIAP to inhibit XIAP degradation, and (4) inhibits CASP-9, -3 and -7 activation. (5) Active CASP-3 may also cleave XIAP into two fragments; BIR1 and -2 and BIR3-RING. (6) BIR1 and -2 have been shown to be more rapidly degraded in comparison to BIR3-RING. (7) BIR3-RING may bind to NICD and (8) both full-length and cleaved XIAP-BIR3-RING/NICD complexes may inhibit caspase activation and apoptosis. Image created by L. Patterson using BioRender.com.

## CHAPTER 5. SUMMARY, CONCLUSIONS AND FUTURE DIRECTIONS

The overall objective of this study was to identify the specific molecular interactions and motifs required for *E. chaffeensis* TRP120-Notch receptor interaction and activation, and to determine the functional outcomes of Notch activation during *E. chaffeensis* infection. This work herein provides evidence that an *E. chaffeensis* TRP120-TR Notch SLiM mimetic motif is directly binding to Notch-1 at a region containing the ligand binding domain to activate Notch signaling. TRP120 Notch activation leads to an increase XIAP expression and subsequent inhibition of caspase activation for *E. chaffeensis* intracellular survival.

In Chapter 3, I demonstrated TRP120 shares sequence homology with canonical and noncanonical Notch ligands at a region located at the C-terminus of the tandem repeat (TR) domain. In addition to this data, *in silico* prediction software predicted TRP120 to share a similar biological function with Notch ligands, in which part of the sequence responsible for the similarity in biological function was also located at the C-terminus of the tandem repeat (TR) domain. Using His-tag pull down assays, SPR and confocal immunofluorescent microscopy, we confirmed TRP120-TR to be the domain responsible for TRP120 Notch activation. Upregulation of Notch downstream targets using a Notch signaling pathway gene array was utilized to confirm TRP120-TR as the Notch activating domain. Furthermore, we identified the TRP120-TR Notch SLiM mimetic motif (TRP120-TR-P6; EDEIVSQPSSE) responsible for Notch activation. TRP120-TR-P6 Notch SLiM mimetic motif correlated with both sequence homology and *in silico* prediction data. Furthermore, TRP120-TR-P6 caused upregulation of Notch downstream targets in a dose-dependent manner. Alanine mutagenesis was used to determine that the entire 11-amino acid motif is required for Notch activation. Importantly, pretreatment with a purified rabbit polyclonal antibody generated against the TRP120-N1-P6 SLiM blocked Notch activation indicating that the TRP120 Notch mimetic is solely responsible for Notch activation by *E. chaffeensis*.

Several questions pertaining to Aim 1 remain unanswered. Previous published data demonstrated interaction of TRP120 and Notch activating metalloprotease, ADAM17 [60]. How and why interaction between TRP120 and ADAM17 occurs still needs to be explored. ADAM17 is known to have a diverse array of substrates that regulates its enzymatic activity [276]. Whether or not TRP120 shares sequence homology with known ADAM17 substrates needs to be determined. In addition, the dynamics of how TRP120 binds to the Notch-1 receptor and ADAM17 to activate Notch signaling needs to be investigated.

Several Notch regulators play a key role in tight regulation of Notch signaling. Exploring possible interaction and degradation of various Notch regulators may explain why host cells infected with *E. chaffeensis* do not maintain tight regulation. Furthermore, several conserved signaling pathways have been shown to be activated by TRP120 ligand mimicry. Understanding how crosstalk between these conserved signaling pathways occurs and whether other secreted TRP effectors play a significant role in regulation of these pathways still needs to be explored.

In Chapter 4, I demonstrated an increase in XIAP expression during *E. chaffeensis* infection. Significant temporal increase in XIAP levels were detected in cells treated with rTRP120-TR or TRP120-TR-P6 peptide, demonstrating *E. chaffeensis* TRP120 promotes increased XIAP levels. Using confocal immunofluorescent microscopy and co-immunoprecipitation, we determined that the increase in XIAP levels was a direct result of Notch activation by demonstrating direct interaction of NICD with XIAP during infection. Pre-treatment of  $\gamma$ -secretase inhibitor, DAPT, exhibited decreased XIAP levels during the course of infection. In addition, treatment with DAPT in combination with Smac-mimetic inhibitor, SM-164 displayed significant cell death, and had significantly decreased ehrlichial load suggesting that XIAP is stabilized by NICD during *E. chaffeensis* infection.

We further demonstrated that NICD stabilization of XIAP results in antiapoptotic activity and increased infection through siRNA knockdown of XIAP. XIAP KD cells displayed a significant decrease in ehrlichial load which was determined to be caused by the induction of apoptosis due to XIAP destabilization. Additionally, SM-164 treatment was utilized to

demonstrate that XIAP stabilizes pro-caspase levels to inhibit apoptosis. Cells treated with SM-164/TNF- $\alpha$  had a significant decrease in viability and exhibited morphological changes of apoptosis. Importantly, pre-incubation with Caspase-9 inhibitor, Z-LEHD-FMK TFA, prior to SM-164/TNF- $\alpha$  treatment reversed apoptotic effects demonstrated with SM-164/TNF- $\alpha$ , demonstrating that increases in XIAP levels inhibit intrinsic apoptosis during *E. chaffeensis* infection. We determined that temporal levels of Caspases-3, -7 and -9 increased during infection. Treatment with SM-164/TNF- $\alpha$  resulted in lower levels of pro-Caspases-9 and -3, and significantly increased levels of cleaved (active) Caspases-9 and -3. Moreover, treatment with SM-164/TNF- $\alpha$  resulted in a significant increase in the percentage of caspase+/dead cells, demonstrating increased XIAP levels inhibit caspase activation and apoptosis during *E. chaffeensis* infection. Finally, by ectopically expressing catalytic-inactive TRP120 (TRP120-C520S) in Hela cells and treating with TRP120-N1-P6 Notch memetic peptide to activate Notch signaling we determined that TRP120 FBW7 degradation stabilizes NICD for subsequent increased XIAP expression and inhibition of caspase activation during *E. chaffeensis* infection.

Future studies for Aim 2 include investigating if other IAPs may play a role during *E. chaffeensis* infection. IAP-1 and -2 are known to form complexes with XIAP to inhibit apoptosis. More investigation is needed to determine IAP-IAP complexes as a possible mechanism for the inhibition of apoptosis. The current study reveals an *E. chaffeensis* initiated, Notch signaling regulated, antiapoptotic mechanism involving inhibitor of apoptosis proteins (IAPs). We have also demonstrated TRP120 activates the Hedgehog signaling pathway to inhibit apoptosis through a different mechanism for ehrlichial survival. How these two conserved signaling pathways may cross talk for execution of apoptosis inhibition needs to be investigated.

### **Possible Clinical Outcomes**

The current recommended treatments for HME include doxycycline, tetracycline and recently rifampin [11]. Therefore, alternative and improved therapeutic modalities for ehrlichiosis are needed for patient populations by which these antibiotics are contraindicated.

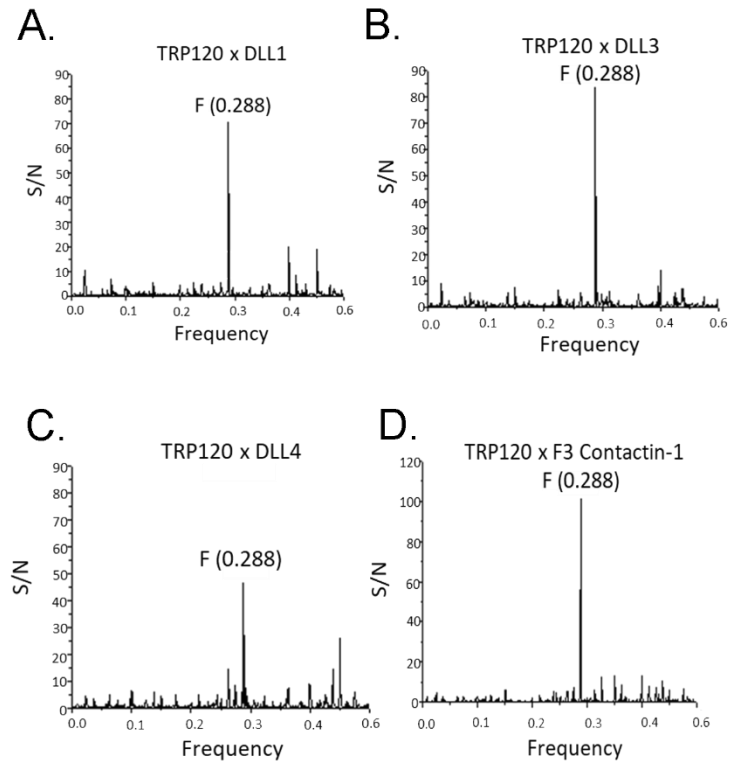
This study has identified a novel Notch mimetic motif that activates Notch signaling. Specifics on TRP120-N1-P6 as a treatment for HME need to be elucidated, including the dose administered, delivery methods, off-target effects and clinical effectiveness. Nevertheless, TRP120-N1-P6 may prove to be an appropriate target for HME.

We have utilized a polyclonal antibody against the Notch mimetic motif which successfully inhibited Notch activation. Various Notch inhibitors have been generated as anti-cancer therapies. Notch inhibitors include gamma-secretase inhibitors (GSIs), alpha-secretase inhibitors (ASIs), endosomal acidification inhibitors, antibody inhibitors of Notch activity and RNA interference [277]. Currently, GSIs and antibodies blocking specific protein-protein interactions have made clinical trials. Navicixizumab is an anti-DLL4/VEGF monoclonal antibody that is currently being used in an ongoing Phase 1b study in combination with paclitaxel to treat resistant ovarian cancer. Currently, targeting DLL4-Notch interaction has shown promising results as a cancer treatment. Therefore, peptide or antibody treatments against the TRP120-N1-P6 mimetic motif may be a potential therapeutic agent for both HME and cancer in the future; however, further studies are needed to confirm TRP120-N1-P6 as a potential therapeutic target.

In summary, *E. chaffeensis* survives by utilizing various molecular based strategies that are critical for cell survival, including exploitation of conserved cellular signaling pathways and modulation of apoptosis. This investigation reveals an *E. chaffeensis* initiated, Notch signaling regulated, antiapoptotic mechanism involving inhibitor of apoptosis proteins (IAPs). Herein, we demonstrate that *E. chaffeensis* utilizes ligand mimicry as a host hijacking mechanism to induce Notch activation for Notch intracellular domain stabilization of X-linked inhibitor of apoptosis protein (XIAP) to inhibit intrinsic apoptosis. This study highlights a novel mechanistic strategy whereby intracellular pathogens repurpose evolutionarily conserved eukaryotic signaling pathways to engage an antiapoptotic program for intracellular survival.

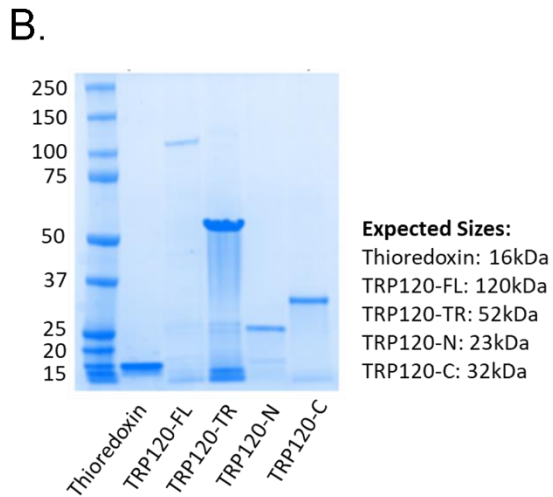
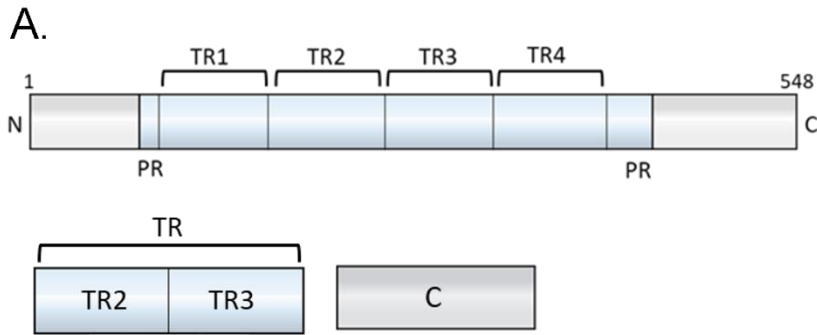
## APPENDICES

### Appendix A: Fig S1. TRP120 shares biological function with canonical and noncanonical Notch ligands.



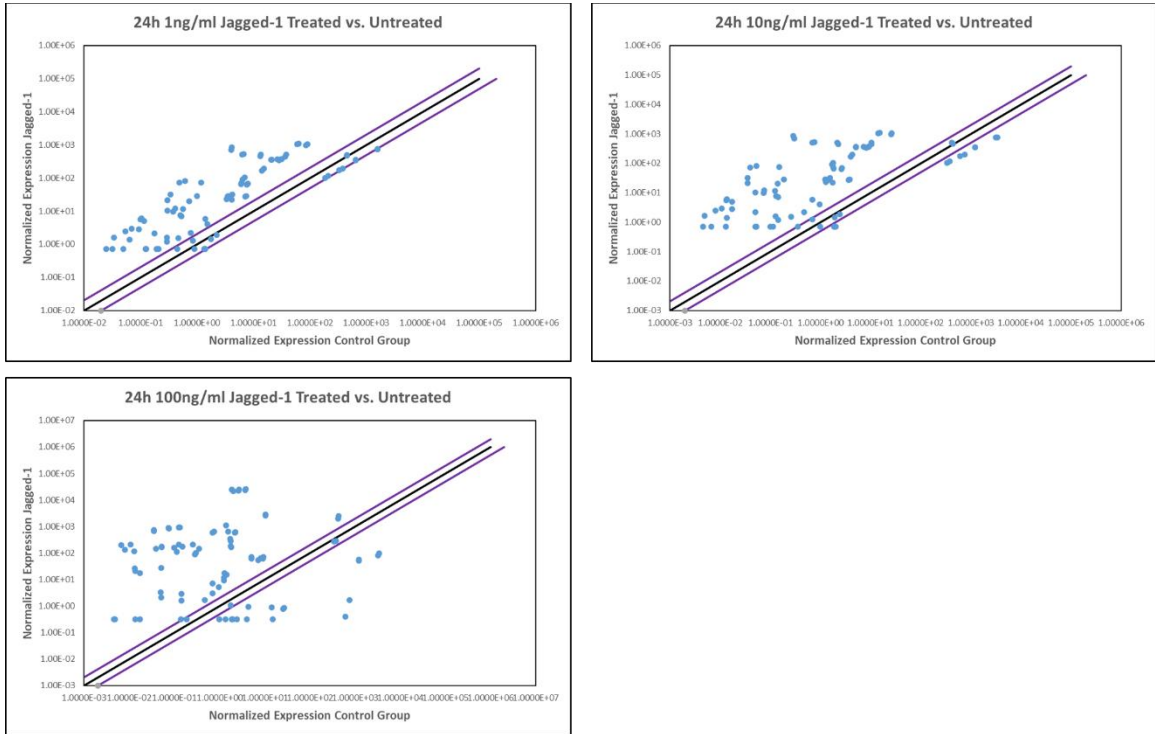
Informational Spectrum Method (ISM) was used to predict if TRP120 shared a similar biological function with endogenous canonical and noncanonical Notch ligands. The primary sequence of TRP120 and endogenous Notch ligands were converted into a numerical sequence using each amino acid's electron-ion interaction potential (EIIP). Numerical sequences were converted into a spectrum using Fourier transform. To determine if proteins shared a similar biological function and cross spectra analysis was performed with TRP120 and Notch ligands individually. A similar biological function is denoted by a peak at a frequency of F(0.288). TRP120 was predicted to share a similar biological function as canonical Notch ligands (A) DLL1, (B) DLL3 and (C) DLL4 and (D) noncanonical Notch ligand, F3 Contactin-1.

**Appendix B: Fig S2. Purification OF RECOMBINANT TRP120 PROTEINS.**



(A) Schematic of TRP120-FL, -TR, and -C terminus recombinant proteins. TRP120-TR is expressed and purified as two tandem repeat domains. (B) Coomassie Blue stained gel displaying an expression of purified TRP120-FL, -TR, -N, -C terminus, and TRX recombinant proteins. All listed recombinant proteins were expressed in a pBAD vector containing a His tag.

**Appendix C: Fig S3. Jagged-1 activates Notch gene expression in a concentration-dependent manner.**



Scatter plots of expression array analysis of 84 Notch signaling pathway genes to determine Notch gene expression with 1 ng/mL (top left), 10 ng/mL (top right), 100 ng/mL (bottom left) of recombinant Jagged-1 at 24 h pt. Purple lines denote a 2-fold upregulation or downregulation in comparison to control, and the black lines denote no change.

**Appendix D: Table S1. TRP120 IDD and SLiM memetic peptides activate Notch gene expression in a concentration-dependent manner.**

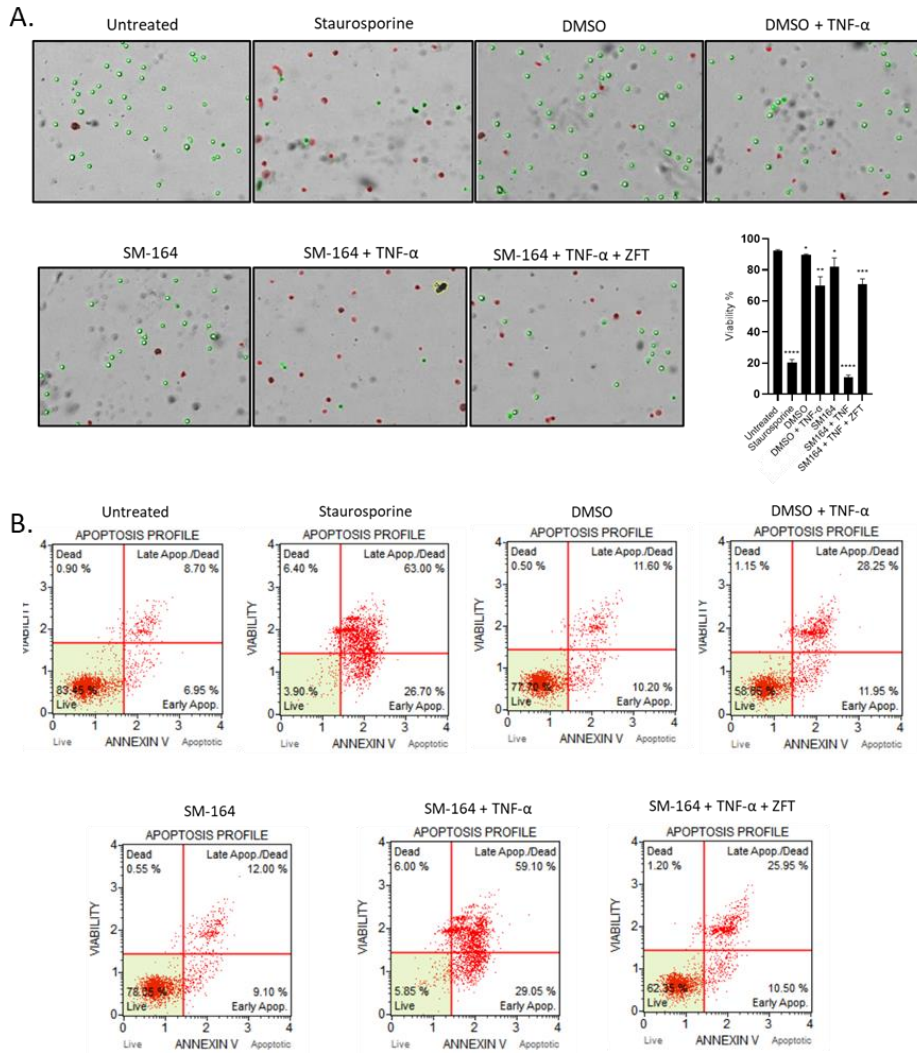
<b>Table S1A</b>				<b>Table S1B</b>			
Symbol	Fold Up- or Down-Regulation (1 ng/ml)	Fold Up- or Down-Regulation (10 ng/ml)	Fold Up- or Down-Regulation (100 ng/ml)	Symbol	Fold Up- or Down-Regulation (1ng/ml)	Fold Up- or Down-Regulation (10ng/ml)	Fold Up- or Down-Regulation (100ng/ml)
ADAM10	-5.24	10.8	18795.34	ADAM10	-62.99	13.49	5145.96
ADAM17	-5.22	9.84	15527.42	ADAM17	-64.01	14.29	4330.4
AES	-2.26	761.37	17744159	AES	-11.32	796.84	50151.56
AXIN1	-2.35	584.87	9243494	AXIN1	-10.9	33.38	26632.86
CBL	4.44	70.52	2259.89	CBL	-7.5	93.74	1186.1
CCND1	4.23	69.23	1811.92	CCND1	-8.34	93.64	1222.11
CCNE1	1.5	10.19	373.62	CCNE1	-14.26	22.12	423.87
CD44	1.22	9.77	289.4	CD44	-16.14	20.74	403.94
CDKN1A	-25.94	-2.69	1569.38	CDKN1A	-29.84	2.05	955.01
CFLAR	-42.34	-1.67	1258.74	CFLAR	-24.86	1.34	775.9
CHUK	-1.85	15.89	9780.16	CHUK	-4.4	28.12	212.35
CTNNB1	-1.73	15.3	8318.63	CTNNB1	-3.79	23.3	169.43
DLL1	-4.45	11.16	17155.54	DLL1	-55.82	15.53	5066.27
DLL3	-5.2	10.14	13489.23	DLL3	-67.45	12.75	4386.8
DLL4	-2.04	436.97	4759582	DLL4	-9.16	407.22	5247.87
DTX1	-2.28	538.76	5976407	DTX1	-10.55	477.81	18759.22
EP300	4.35	73.16	2115.2	EP300	-7.21	102.63	1180.69
ERBB2	4.67	74.69	1655.05	ERBB2	-7.66	93.26	1169.59
FIGF	1.34	9.82	297.41	FIGF	-15.67	20.38	370.13
FOS	1.57	11.32	274.14	FOS	-12.88	21.22	346.8
FOSL1	-44.76	-2.52	1343.81	FOSL1	-28.27	1.53	829.48
FZD2	-21.28	-2.77	1058.9	FZD2	-25.22	1.27	742.01
FZD3	-1.42	17.8	7414.3	FZD3	-4.08	23.7	177.09
FZD4	-1.63	18.4	7858.77	FZD4	-3.96	22.17	194.45
FZD7	2.37	30.26	695.01	FZD7	-24.58	42.3	547.95
GLI1	2.43	36.43	552.66	GLI1	-19.53	39.78	620.7
GSK3B	93.94	1265.58	4309.76	GSK3B	3.89	1627.24	11.44
HDAC1	32.38	609.4	4265.23	HDAC1	-1.1	822.35	12.79
HES1	-2.52	86.35	125699.8	HES1	-5.04	25.77	3618.7
HES5	1.01	43.98	155836.3	HES5	-3.9	220.74	4419.64
HEY1	3.22	108.88	12807.99	HEY1	3.01	145.4	92.49
HEY2	7.87	205.31	15425.43	HEY2	4.39	193.21	146.43
HEYL	-1.95	2.47	258.91	HEYL	-32.91	5.73	340.69
HOXB4	-2.04	2.53	227.7	HOXB4	-29.49	4.33	306.41
HR	21.54	30.44	20.75	HR	-13.12	86.62	64.58

ID1	12.24	24.54	14.37		ID1	-39.92	62.75	39.66
IFNG	1.79	30.81	651.91		IFNG	-25.54	36.92	615.18
IL17B	2.41	33.58	693.47		IL17B	-22.6	53.03	616.93
IL2RA	82.14	1479.42	3990.42		IL2RA	3.92	1683.42	25.12
JAG1	14.99	654.18	4258.14		JAG1	1.69	723.27	11.3
JAG2	-1.14	90.37	179285.9		JAG2	-2.05	46.73	4481.5
KRT1	-1.33	66.7	148379.9		KRT1	-4.04	103.61	4634.66
LFNG	-2.74	69.88	14457.78		LFNG	-6.51	40.87	93.67
LMO2	7.23	176.02	12533.04		LMO2	6.37	171.76	99.07
LOR	-2.2	2.59	221.37		LOR	-35.84	4.16	296.2
LRP5	-2.51	2.41	194.62		LRP5	-38.31	4.06	325.06
MAML1	13.87	32.92	22.62		MAML1	-83.1	50.46	48.59
MAML2	35.54	34.17	10.68		MAML2	-13.75	92.38	42.78
MFNG	8.31	3.15	8.12		MFNG	-54.09	12.16	244
MMP7	6.61	9.6	-1.6		MMP7	-30.69	12.45	222.52
NCOR2	4.54	171.28	32775.36		NCOR2	-11.54	354.31	4079.32
NCSTN	2.77	171.77	14890.95		NCSTN	-33.59	332.08	7564.54
NEURL1	-1.33	201.57	202795.4		NEURL1	-167.98	170.05	60342.94
NFKB1	-1.33	47.7	29898.63		NFKB1	-140.04	71.13	8679.35
NFKB2	-51.03	1.57	22688.16		NFKB2	-249.12	-1.21	55186.05
NOTCH1	-30.08	4.36	18030.16		NOTCH1	-230.64	2.15	71210.74
NOTCH2	1	-2.43	-3.59		NOTCH2	-41.2	-1.16	9.84
NOTCH2NL	24.72	2.28	-2.52		NOTCH2NL	2.14	3.05	12.05
NOTCH3	14.34	112.67	218.31		NOTCH3	-1.93	223.35	7.8
NOTCH4	2.54	40.51	174.47		NOTCH4	-17.57	88.49	2.71
NR4A2	6.45	5.13	3.06		NR4A2	-136.29	4.26	199.78
NUMB	6.91	2.52	2.5		NUMB	-73.74	22.49	186.65
PAX5	4.46	1622.97	21151.95		PAX5	-10.99	349.38	4745.94
POFUT1	4.27	82.42	4754.48		POFUT1	-12.84	177.47	1037.37
PPARG	-1.37	46.65	162607.4		PPARG	-140.89	192.04	124761.22
PSEN1	-1.49	64.59	16191.85		PSEN1	-158.86	52.4	2513.53
PSEN2	-29.22	26.79	7155.42		PSEN2	-204.6	2.14	23746.21
PSENE1	-68.96	1.82	8175.69		PSENE1	-175.41	2.04	25153.28
PTCRA	-2.6	-1.94	-18.24		PTCRA	-13.78	1.37	10.84
RBPJL	3.8	-1.13	-1.51		RBPJL	-4.94	1.43	8.41
RFNG	13.9	13.14	203.84		RFNG	-6.83	150.54	2.54
RUNX1	44.38	185.53	108.45		RUNX1	-1.14	325.26	7.33
SEL1L	-1.12	6.25	-12.86		SEL1L	1.68	-4.14	-1.98
SH2D1A	-1.48	-7.67	-15.83		SH2D1A	-2.17	-8.36	-1.7
SHH	-9.69	1.13	148.76		SHH	2.16	1.52	2.27
SMO	-4.28	1.29	137.15		SMO	3.23	1.74	2.64

SNW1	25.69	-6.57	-51.05		SNW1	-3.39	7.44	1.66
STAT6	7.68	1.35	-7.21		STAT6	-27.08	6.02	1.65
STIL	22.31	10.03	135.04		STIL	-12.8	157.74	51.89
SUFU	21.46	126.99	107.78		SUFU	-12.74	157.74	46.7
TLE1	57.96	27.83	-1.05		TLE1	-3.72	23.98	6.77
WISP1	60.58	27.66	-1.2		WISP1	-3.21	24.77	7.04
WNT11	397.11	60518.21	82891.56		WNT11	-1.28	87724.56	954.21
ZIC2	1277.02	38367.79	31043.64		ZIC2	2.21	56529.83	109.89

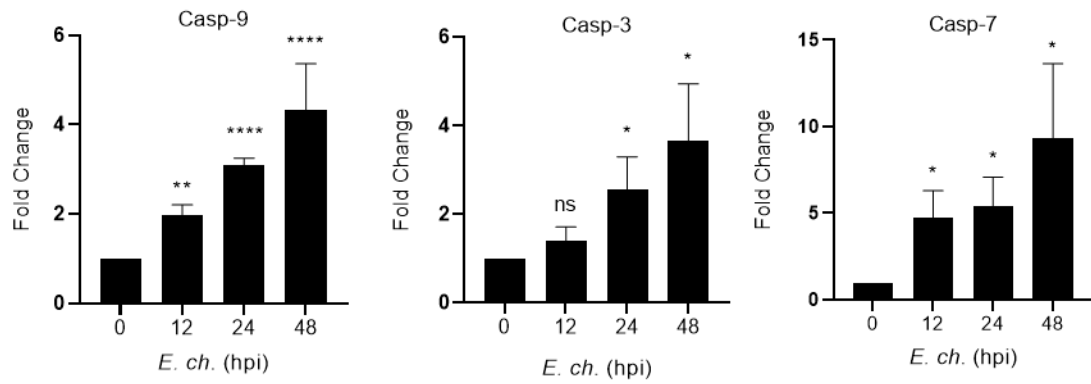
List of 84 Notch signaling pathway genes with their fold change displaying differential expression (upregulation and downregulation) at 24 h pt. with 1 ng/mL, 10 ng/mL, or 100 ng/mL of (A) TRP120-N1-P3 peptide or (B) TRP120-N1-P6 peptide.

**Appendix E: Fig S4. Inhibition of XIAP enhances apoptosis in *E.ch.*-infected cells.**



*E. ch.*-infected THP-1 cells (MOI 50) were pre-treated with DMSO or SM-164 alone (100nM, 12h) or SM164 (100nM, 12h) in combination with caspase-9 inhibitor, Z-LEHD-FMK TFA (20μM, 2h). Cell death was stimulated with TNF-α (100 ng/ml) or staurosporine (100 ng/ml, positive apoptosis control) in the indicated samples. (A) Cell viability was determined by trypan blue exclusion on the indicated treated cells. Quantification of live vs. dead cells were analyzed by Brightfield cell counting using the automated Cellometer Mini. Brightfield images were taken from the counts. Live cells are shown in green and dead cells are shown in red. (B) Percentages of live, early apoptotic, late apoptotic, total apoptotic, and dead cells were determined by the Muse® Annexin V & Dead Cell Kit. Bar graphs represent means ± SD. \*\*\*\*, P < 0.0001. Experiments were performed in triplicate (n=3) and representative images are shown.

**Appendix F: Fig S5. Pro-Caspase transcript levels are increased during *E. chaffeensis* infection.**



Changes in Caspase-9, -3 and -7 transcript levels in *E.ch.* infected and uninfected THP-1 cells (0 hpi), as measured by RT-qPCR analysis. Bar graphs represent means  $\pm$  SD. \*\*\*\*,  $P < 0.0001$ . Experiments were performed in triplicate ( $n=3$ ) and representative images are shown.

## BIBLIOGRAPHY/REFERENCES

1. Glushko, G.M., *Human ehrlichiosis. [Review] [11 refs]*. Postgraduate Medicine, 1997. **101**(6): p. 225-230.
2. Jacobs, R.F. and G.E. Schutze, *Ehrlichiosis in children. [Review] [90 refs]*. Journal of Pediatrics, 1997. **131**(2): p. 184-192.
3. Schutze, G.E., et al., *Human monocytic ehrlichiosis in children*. Pediatr Infect Dis J, 2007. **26**(6): p. 475-9.
4. Mogg, M., et al., *Increased Incidence of Ehrlichia chaffeensis Infections in the United States, 2012 Through 2016*. Vector Borne Zoonotic Dis, 2020. **20**(7): p. 547-550.
5. Childs, J.E., et al., *Outcome of diagnostic tests using samples from patients with culture-proven human monocytic ehrlichiosis: implications for surveillance*. J.Clin.Microbiol., 1999. **37**(9): p. 2997-3000.
6. McQuiston, J.H., et al., *The human ehrlichioses in the United States*. Emerg Infect Dis, 1999. **5**(5): p. 635-42.
7. Nichols Heitman, K., et al., *Increasing Incidence of Ehrlichiosis in the United States: A Summary of National Surveillance of Ehrlichia chaffeensis and Ehrlichia ewingii Infections in the United States, 2008-2012*. Am J Trop Med Hyg, 2016. **94**(1): p. 52-60.
8. Lina, T.T., et al., *Hacker within! Ehrlichia chaffeensis Effector Driven Phagocyte Reprogramming Strategy*. Front Cell Infect Microbiol, 2016. **6**: p. 58.
9. Schutze, G.E. and R.F. Jacobs, *Human monocytic ehrlichiosis in children*. Pediatrics, 1997. **100**(1): p. E10.
10. Olano, J.P., et al., *Clinical manifestations, epidemiology, and laboratory diagnosis of human monocytotropic ehrlichiosis in a commercial laboratory setting*. Clin.Diagn.Lab Immunol., 2003. **10**(5): p. 891-896.
11. Abusaada, K., S. Ajmal, and L. Hughes, *Successful Treatment of Human Monocytic Ehrlichiosis with Rifampin*. Cureus, 2016. **8**(1): p. e444.
12. Hamburg, B.J., et al., *The importance of early treatment with doxycycline in human ehrlichiosis*. Medicine (Baltimore), 2008. **87**(2): p. 53-60.
13. McBride, J.W. and D.H. Walker, *Molecular and cellular pathobiology of Ehrlichia infection: targets for new therapeutics and immunomodulation strategies*. Expert Rev Mol Med, 2011. **13**: p. e3.
14. !!! INVALID CITATION !!! [12, 13].
15. Paddock, C.D. and J.E. Childs, *Ehrlichia chaffeensis: a prototypical emerging pathogen*. Clin Microbiol Rev, 2003. **16**(1): p. 37-64.
16. Eedunuri, V.K., et al., *Protein and DNA synthesis demonstrated in cell-free Ehrlichia chaffeensis organisms in axenic medium*. Sci Rep, 2018. **8**(1): p. 9293.
17. Jaworski, D.C., et al., *Amblyomma americanum ticks infected with in vitro cultured wild-type and mutants of Ehrlichia chaffeensis are competent to produce infection in naive deer and dogs*. Ticks Tick Borne Dis, 2017. **8**(1): p. 60-64.
18. Anderson, B.E., et al., *Amblyomma americanum: a potential vector of human ehrlichiosis*. Am.J.Trop.Med.Hyg., 1993. **49**(2): p. 239-244.
19. Rikihisa, Y., *Anaplasma phagocytophilum and Ehrlichia chaffeensis: subversive manipulators of host cells*. Nat Rev Microbiol, 2010. **8**(5): p. 328-39.
20. Kocan, A.A., et al., *Attempted transmission of Ehrlichia chaffeensis among white-tailed deer by Amblyomma maculatum*. J Wildl Dis, 2000. **36**(3): p. 592-594.

21. Budachetri, K., et al., *An Entry-Triggering Protein of Ehrlichia Is a New Vaccine Candidate against Tick-Borne Human Monocytic Ehrlichiosis*. mBio, 2020. **11**(4).
22. Popov, V.L., et al., *Ultrastructural variation of cultured Ehrlichia chaffeensis*. J.Med.Microbiol., 1995. **43**(6): p. 411-421.
23. Mohan Kumar, D., et al., *Ehrlichia chaffeensis uses its surface protein EtpE to bind GPI-anchored protein DNase X and trigger entry into mammalian cells*. PLoS Pathog, 2013. **9**(10): p. e1003666.
24. Zhang, J.Z., et al., *The developmental cycle of Ehrlichia chaffeensis in vertebrate cells*. Cell Microbiol., 2007. **9**(3): p. 610-618.
25. Rikihisa, Y., *Molecular events involved in cellular invasion by Ehrlichia chaffeensis and Anaplasma phagocytophilum*. Vet Parasitol, 2010. **167**(2-4): p. 155-66.
26. Bao, W., et al., *Four VirB6 paralogs and VirB9 are expressed and interact in Ehrlichia chaffeensis-containing vacuoles*. J Bacteriol, 2009. **191**(1): p. 278-86.
27. Rikihisa, Y., et al., *Type IV secretion system of Anaplasma phagocytophilum and Ehrlichia chaffeensis*. Ann N Y Acad Sci, 2009. **1166**: p. 106-11.
28. Morgan, J.L.W., J.F. Acheson, and J. Zimmer, *Structure of a Type-1 Secretion System ABC Transporter*. Structure, 2017. **25**(3): p. 522-529.
29. Spitz, O., et al., *Type I Secretion Systems-One Mechanism for All?* Microbiol Spectr, 2019. **7**(2).
30. Alav, I., et al., *Structure, Assembly, and Function of Tripartite Efflux and Type 1 Secretion Systems in Gram-Negative Bacteria*. Chem Rev, 2021. **121**(9): p. 5479-5596.
31. Rego, A.T., V. Chandran, and G. Waksman, *Two-step and one-step secretion mechanisms in Gram-negative bacteria: contrasting the type IV secretion system and the chaperone-usher pathway of pilus biogenesis*. Biochem J, 2010. **425**(3): p. 475-88.
32. Masi, M. and C. Wandersman, *Multiple signals direct the assembly and function of a type 1 secretion system*. J Bacteriol, 2010. **192**(15): p. 3861-9.
33. Linhartova, I., et al., *RTX proteins: a highly diverse family secreted by a common mechanism*. FEMS Microbiol Rev, 2010. **34**(6): p. 1076-112.
34. Wakeel, A., et al., *Ehrlichia chaffeensis tandem repeat proteins and Ank200 are type 1 secretion system substrates related to the repeats-in-toxin exoprotein family*. Front Cell Infect Microbiol, 2011. **1**: p. 22.
35. Cheng, Z., X. Wang, and Y. Rikihisa, *Regulation of type IV secretion apparatus genes during Ehrlichia chaffeensis intracellular development by a previously unidentified protein*. J Bacteriol, 2008. **190**(6): p. 2096-105.
36. Rikihisa, Y., *The "Biological Weapons" of Ehrlichia chaffeensis: Novel Molecules and Mechanisms to Subjugate Host Cells*. Front Cell Infect Microbiol, 2021. **11**: p. 830180.
37. Yan, Q., et al., *Ehrlichia type IV secretion system effector Etf-2 binds to active RAB5 and delays endosome maturation*. Proc Natl Acad Sci U S A, 2018. **115**(38): p. E8977-E8986.
38. Elkhaily, H., C.A. Balbin, and J. Siltberg-Liberles, *Comparative Analysis of Structural Features in SLiMs from Eukaryotes, Bacteria, and Viruses with Importance for Host-Pathogen Interactions*. Pathogens, 2022. **11**(5).
39. Via, A., et al., *How pathogens use linear motifs to perturb host cell networks*. Trends Biochem Sci, 2015. **40**(1): p. 36-48.
40. Davey, N.E., G. Trave, and T.J. Gibson, *How viruses hijack cell regulation*. Trends Biochem Sci, 2011. **36**(3): p. 159-69.

41. Ko, Y., et al., *Active escape of Orientia tsutsugamushi from cellular autophagy*. Infect Immun, 2013. **81**(2): p. 552-9.
42. Niu, H. and Y. Rikihisa, *Ats-1: a novel bacterial molecule that links autophagy to bacterial nutrition*. Autophagy, 2013. **9**(5): p. 787-8.
43. Henderson, B., S. Poole, and M. Wilson, *Bacterial modulins: a novel class of virulence factors which cause host tissue pathology by inducing cytokine synthesis*. Microbiol Rev, 1996. **60**(2): p. 316-341.
44. Arena, E.T., et al., *The deubiquitinase activity of the Salmonella pathogenicity island 2 effector, SseL, prevents accumulation of cellular lipid droplets*. Infect Immun, 2011. **79**(11): p. 4392-400.
45. Saka, H.A. and R.H. Valdivia, *Acquisition of nutrients by Chlamydiae: unique challenges of living in an intracellular compartment*. Curr Opin Microbiol, 2010. **13**(1): p. 4-10.
46. Rikihisa, Y. and M. Lin, *Anaplasma phagocytophilum and Ehrlichia chaffeensis type IV secretion and Ank proteins*. Curr Opin Microbiol, 2010. **13**(1): p. 59-66.
47. Kubori, T. and H. Nagai, *Bacterial effector-involved temporal and spatial regulation by hijack of the host ubiquitin pathway*. Front Microbiol, 2011. **2**: p. 145.
48. Lafont, F. and F.G. van der Goot, *Bacterial invasion via lipid rafts*. Cell Microbiol, 2005. **7**(5): p. 613-20.
49. Moumene, A. and D.F. Meyer, *Ehrlichia's molecular tricks to manipulate their host cells*. Microbes Infect, 2016. **18**(3): p. 172-9.
50. Byerly, C.D., L.L. Patterson, and J.W. McBride, *Ehrlichia TRP effectors: moonlighting, mimicry and infection*. Pathog Dis, 2021. **79**(5).
51. Luo, T., P.S. Dunphy, and J.W. McBride, *Ehrlichia chaffeensis tandem repeat effector targets differentially influence infection*. Front Cell Infect Microbiol, 2017. **7**: p. 178.
52. Luo, T., et al., *Molecular characterization of antibody epitopes of Ehrlichia chaffeensis ankryin protein 200 and tandem repeat protein 47 and evaluation of synthetic immunodeterminants for serodiagnosis of human monocytotropic ehrlichiosis*. Clin Vaccine Immunol, 2010. **17**(1): p. 87-97.
53. Luo, T., X. Zhang, and J.W. McBride, *Major species-specific antibody epitopes of the Ehrlichia chaffeensis p120 and E. canis p140 orthologs in surface-exposed tandem repeat regions*. Clin Vaccine Immunol, 2009. **16**(7): p. 982-90.
54. Doyle, C.K., et al., *Differentially expressed and secreted major immunoreactive protein orthologs of Ehrlichia canis and E. chaffeensis elicit early antibody responses to epitopes on glycosylated tandem repeats*. Infect Immun, 2006. **74**(1): p. 711-20.
55. Luo, T., et al., *A variable-length PCR target protein of Ehrlichia chaffeensis contains major species-specific antibody epitopes in acidic serine-rich tandem repeats*. Infect Immun, 2008. **76**(4): p. 1572-80.
56. Luo, T., S. Mitra, and J.W. McBride, *Ehrlichia chaffeensis TRP75 interacts with host cell targets involved in homeostasis, cytoskeleton organization, and apoptosis regulation to promote infection*. mSphere, 2018. **3**(2).
57. McBride, J.W., et al., *Tyrosine-phosphorylated Ehrlichia chaffeensis and Ehrlichia canis tandem repeat orthologs contain a major continuous cross-reactive antibody epitope in lysine-rich repeats*. Infect Immun, 2011. **79**(8): p. 3178-87.
58. Wakeel, A., X. Zhang, and J.W. McBride, *Mass spectrometric analysis of Ehrlichia chaffeensis tandem repeat proteins reveals evidence of phosphorylation and absence of glycosylation*. PLoS One, 2010. **5**(3): p. e9552.

59. Popov, V.L., X. Yu, and D.H. Walker, *The 120 kDa outer membrane protein of Ehrlichia chaffeensis: preferential expression on dense-core cells and gene expression in Escherichia coli associated with attachment and entry*. Microb Pathog, 2000. **28**(2): p. 71-80.
60. Luo, T., et al., *Ehrlichia chaffeensis TRP120 interacts with a diverse array of eukaryotic proteins involved in transcription, signaling, and cytoskeleton organization*. Infect Immun, 2011. **79**(11): p. 4382-91.
61. Luo, T. and J.W. McBride, *Ehrlichia chaffeensis TRP32 interacts with host cell targets that influence intracellular survival*. Infect Immun, 2012. **80**(7): p. 2297-306.
62. Kibler, C.E., et al., *Ehrlichia chaffeensis TRP47 enters the nucleus via a MYND-binding domain-dependent mechanism and predominantly binds enhancers of host genes associated with signal transduction, cytoskeletal organization, and immune response*. PLoS One, 2018. **13**(11): p. e0205983.
63. Dunphy, P.S., T. Luo, and J.W. McBride, *Ehrlichia chaffeensis exploits host SUMOylation pathways to mediate effector-host interactions and promote intracellular survival*. Infect Immun, 2014. **82**(10): p. 4154-68.
64. Wang, J.Y., et al., *Ehrlichia chaffeensis TRP120-mediated ubiquitination and proteasomal degradation of tumor suppressor FBW7 increases oncoprotein stability and promotes infection*. PLoS Pathog, 2020. **16**(4): p. e1008541.
65. Zhu, B., et al., *Ehrlichia chaffeensis TRP120 moonlights as a HECT E3 ligase involved in self- and host ubiquitination to influence protein interactions and stability for intracellular survival*. Infect Immun, 2017. **85**(9).
66. Klema, V.J., et al., *Ehrlichia chaffeensis TRP120 nucleomodulin binds DNA with disordered tandem repeat domain*. PLoS One, 2018. **13**(4): p. e0194891.
67. Farris, T.R., et al., *Ehrlichia chaffeensis TRP32 is a Nucleomodulin that Directly Regulates Expression of Host Genes Governing Differentiation and Proliferation*. Infect Immun, 2016. **84**(11): p. 3182-3194.
68. Zhu, B., et al., *Ehrlichia chaffeensis TRP120 binds a G+C-rich motif in host cell DNA and exhibits eukaryotic transcriptional activator function*. Infect Immun, 2011. **79**(11): p. 4370-81.
69. Mitra, S., et al., *Ehrlichia chaffeensis TRP120 effector targets and recruits host polycomb group proteins for degradation to promote intracellular infection*. Infect Immun, 2018. **86**(4).
70. van der Lee, R., et al., *Classification of intrinsically disordered regions and proteins*. Chem Rev, 2014. **114**(13): p. 6589-631.
71. Van Roey, K., et al., *Short linear motifs: ubiquitous and functionally diverse protein interaction modules directing cell regulation*. Chem Rev, 2014. **114**(13): p. 6733-78.
72. Davey, N.E., et al., *Attributes of short linear motifs*. Mol Biosyst, 2012. **8**(1): p. 268-81.
73. Dinkel, H., et al., *ELM--the database of eukaryotic linear motifs*. Nucleic Acids Res, 2012. **40**(Database issue): p. D242-51.
74. Davey, N.E., et al., *SLiMSearch 2.0: biological context for short linear motifs in proteins*. Nucleic Acids Res, 2011. **39**(Web Server issue): p. W56-60.
75. Samano-Sanchez, H. and T.J. Gibson, *Mimicry of Short Linear Motifs by Bacterial Pathogens: A Drugging Opportunity*. Trends Biochem Sci, 2020. **45**(6): p. 526-544.
76. Ijdo, J.W., A.C. Carlson, and E.L. Kennedy, *Anaplasma phagocytophilum AnkA is tyrosine-phosphorylated at EPIYA motifs and recruits SHP-1 during early infection*. Cell Microbiol., 2007. **9**(5): p. 1284-1296.

77. Tompa, P., et al., *A million peptide motifs for the molecular biologist*. Mol Cell, 2014. **55**(2): p. 161-9.
78. Kumar, M., et al., *ELM-the eukaryotic linear motif resource in 2020*. Nucleic Acids Res, 2020. **48**(D1): p. D296-D306.
79. Rogan, M.R., et al., *Ehrlichia chaffeensis TRP120 is a Wnt ligand mimetic that interacts with Wnt receptors and contains a novel repetitive short linear motif that activates Wnt signaling*. mSphere, 2021. **6**(2).
80. Byerly, C.D., et al., *Ehrlichia SLiM ligand mimetic activates Hedgehog signaling to engage a BCL-2 anti-apoptotic cellular program*. PLoS Pathog, 2022. **18**(5): p. e1010345.
81. Patterson, L.L., et al., *Ehrlichia SLiM ligand mimetic activates Notch signaling in human monocytes*. mBio, 2022. **13**(2): p. e0007622.
82. Galan, J.E., *Common themes in the design and function of bacterial effectors*. Cell Host Microbe, 2009. **5**(6): p. 571-9.
83. Zhu, B. and J.W. McBride, *Alpha Enolase 1 Ubiquitination and Degradation Mediated by Ehrlichia chaffeensis TRP120 Disrupts Glycolytic Flux and Promotes Infection*. Pathogens, 2021. **10**(8).
84. Lina, T.T., et al., *Ehrlichia Activation of Wnt-PI3K-mTOR Signaling Inhibits Autolysosome Generation and Autophagic Destruction by the Mononuclear Phagocyte*. Infect Immun, 2017. **85**(12).
85. Luo, T., et al., *Ehrlichia chaffeensis exploits canonical and noncanonical host Wnt signaling pathways to stimulate phagocytosis and promote intracellular survival*. Infect Immun, 2015. **84**(3): p. 686-700.
86. Nusse, R., *Wnt signaling*. Cold Spring Harb Perspect Biol, 2012. **4**(5).
87. Jamieson, C., M. Sharma, and B.R. Henderson, *Wnt signaling from membrane to nucleus: beta-catenin caught in a loop*. Int J Biochem Cell Biol, 2012. **44**(6): p. 847-50.
88. Polakis, P., *Wnt signaling in cancer*. Cold Spring Harb Perspect Biol, 2012. **4**(5).
89. Voloshanenko, O., et al., *Mapping of Wnt-Frizzled interactions by multiplex CRISPR targeting of receptor gene families*. FASEB J, 2017. **31**(11): p. 4832-4844.
90. Jia, Y., Y. Wang, and J. Xie, *The Hedgehog pathway: role in cell differentiation, polarity and proliferation*. Arch Toxicol, 2015. **89**(2): p. 179-91.
91. Varjosalo, M. and J. Taipale, *Hedgehog signaling*. J Cell Sci, 2007. **120**(Pt 1): p. 3-6.
92. Kanda, S., et al., *Anti-apoptotic role of the sonic hedgehog signaling pathway in the proliferation of ameloblastoma*. Int J Oncol, 2013. **43**(3): p. 695-702.
93. Zhu, S.L., et al., *Sonic hedgehog signalling pathway regulates apoptosis through Smo protein in human umbilical vein endothelial cells*. Rheumatology (Oxford), 2015. **54**(6): p. 1093-102.
94. Lina, T.T., et al., *Ehrlichia chaffeensis TRP120 Activates Canonical Notch Signaling To Downregulate TLR2/4 Expression and Promote Intracellular Survival*. mBio, 2016. **7**(4).
95. Kim, M.Y., et al., *Downregulation by lipopolysaccharide of Notch signaling, via nitric oxide*. J Cell Sci, 2008. **121**(Pt 9): p. 1466-76.
96. Tsao, P.N., et al., *Lipopolysaccharide-induced Notch signaling activation through JNK-dependent pathway regulates inflammatory response*. J Biomed Sci, 2011. **18**: p. 56.
97. Singh, S.B., et al., *Notch Signaling Pathway Is Activated by Sulfate Reducing Bacteria*. Front Cell Infect Microbiol, 2021. **11**: p. 695299.

98. Narayana, Y. and K.N. Balaji, *NOTCH1 up-regulation and signaling involved in Mycobacterium bovis BCG-induced SOCS3 expression in macrophages*. J Biol Chem, 2008. **283**(18): p. 12501-11.
99. Hori, K., A. Sen, and S. Artavanis-Tsakonas, *Notch signaling at a glance*. J Cell Sci, 2013. **126**(Pt 10): p. 2135-40.
100. Borggreffe, T. and F. Oswald, *The Notch signaling pathway: transcriptional regulation at Notch target genes*. Cell Mol Life Sci, 2009. **66**(10): p. 1631-46.
101. Artavanis-Tsakonas, S., M.D. Rand, and R.J. Lake, *Notch signaling: cell fate control and signal integration in development*. Science, 1999. **284**(5415): p. 770-6.
102. Kwon, C., et al., *Notch post-translationally regulates beta-catenin protein in stem and progenitor cells*. Nat Cell Biol, 2011. **13**(10): p. 1244-51.
103. Tasca, A., et al., *Notch signaling induces either apoptosis or cell fate change in multiciliated cells during mucociliary tissue remodeling*. Dev Cell, 2021. **56**(4): p. 525-539 e6.
104. Zweidler-McKay, P.A., et al., *Notch signaling is a potent inducer of growth arrest and apoptosis in a wide range of B-cell malignancies*. Blood, 2005. **106**(12): p. 3898-906.
105. Palaga, T., et al., *Notch signaling is activated by TLR stimulation and regulates macrophage functions*. Eur J Immunol, 2008. **38**(1): p. 174-83.
106. Urbanek, K., et al., *Notch signaling pathway and gene expression profiles during early in vitro differentiation of liver-derived mesenchymal stromal cells to osteoblasts*. Lab Invest, 2017. **97**(10): p. 1225-1234.
107. De Falco, F., et al., *Notch signaling sustains the expression of Mcl-1 and the activity of eIF4E to promote cell survival in CLL*. Oncotarget, 2015. **6**(18): p. 16559-72.
108. Guruharsha, K.G., M.W. Kankel, and S. Artavanis-Tsakonas, *The Notch signalling system: recent insights into the complexity of a conserved pathway*. Nat Rev Genet, 2012. **13**(9): p. 654-66.
109. Radtke, F., et al., *Deficient T cell fate specification in mice with an induced inactivation of Notch1*. Immunity, 1999. **10**(5): p. 547-58.
110. Zhang, Q., et al., *Notch signal suppresses Toll-like receptor-triggered inflammatory responses in macrophages by inhibiting extracellular signal-regulated kinase 1/2-mediated nuclear factor kappaB activation*. J Biol Chem, 2012. **287**(9): p. 6208-17.
111. Nakano, N., et al., *Notch1-mediated signaling induces MHC class II expression through activation of class II transactivator promoter III in mast cells*. J Biol Chem, 2011. **286**(14): p. 12042-8.
112. Radtke, F., H.R. MacDonald, and F. Tacchini-Cottier, *Regulation of innate and adaptive immunity by Notch*. Nat Rev Immunol, 2013. **13**(6): p. 427-37.
113. Pancewicz, J. and C. Nicot, *Current views on the role of Notch signaling and the pathogenesis of human leukemia*. BMC Cancer, 2011. **11**: p. 502.
114. Katoh, M., *Networking of WNT, FGF, Notch, BMP, and Hedgehog signaling pathways during carcinogenesis*. Stem Cell Rev, 2007. **3**(1): p. 30-8.
115. Mizuno, T., et al., *Clinical and Genetic Aspects of CADASIL*. Front Aging Neurosci, 2020. **12**: p. 91.
116. Masek, J. and E.R. Andersson, *The developmental biology of genetic Notch disorders*. Development, 2017. **144**(10): p. 1743-1763.
117. Larabee, J. and J. Ballard, *Modulation of Notch signaling by intracellular bacterial toxins*. FASEB Journal, 2014. **28**(1).

118. Kopan, R. and M.X. Ilagan, *The canonical Notch signaling pathway: unfolding the activation mechanism*. Cell, 2009. **137**(2): p. 216-33.
119. D'Souza, B., A. Miyamoto, and G. Weinmaster, *The many facets of Notch ligands*. Oncogene, 2008. **27**(38): p. 5148-67.
120. Wang, M.M., *Notch signaling and Notch signaling modifiers*. Int J Biochem Cell Biol, 2011. **43**(11): p. 1550-62.
121. Sprinzak, D. and S.C. Blacklow, *Biophysics of Notch Signaling*. Annu Rev Biophys, 2021. **50**: p. 157-189.
122. Gomez-Lamarca, M.J., et al., *Activation of the Notch Signaling Pathway In Vivo Elicits Changes in CSL Nuclear Dynamics*. Dev Cell, 2018. **44**(5): p. 611-623 e7.
123. Krejci, A. and S. Bray, *Notch activation stimulates transient and selective binding of Su(H)/CSL to target enhancers*. Genes Dev, 2007. **21**(11): p. 1322-7.
124. Chillakuri, C.R., et al., *Notch receptor-ligand binding and activation: insights from molecular studies*. Semin Cell Dev Biol, 2012. **23**(4): p. 421-8.
125. Brou, C., et al., *A novel proteolytic cleavage involved in Notch signaling: the role of the disintegrin-metalloprotease TACE*. Mol Cell, 2000. **5**(2): p. 207-16.
126. Bozkulak, E.C. and G. Weinmaster, *Selective use of ADAM10 and ADAM17 in activation of Notch1 signaling*. Mol Cell Biol, 2009. **29**(21): p. 5679-95.
127. Logeat, F., et al., *The Notch1 receptor is cleaved constitutively by a furin-like convertase*. Proc Natl Acad Sci U S A, 1998. **95**(14): p. 8108-12.
128. Hambleton, S., et al., *Structural and functional properties of the human notch-1 ligand binding region*. Structure, 2004. **12**(12): p. 2173-83.
129. Stephenson, N.L. and J.M. Avis, *Direct observation of proteolytic cleavage at the S2 site upon forced unfolding of the Notch negative regulatory region*. Proc Natl Acad Sci U S A, 2012. **109**(41): p. E2757-65.
130. Sorensen, E.B. and S.D. Conner, *gamma-secretase-dependent cleavage initiates notch signaling from the plasma membrane*. Traffic, 2010. **11**(9): p. 1234-45.
131. Barrick, D. and R. Kopan, *The Notch transcription activation complex makes its move*. Cell, 2006. **124**(5): p. 883-5.
132. Moellering, R.E., et al., *Direct inhibition of the NOTCH transcription factor complex*. Nature, 2009. **462**(7270): p. 182-8.
133. Monahan, P., S. Rybak, and L.T. Raetzman, *The notch target gene HES1 regulates cell cycle inhibitor expression in the developing pituitary*. Endocrinology, 2009. **150**(9): p. 4386-94.
134. Fischer, A., et al., *The Notch target genes Hey1 and Hey2 are required for embryonic vascular development*. Genes Dev, 2004. **18**(8): p. 901-11.
135. Pandey, A., et al., *Glycosylation of Specific Notch EGF Repeats by O-Fut1 and Fringe Regulates Notch Signaling in Drosophila*. Cell Rep, 2019. **29**(7): p. 2054-2066 e6.
136. Yamamoto, S., W.L. Charng, and H.J. Bellen, *Endocytosis and intracellular trafficking of Notch and its ligands*. Curr Top Dev Biol, 2010. **92**: p. 165-200.
137. Moretti, J. and C. Brou, *Ubiquitinations in the notch signaling pathway*. Int J Mol Sci, 2013. **14**(3): p. 6359-81.
138. Cornell, M., et al., *The Drosophila melanogaster Suppressor of deltex gene, a regulator of the Notch receptor signaling pathway, is an E3 class ubiquitin ligase*. Genetics, 1999. **152**(2): p. 567-76.
139. Wilkin, M.B., et al., *Regulation of notch endosomal sorting and signaling by Drosophila Nedd4 family proteins*. Curr Biol, 2004. **14**(24): p. 2237-44.

140. Monticone, G., et al., *Targeting the Cbl-b-Notch1 axis as a novel immunotherapeutic strategy to boost CD8+ T-cell responses*. Front Immunol, 2022. **13**: p. 987298.
141. Kim, H. and Z.A. Ronai, *Rewired Notch/p53 by Numb'ing Mdm2*. J Cell Biol, 2018. **217**(2): p. 445-446.
142. Matsumoto, A., et al., *Fbxw7-dependent degradation of Notch is required for control of "stemness" and neuronal-glia differentiation in neural stem cells*. J Biol Chem, 2011. **286**(15): p. 13754-64.
143. Kar, R., et al., *The FBXW7-NOTCH interactome: A ubiquitin proteasomal system-induced crosstalk modulating oncogenic transformation in human tissues*. Cancer Rep (Hoboken), 2021. **4**(4): p. e1369.
144. Yeh, C.H., M. Bellon, and C. Nicot, *FBXW7: a critical tumor suppressor of human cancers*. Mol Cancer, 2018. **17**(1): p. 115.
145. Davis, R.J., M. Welcker, and B.E. Clurman, *Tumor suppression by the Fbw7 ubiquitin ligase: mechanisms and opportunities*. Cancer Cell, 2014. **26**(4): p. 455-64.
146. Rand, M.D., et al., *Calcium depletion dissociates and activates heterodimeric notch receptors*. Mol Cell Biol, 2000. **20**(5): p. 1825-35.
147. Steinbuck, M.P. and S. Winandy, *A Review of Notch Processing With New Insights Into Ligand-Independent Notch Signaling in T-Cells*. Front Immunol, 2018. **9**: p. 1230.
148. Wang, W., T. Okajima, and H. Takeuchi, *Significant Roles of Notch O-Glycosylation in Cancer*. Molecules, 2022. **27**(6).
149. Habets, R.A., et al., *Human NOTCH2 Is Resistant to Ligand-independent Activation by Metalloprotease Adam17*. J Biol Chem, 2015. **290**(23): p. 14705-16.
150. Tosello, V. and A.A. Ferrando, *The NOTCH signaling pathway: role in the pathogenesis of T-cell acute lymphoblastic leukemia and implication for therapy*. Ther Adv Hematol, 2013. **4**(3): p. 199-210.
151. Lubman, O.Y., S.V. Korolev, and R. Kopan, *Anchoring notch genetics and biochemistry; structural analysis of the ankyrin domain sheds light on existing data*. Mol Cell, 2004. **13**(5): p. 619-26.
152. D'Souza, B., L. Meloty-Kapella, and G. Weinmaster, *Canonical and non-canonical Notch ligands*. Curr Top Dev Biol, 2010. **92**: p. 73-129.
153. Cordle, J., et al., *A conserved face of the Jagged/Serrate DSL domain is involved in Notch trans-activation and cis-inhibition*. Nat Struct Mol Biol, 2008. **15**(8): p. 849-57.
154. Andrawes, M.B., et al., *Intrinsic selectivity of Notch 1 for Delta-like 4 over Delta-like 1*. J Biol Chem, 2013. **288**(35): p. 25477-25489.
155. Handford, P.A., et al., *Structural Insights into Notch Receptor-Ligand Interactions*. Adv Exp Med Biol, 2018. **1066**: p. 33-46.
156. Hirano, K.I., et al., *Delta-like 1 and Delta-like 4 differently require their extracellular domains for triggering Notch signaling in mice*. Elife, 2020. **9**.
157. Vitt, U.A., S.Y. Hsu, and A.J. Hsueh, *Evolution and classification of cystine knot-containing hormones and related extracellular signaling molecules*. Mol Endocrinol, 2001. **15**(5): p. 681-94.
158. Shaye, D.D. and I. Greenwald, *LIN-12/Notch trafficking and regulation of DSL ligand activity during vulval induction in Caenorhabditis elegans*. Development, 2005. **132**(22): p. 5081-92.
159. Pintar, A., et al., *The intracellular region of Notch ligands: does the tail make the difference?* Biol Direct, 2007. **2**: p. 19.

160. Mizuhara, E., et al., *MAG11 recruits Dll1 to cadherin-based adherens junctions and stabilizes it on the cell surface*. J Biol Chem, 2005. **280**(28): p. 26499-507.
161. Hu, B., et al., *[Over-expression of human Notch ligand Delta-like 3 promotes proliferation of human gastric cancer cells in vitro]*. Nan Fang Yi Ke Da Xue Xue Bao, 2018. **38**(1): p. 14-19.
162. Ladi, E., et al., *The divergent DSL ligand Dll3 does not activate Notch signaling but cell autonomously attenuates signaling induced by other DSL ligands*. J Cell Biol, 2005. **170**(6): p. 983-92.
163. Chapman, G., et al., *Notch inhibition by the ligand DELTA-LIKE 3 defines the mechanism of abnormal vertebral segmentation in spondylocostal dysostosis*. Hum Mol Genet, 2011. **20**(5): p. 905-16.
164. Shimizu, K., et al., *Mouse jagged1 physically interacts with notch2 and other notch receptors. Assessment by quantitative methods*. J Biol Chem, 1999. **274**(46): p. 32961-9.
165. Luca, V.C., et al., *Notch-Jagged complex structure implicates a catch bond in tuning ligand sensitivity*. Science, 2017. **355**(6331): p. 1320-1324.
166. Luca, V.C., et al., *Structural biology. Structural basis for Notch1 engagement of Delta-like 4*. Science, 2015. **347**(6224): p. 847-53.
167. Kershaw, N.J., et al., *Notch ligand delta-like1: X-ray crystal structure and binding affinity*. Biochem J, 2015. **468**(1): p. 159-66.
168. Hu, Q.D., et al., *F3/contactin acts as a functional ligand for Notch during oligodendrocyte maturation*. Cell, 2003. **115**(2): p. 163-75.
169. Eiraku, M., et al., *DNER acts as a neuron-specific Notch ligand during Bergmann glial development*. Nat Neurosci, 2005. **8**(7): p. 873-80.
170. Bray, S.J., et al., *The atypical mammalian ligand Delta-like homologue 1 (Dlk1) can regulate Notch signalling in Drosophila*. BMC Dev Biol, 2008. **8**: p. 11.
171. Baladron, V., et al., *dlk acts as a negative regulator of Notch1 activation through interactions with specific EGF-like repeats*. Exp Cell Res, 2005. **303**(2): p. 343-59.
172. Finn, J., et al., *Dlk1-Mediated Temporal Regulation of Notch Signaling Is Required for Differentiation of Alveolar Type II to Type I Cells during Repair*. Cell Rep, 2019. **26**(11): p. 2942-2954 e5.
173. Komatsu, H., et al., *OSM-11 facilitates LIN-12 Notch signaling during Caenorhabditis elegans vulval development*. PLoS Biol, 2008. **6**(8): p. e196.
174. Greene, M., et al., *Delta/Notch-Like EGF-Related Receptor (DNER) Is Not a Notch Ligand*. PLoS One, 2016. **11**(9): p. e0161157.
175. Meng, H., et al., *Thrombospondin 2 potentiates notch3/jagged1 signaling*. J Biol Chem, 2009. **284**(12): p. 7866-74.
176. Lu, Z.H., J.T. Books, and T.J. Ley, *Cold shock domain family members YB-1 and MSY4 share essential functions during murine embryogenesis*. Mol Cell Biol, 2006. **26**(22): p. 8410-7.
177. Rauen, T., et al., *YB-1 acts as a ligand for Notch-3 receptors and modulates receptor activation*. J Biol Chem, 2009. **284**(39): p. 26928-40.
178. Nichol, D., et al., *Impaired angiogenesis and altered Notch signaling in mice overexpressing endothelial Eglf7*. Blood, 2010. **116**(26): p. 6133-43.
179. Best, S.M., *Viral subversion of apoptotic enzymes: escape from death row*. Annu Rev Microbiol, 2008. **62**: p. 171-92.
180. Zhang, J.Z., et al., *Survival strategy of obligately intracellular Ehrlichia chaffeensis: novel modulation of immune response and host cell cycles*. Infect Immun, 2004. **72**(1): p. 498-507.

181. Faherty, C.S. and A.T. Maurelli, *Staying alive: bacterial inhibition of apoptosis during infection*. Trends Microbiol, 2008. **16**(4): p. 173-80.
182. Fu, T.M., et al., *Cryo-EM Structure of Caspase-8 Tandem DED Filament Reveals Assembly and Regulation Mechanisms of the Death-Inducing Signaling Complex*. Mol Cell, 2016. **64**(2): p. 236-250.
183. Hughes, M.A., et al., *Co-operative and Hierarchical Binding of c-FLIP and Caspase-8: A Unified Model Defines How c-FLIP Isoforms Differentially Control Cell Fate*. Mol Cell, 2016. **61**(6): p. 834-49.
184. Beaudouin, J., et al., *Caspase-8 cleaves its substrates from the plasma membrane upon CD95-induced apoptosis*. Cell Death Differ, 2013. **20**(4): p. 599-610.
185. Fulda, S. and K.M. Debatin, *Extrinsic versus intrinsic apoptosis pathways in anticancer chemotherapy*. Oncogene, 2006. **25**(34): p. 4798-811.
186. Kim, H.E., et al., *Formation of apoptosome is initiated by cytochrome c-induced dATP hydrolysis and subsequent nucleotide exchange on Apaf-1*. Proc Natl Acad Sci U S A, 2005. **102**(49): p. 17545-50.
187. Brentnall, M., et al., *Caspase-9, caspase-3 and caspase-7 have distinct roles during intrinsic apoptosis*. BMC Cell Biol, 2013. **14**: p. 32.
188. Riedl, S.J. and Y. Shi, *Molecular mechanisms of caspase regulation during apoptosis*. Nat Rev Mol Cell Biol, 2004. **5**(11): p. 897-907.
189. Rikihisa, Y., *Ehrlichia subversion of host innate responses*. Curr Opin Microbiol, 2006. **9**(1): p. 95-101.
190. Liu, H., et al., *Ehrlichia type IV secretion effector ECH0825 is translocated to mitochondria and curbs ROS and apoptosis by upregulating host MnSOD*. Cell Microbiol, 2012. **14**(7): p. 1037-50.
191. Schimmer, A.D., *Inhibitor of apoptosis proteins: translating basic knowledge into clinical practice*. Cancer Res, 2004. **64**(20): p. 7183-90.
192. Silke, J. and P. Meier, *Inhibitor of apoptosis (IAP) proteins-modulators of cell death and inflammation*. Cold Spring Harb Perspect Biol, 2013. **5**(2).
193. Duckett, C.S., et al., *A conserved family of cellular genes related to the baculovirus iap gene and encoding apoptosis inhibitors*. EMBO J, 1996. **15**(11): p. 2685-94.
194. Riedl, S.J., et al., *Structural basis for the inhibition of caspase-3 by XIAP*. Cell, 2001. **104**(5): p. 791-800.
195. Rajalingam, K., et al., *IAP-IAP complexes required for apoptosis resistance of C. trachomatis-infected cells*. PLoS Pathog, 2006. **2**(10): p. e114.
196. Deveraux, Q.L., et al., *Cleavage of human inhibitor of apoptosis protein XIAP results in fragments with distinct specificities for caspases*. EMBO J, 1999. **18**(19): p. 5242-51.
197. Scott, F.L., et al., *XIAP inhibits caspase-3 and -7 using two binding sites: evolutionarily conserved mechanism of IAPs*. EMBO J, 2005. **24**(3): p. 645-55.
198. Lu, M., et al., *XIAP induces NF-kappaB activation via the BIR1/TAB1 interaction and BIR1 dimerization*. Mol Cell, 2007. **26**(5): p. 689-702.
199. Sun, C., et al., *NMR structure and mutagenesis of the third Bir domain of the inhibitor of apoptosis protein XIAP*. J Biol Chem, 2000. **275**(43): p. 33777-81.
200. Shiozaki, E.N., et al., *Mechanism of XIAP-mediated inhibition of caspase-9*. Mol Cell, 2003. **11**(2): p. 519-27.
201. Hornle, M., et al., *Caspase-3 cleaves XIAP in a positive feedback loop to sensitize melanoma cells to TRAIL-induced apoptosis*. Oncogene, 2011. **30**(5): p. 575-87.

202. Galban, S. and C.S. Duckett, *XIAP as a ubiquitin ligase in cellular signaling*. Cell Death Differ, 2010. **17**(1): p. 54-60.
203. Srinivasula, S.M., et al., *A conserved XIAP-interaction motif in caspase-9 and Smac/DIABLO regulates caspase activity and apoptosis*. Nature, 2001. **410**(6824): p. 112-6.
204. Liu, W.H., et al., *Notch inhibits apoptosis by direct interference with XIAP ubiquitination and degradation*. EMBO J, 2007. **26**(6): p. 1660-9.
205. Olano, J.P., et al., *Human monocytotropic ehrlichiosis, Missouri*. Emerg.Infect.Dis., 2003. **9**(12): p. 1579-1586.
206. Fishbein, D.B., J.E. Dawson, and L.E. Robinson, *Human ehrlichiosis in the United States, 1985 to 1990*. Ann.Intern.Med., 1994. **120**(9): p. 736-743.
207. Paparone, P.W., et al., *Ehrlichiosis with pancytopenia and ARDS*. New Jersey Med., 1995. **92**(6): p. 381-385.
208. Patel, R.G. and M.A. Byrd, *Near fatal acute respiratory distress syndrome in a patient with human ehrlichiosis*. South Med.J., 1999. **92**(3): p. 333-335.
209. Dumler, J.S., et al., *Ehrlichioses in humans: epidemiology, clinical presentation, diagnosis, and treatment*. Clin.Infect.Dis., 2007. **45 Suppl 1**: p. S45-S51.
210. Keewan, E. and S.A. Naser, *Notch-1 Signaling Modulates Macrophage Polarization and Immune Defense against Mycobacterium avium paratuberculosis Infection in Inflammatory Diseases*. Microorganisms, 2020. **8**(7).
211. Palaga, T., et al., *Notch signaling regulates expression of Mcl-1 and apoptosis in PPD-treated macrophages*. Cell Mol Immunol, 2013. **10**(5): p. 444-52.
212. Rikihisa, Y., *Molecular Pathogenesis of Ehrlichia chaffeensis Infection*. Annu Rev Microbiol, 2015. **69**: p. 283-304.
213. Velayutham, T.S., et al., *Ehrlichia chaffeensis outer membrane protein 1-specific human antibody-mediated immunity is defined by intracellular TRIM21-dependent innate immune activation and extracellular neutralization*. Infect Immun, 2019. **87**(12).
214. Baonza, A. and A. Garcia-Bellido, *Notch signaling directly controls cell proliferation in the Drosophila wing disc*. Proc Natl Acad Sci U S A, 2000. **97**(6): p. 2609-14.
215. Hoyne, G.F., *Notch signaling in the immune system*. J Leukoc Biol, 2003. **74**(6): p. 971-81.
216. Sarin, A. and N. Marcel, *The NOTCH1-autophagy interaction: Regulating self-eating for survival*. Autophagy, 2017. **13**(2): p. 446-447.
217. Miele, L. and B. Osborne, *Arbiter of differentiation and death: Notch signaling meets apoptosis*. J Cell Physiol, 1999. **181**(3): p. 393-409.
218. Edwards, R.J., et al., *Interactome-wide prediction of short, disordered protein interaction motifs in humans*. Mol Biosyst, 2012. **8**(1): p. 282-95.
219. Symmons, M.F., et al., *The assembled structure of a complete tripartite bacterial multidrug efflux pump*. Proc Natl Acad Sci U S A, 2009. **106**(17): p. 7173-8.
220. Chemes, L.B., G. de Prat-Gay, and I.E. Sanchez, *Convergent evolution and mimicry of protein linear motifs in host-pathogen interactions*. Curr Opin Struct Biol, 2015. **32**: p. 91-101.
221. Drayman, N., et al., *Pathogens use structural mimicry of native host ligands as a mechanism for host receptor engagement*. Cell Host Microbe, 2013. **14**(1): p. 63-73.
222. Price, C.T., et al., *Molecular mimicry by an F-box effector of Legionella pneumophila hijacks a conserved polyubiquitination machinery within macrophages and protozoa*. PLoS Pathog, 2009. **5**(12): p. e1000704.

223. Veljkovic, V., et al., *Use of the informational spectrum methodology for rapid biological analysis of the novel coronavirus 2019-nCoV: prediction of potential receptor, natural reservoir, tropism and therapeutic/vaccine target.* F1000Res, 2020. **9**: p. 52.
224. Whiteman, P., et al., *Molecular basis for Jagged-1/Serrate ligand recognition by the Notch receptor.* J Biol Chem, 2013. **288**(10): p. 7305-12.
225. Bruckner, A., et al., *Yeast two-hybrid, a powerful tool for systems biology.* Int J Mol Sci, 2009. **10**(6): p. 2763-88.
226. Gomez-Valero, L., et al., *Comparative and functional genomics of legionella identified eukaryotic like proteins as key players in host-pathogen interactions.* Front Microbiol, 2011. **2**: p. 208.
227. Roy, C.R., *The Dot/lcm transporter of Legionella pneumophila: a bacterial conductor of vesicle trafficking that orchestrates the establishment of a replicative organelle in eukaryotic hosts.* Int J Med Microbiol, 2002. **291**(6-7): p. 463-7.
228. Nagai, H. and C.R. Roy, *The DotA protein from Legionella pneumophila is secreted by a novel process that requires the Dot/lcm transporter.* EMBO J, 2001. **20**(21): p. 5962-70.
229. Huang, L., et al., *The E Block motif is associated with Legionella pneumophila translocated substrates.* Cell Microbiol, 2011. **13**(2): p. 227-45.
230. Ravi Chandra, B., et al., *Distribution of proline-rich (PxxP) motifs in distinct proteomes: functional and therapeutic implications for malaria and tuberculosis.* Protein Eng Des Sel, 2004. **17**(2): p. 175-82.
231. Semenova, D., et al., *Dose-dependent mechanism of Notch action in promoting osteogenic differentiation of mesenchymal stem cells.* Cell Tissue Res, 2020. **379**(1): p. 169-179.
232. Maveyraud, L. and L. Mourey, *Protein X-ray Crystallography and Drug Discovery.* Molecules, 2020. **25**(5).
233. Zhu, B., et al., *Analysis of Ehrlichia chaffeensis Multifunctional TRP120 Effector Ubiquitinylation by Microfluidic Peptide Array.*, in *American Society of Microbiology Annual Meeting.* 2015.
234. Luo, T., et al., *Ehrlichia chaffeensis and E. canis hypothetical protein immunoanalysis reveals small secreted immunodominant proteins and conformation-dependent antibody epitopes.* NPJ Vaccines, 2020. **5**: p. 85.
235. Kuriakose, J.A., et al., *Molecular basis of antibody mediated immunity against Ehrlichia chaffeensis involves species-specific linear epitopes in tandem repeat proteins.* Microbes Infect, 2012. **14**(12): p. 1054-63.
236. McBride, J.W., J.E. Comer, and D.H. Walker, *Novel Immunoreactive glycoprotein orthologs of Ehrlichia spp.* Ann N Y Acad Sci, 2003. **990**: p. 678-84.
237. McBride, J.W., et al., *Kinetics of antibody response to Ehrlichia canis immunoreactive proteins.* Infect Immun, 2003. **71**(5): p. 2516-24.
238. Bock, F.J. and S.W.G. Tait, *Mitochondria as multifaceted regulators of cell death.* Nat Rev Mol Cell Biol, 2020. **21**(2): p. 85-100.
239. Abe, Y., et al., *Hedgehog signaling overrides p53-mediated tumor suppression by activating Mdm2.* Proc Natl Acad Sci U S A, 2008. **105**(12): p. 4838-43.
240. Elmore, S., *Apoptosis: a review of programmed cell death.* Toxicol Pathol, 2007. **35**(4): p. 495-516.
241. Shang, Y., S. Smith, and X. Hu, *Role of Notch signaling in regulating innate immunity and inflammation in health and disease.* Protein Cell, 2016. **7**(3): p. 159-74.
242. Lin, M. and Y. Rikihisa, *Ehrlichia chaffeensis downregulates surface Toll-like receptors 2/4, CD14 and transcription factors PU.1 and inhibits*

- lipopolysaccharide activation of NF-kappa B, ERK 1/2 and p38 MAPK in host monocytes.* Cell Microbiol, 2004. **6**(2): p. 175-86.
243. Strasser, A., L. O'Connor, and V.M. Dixit, *Apoptosis signaling.* Annu Rev Biochem, 2000. **69**: p. 217-45.
244. Suzuki, Y., Y. Nakabayashi, and R. Takahashi, *Ubiquitin-protein ligase activity of X-linked inhibitor of apoptosis protein promotes proteasomal degradation of caspase-3 and enhances its anti-apoptotic effect in Fas-induced cell death.* Proc Natl Acad Sci U S A, 2001. **98**(15): p. 8662-7.
245. Ge, Y. and Y. Rikihisa, *Anaplasma phagocytophilum delays spontaneous human neutrophil apoptosis by modulation of multiple apoptotic pathways.* Cell Microbiol, 2006. **8**(9): p. 1406-16.
246. Peterson, Q.P., et al., *Preparation of the caspase-3/7 substrate Ac-DEVD-pNA by solution-phase peptide synthesis.* Nat Protoc, 2010. **5**(2): p. 294-302.
247. Creagh, E.M., et al., *Smac/Diablo antagonizes ubiquitin ligase activity of inhibitor of apoptosis proteins.* J Biol Chem, 2004. **279**(26): p. 26906-14.
248. Liu, Y., et al., *Obligate intracellular bacterium Ehrlichia inhibiting mitochondrial activity.* Microbes Infect, 2011. **13**(3): p. 232-8.
249. Lin, M., et al., *Ehrlichia secretes Etf-1 to induce autophagy and capture nutrients for its growth through RAB5 and class III phosphatidylinositol 3-kinase.* Autophagy, 2016. **12**(11): p. 2145-2166.
250. Choi, K.S., et al., *Differential innate immune cell activation and proinflammatory response in Anaplasma phagocytophilum infection.* Infect Immun, 2007. **75**(6): p. 3124-30.
251. Fischer, A., et al., *Chlamydia trachomatis-containing vacuole serves as deubiquitination platform to stabilize Mcl-1 and to interfere with host defense.* Elife, 2017. **6**.
252. Forsberg, M., et al., *Differential effects of invasion by and phagocytosis of Salmonella typhimurium on apoptosis in human macrophages: potential role of Rho-GTPases and Akt.* J Leukoc Biol, 2003. **74**(4): p. 620-9.
253. Ge, Y., et al., *Anaplasma phagocytophilum inhibits human neutrophil apoptosis via upregulation of bfl-1, maintenance of mitochondrial membrane potential and prevention of caspase 3 activation.* Cell Microbiol, 2005. **7**(1): p. 29-38.
254. Holla, S., et al., *Mycobacterium bovis BCG promotes tumor cell survival from tumor necrosis factor-alpha-induced apoptosis.* Mol Cancer, 2014. **13**: p. 210.
255. Hueffer, K. and J.E. Galan, *Salmonella-induced macrophage death: multiple mechanisms, different outcomes.* Cell Microbiol, 2004. **6**(11): p. 1019-25.
256. Chen, F., et al., *[Induction of IL-8 by Chlamydia trachomatis through MAPK pathway rather than NF-kappaB pathway].* Zhong Nan Da Xue Xue Bao Yi Xue Ban, 2010. **35**(4): p. 307-13.
257. Choi, K.S., J.T. Park, and J.S. Dumler, *Anaplasma phagocytophilum delay of neutrophil apoptosis through the p38 mitogen-activated protein kinase signal pathway.* Infect Immun, 2005. **73**(12): p. 8209-18.
258. Figueiredo, J.F., et al., *Salmonella enterica Typhimurium SipA induces CXC-chemokine expression through p38MAPK and JUN pathways.* Microbes Infect, 2009. **11**(2): p. 302-10.
259. Popa, C.M., M. Tabuchi, and M. Valls, *Modification of Bacterial Effector Proteins Inside Eukaryotic Host Cells.* Frontiers in Cellular and Infection Microbiology, 2016. **6**(73).
260. Balcewicz-Sablinska, M.K., et al., *Pathogenic Mycobacterium tuberculosis evades apoptosis of host macrophages by release of TNF-R2, resulting in inactivation of TNF-alpha.* J Immunol, 1998. **161**(5): p. 2636-41.

261. Bastidas, R.J., et al., *Chlamydial intracellular survival strategies*. Cold Spring Harb Perspect Med, 2013. **3**(5): p. a010256.
262. Artavanis-Tsakonas, S., *The molecular biology of the Notch locus and the fine tuning of differentiation in Drosophila*. Trends Genet, 1988. **4**(4): p. 95-100.
263. Song, B.Q., et al., *Inhibition of Notch Signaling Promotes the Adipogenic Differentiation of Mesenchymal Stem Cells Through Autophagy Activation and PTEN-PI3K/AKT/mTOR Pathway*. Cell Physiol Biochem, 2015. **36**(5): p. 1991-2002.
264. Andersen, P., et al., *Non-canonical Notch signaling: emerging role and mechanism*. Trends Cell Biol, 2012. **22**(5): p. 257-65.
265. Palomero, T., et al., *Mutational loss of PTEN induces resistance to NOTCH1 inhibition in T-cell leukemia*. Nat Med, 2007. **13**(10): p. 1203-10.
266. Zhivotovsky, B., et al., *Caspases: their intracellular localization and translocation during apoptosis*. Cell Death Differ, 1999. **6**(7): p. 644-51.
267. Delbue, D., et al., *Expression of nuclear XIAP associates with cell growth and drug resistance and confers poor prognosis in breast cancer*. Biochim Biophys Acta Mol Cell Res, 2020. **1867**(10): p. 118761.
268. Cao, Z., et al., *X-linked inhibitor of apoptosis protein (XIAP) lacking RING domain localizes to the nuclear and promotes cancer cell anchorage-independent growth by targeting the E2F1/Cyclin E axis*. Oncotarget, 2014. **5**(16): p. 7126-37.
269. Xiao, Y., et al., *Chlamydia trachomatis infection inhibits both Bax and Bak activation induced by staurosporine*. Infect Immun, 2004. **72**(9): p. 5470-4.
270. Banga, S., et al., *Legionella pneumophila inhibits macrophage apoptosis by targeting pro-death members of the Bcl2 protein family*. Proc Natl Acad Sci U S A, 2007. **104**(12): p. 5121-6.
271. Alberdi, P., et al., *Anaplasma phagocytophilum Manipulates Host Cell Apoptosis by Different Mechanisms to Establish Infection*. Vet Sci, 2016. **3**(3).
272. Zhang, J.Z., et al., *Survival strategy of obligately intracellular Ehrlichia chaffeensis: novel modulation of immune response and host cell cycles*. Infect.Immun., 2004. **72**(1): p. 498-507.
273. Lu, J., et al., *SM-164: a novel, bivalent Smac mimetic that induces apoptosis and tumor regression by concurrent removal of the blockade of cIAP-1/2 and XIAP*. Cancer Res, 2008. **68**(22): p. 9384-93.
274. Wei, M.C., et al., *tBID, a membrane-targeted death ligand, oligomerizes BAK to release cytochrome c*. Genes Dev, 2000. **14**(16): p. 2060-71.
275. Lu, J., D. Wang, and J. Shen, *Hedgehog signalling is required for cell survival in Drosophila wing pouch cells*. Sci Rep, 2017. **7**(1): p. 11317.
276. Gooz, M., *ADAM-17: the enzyme that does it all*. Crit Rev Biochem Mol Biol, 2010. **45**(2): p. 146-69.
277. Purow, B., *Notch inhibition as a promising new approach to cancer therapy*. Adv Exp Med Biol, 2012. **727**: p. 305-19.

## VITA

**LaNisha L. Patterson, B.S., M.S.**

### WORK AND RESEARCH EXPERIENCE:

2023 Postdoctoral Fellow  
MD Anderson Cancer Center – Translational Research in Multi-Disciplinary Program (TRIUMPH) Postdoctoral Fellowship

### EDUCATION:

2016- 2022 University of Texas Medical Branch – Galveston, Graduate Student, Cell Biology

2014 - 2016 Texas Southern University - Masters of Science, Biology

2015 Graduate Training  
Graduate Research Assistant, Summer Research Experience  
Department of Pediatrics, Cancer Prevention Research Training Program (National Cancer Institute R25E CA056452 Cancer Prevention Education: Student Research Experiences, Dr. Shine Chang, Principal Investigator)  
The University of Texas MD Anderson Cancer Center, Houston, TX Mentor: Dr. Joya Chandra

2007 – 2012 Marquette University – Bachelors of Science, Biological Sciences

### HONORS AND AWARDS

2022 The American Society of Rickettsiology Travel Award  
The 31st American Society of Rickettsiology Meeting,  
Greenville SC

2022 The McLaughlin Travel Award  
The 2022 McLaughlin Colloquium  
University of Texas Medical Branch, Galveston, TX

2021 The Pathology Research Day Poster Award  
The 26<sup>th</sup> Department of Pathology Research Day  
University of Texas Medical Branch, Galveston, TX

2020 The Pathology Research Day Poster Award  
The 26<sup>th</sup> Department of Pathology Research Day  
University of Texas Medical Branch, Galveston, TX

2020 ASCB Grant - to promote inclusivity of diverse populations in STEM The American Society of Cell Biology 2020 Virtual Conference

2020 First Place Oral Presentation  
7<sup>th</sup> Annual Cell Biology Graduate Program Student Symposium  
University of Texas Medical Branch, Galveston, TX

2019 The Pathology Research Day Poster Award  
25th Annual Department of Pathology Trainee Research Day  
University of Texas Medical Branch, Galveston, TX

2019 Edward S. Reynolds Award  
24th Annual Trainee Research Day  
University of Texas Medical Branch, Galveston, TX

2019 Mikiten Travel Award  
Mikiten Graduate Research Symposium, Graduate Student Association  
UT Health San Antonio, San Antonio, TX

2018 Outstanding Service Award  
Department of Cell Biology, Cell Biology Graduate Program  
University of Texas Medical Branch, Galveston, TX

2016 Outstanding Graduate Student Award  
Masters of Biology Student  
Department of Biology, College of Science and Engineering  
Technology  
Texas Southern University, Houston, TX

2015 Cancer Prevention Research Training Program Certification of Completion  
Graduate Research Assistant, Summer Research Experience  
Department of Pediatrics, Cancer Prevention Research Training Program (National Cancer Institute R25E CA056452 Cancer Prevention Education: Student Research Experiences, Dr. Shine Chang, Principal Investigator)  
The University of Texas MD Anderson Cancer Center, Houston, TX Mentor: Dr. Joya Chandra

2015 Summer Research Experience Certification of Participation in the Elevator Speech Competition  
Graduate Research Assistant, Summer Research Experience  
Department of Pediatrics, Cancer Prevention Research Training Program (National Cancer Institute R25E CA056452 Cancer Prevention Education: Student Research Experiences, Dr. Shine Chang, Principal Investigator)

- The University of Texas MD Anderson Cancer Center, Houston, TX Mentor: Dr. Joya Chandra
- 2015 Summer Research Experience Elevator Speech Competition Best Speech Award Winner  
Graduate Research Assistant, Summer Research Experience Department of Pediatrics, Cancer Prevention Research Training Program (National Cancer Institute R25E CA056452 Cancer Prevention Education: Student Research Experiences, Dr. Shine Chang, Principal Investigator)  
The University of Texas MD Anderson Cancer Center, Houston, TX Mentor: Dr. Joya Chandra
- 2008 “Woman Putting Their Stamp on Metro Milwaukee” Youth Achiever award
- 2007 - Present Bill and Melinda Gates Millennium Scholarship Recipient
- 2007 Brady Corporation Scholarship Recipient

**RESEARCH:**

- 2016 MD Anderson Cancer Center, Department of Pediatrics, Graduate Research Assistant-non-UTHSCH, Summer Research Experience, The University of Texas MD Anderson Cancer Center, Houston, TX Principal Investigator: Dr. Joya Chandra  
*Targeting the Nrf2/HO-1 antioxidant pathway in Flt3-ITD positive AML: A Novel Therapeutic Approach*
- 2014 – 2016 Masters of Biology Student  
Texas Southern University  
Department of Biology  
Advisor: Mario Hollomon, Ph.D.  
*Knockdown of autophagy proteins, ATG5 or LC3, has an opposing effect on anticancer drug treatment in a k-Ras transformed osteosarcoma cell line.*
- 2015 Graduate Research Assistant, Summer Research Experience Department of Pediatrics, Cancer Prevention Research Training Program (National Cancer Institute R25E CA056452 Cancer Prevention Education: Student Research Experiences, Dr. Shine Chang, Principal Investigator),  
The University of Texas MD Anderson Cancer Center, Houston, TX  
Mentor: Dr. Joya Chandra

*Examining the Cooperation Between the Notch Signaling and HO-1 Mediated Antioxidant Pathways in Acute Myeloid Leukemia*

**Manuscripts/Peer Reviews**

Byerly CD, Mitra S, **Patterson LL**, Pittner NA, Velayutham TS, Paessler S, Veljkovic V, McBride JW. Ehrlichia SLiM ligand mimetic activates Hedgehog signaling to engage a BCL-2 anti-apoptotic cellular program. PLoS Pathog. 2022 May 16;18(5):e1010345. doi: 10.1371/journal.ppat.1010345. <https://doi.org/10.1371/journal.ppat.1010345>

Kannan S, Irwin ME, Herbrich SM, Cheng T, **Patterson LL**, Aitken MJL, Bhalla K, You MJ, Konopleva M, Zweidler-McKay PA, Chandra J. Targeting the NRF2/HO-1 Antioxidant Pathway in FLT3-ITD-Positive AML Enhances Therapy Efficacy. Antioxidants (Basel). 2022 Apr 5;11(4):717. doi: 10.3390/antiox11040717. <https://doi.org/10.3390/antiox11040717>

**Patterson LL**, Velayutham TS, Byerly CD, Bui DC, Patel J, Veljkovic V, Paessler S, McBride JW. Ehrlichia SLiM Ligand Mimetic Activates Notch Signaling in Human Monocytes. mBio. 2022 Apr 26;13(2):e0007622. doi: 10.1128/mbio.00076-22. Epub 2022 Mar 31. <https://doi.org/10.1128/mbio.00076-22>

Byerly CD, **Patterson LL**, McBride JW. Ehrlichia TRP effectors: moonlighting, mimicry and infection. Pathog Dis. (2021) 79(5):ftab026. <https://doi.org/10.1093/femspd/ftab026>

**Patterson LL**, Byerly CB, McBride JW. *Anaplasmatocae*: Dichotomous Autophagic Interplay for Infection, Frontiers in Immunology (2021) 12:642771. <https://doi.org/10.3389/fimmu.2021.642771>

Rogan MR, **Patterson LL**, Byerly C, Luo T, Paessler S, Veljkovic V, Quade B, McBride JW. *Ehrlichia chaffeensis* TRP120 is a Wnt Ligand Mimetic that Interacts with Wnt Receptors and Contains a Novel Repetitive Short Linear Motif that Activates Wnt Signaling. mSphere (2021) 6:e00216-21. <https://doi.org/10.1128/msphere.00216-21>

Wang JY, Zhu B, **Patterson LL**, Kibler CE, McBride JW. *Ehrlichia chaffeensis* TRP120-mediated ubiquitination and proteasomal degradation of tumor suppressor FBW7 increases oncoprotein stability and promotes infection, PLoS Pathogens. (2019). 16(4): e1008541. <https://doi.org/10.1371/journal.ppat.1008541>

Hollomon, MG, **Patterson L**, Santiago-O'Farrill J, Kleinerman ES, Gordon N. Knockdown of Fas-Associated Protein with Death Domain (FADD) Sensitizes Osteosarcoma to TNF $\alpha$ -induced Cell Death, *Journal of Cancer*. (2020). 11(7):1657-1667. doi: 10.7150/jca.38721. <https://pubmed.ncbi.nlm.nih.gov/32194778/>

Rogan MR, **Patterson LL**, Wang JY, McBride JW. Bacterial Manipulation of Wnt Signaling: A Host-Pathogen Tug-of-Wnt, *Frontiers*. (2019). 10:2390. <https://doi.org/10.3389/fimmu.2019.02390>

### Abstracts

Hornbaker MJ, Irwin ME, **Patterson L**, Herbrich SM, Zweidler-McKay P, and Chandra J. (2015). Targeting the NRF2/HO-1 Antioxidant Pathway with Consequences for Notch Signaling in FLT3-ITD Positive AML: A Novel Therapeutic Approach, *Blood*, 126(23), 2470.

### PRESENTATIONS

- 2022 Patterson, L. *Ehrlichia* SLiM Ligand Mimetic Activates Notch Signaling in Human Monocytes. Oral Presentation at the 31st American Society of Rickettsiology Meeting, Greenville SC.
- 2022 Patterson, L. *Ehrlichia chaffeensis* activation of notch signaling stabilizes XIAP expression to inhibit caspase activation. Poster Presentation at the 31st American Society of Rickettsiology Meeting, Greenville SC.
- 2021 Patterson, L. *Ehrlichia chaffeensis* TRP120 Notch Ligand Memetic Motif Interacts with Notch Epidermal Growth Factor Domains to Activate Notch Signaling. Virtual poster presentation at the UTMB 27<sup>th</sup> Annual Pathology Department Trainee Research Day.
- 2021 Patterson, L. *Ehrlichia chaffeensis* TRP120 Notch Ligand Memetic Motif Interacts with Notch Epidermal Growth Factor Domains to Activate Notch Signaling. Virtual poster presentation at the American Society of Cell Biology EMBO Meeting.
- 2021 Patterson, L. *Ehrlichia chaffeensis* TRP120 Notch Ligand Memetic Motif Interacts with Notch Epidermal Growth Factor Domains to Activate Notch Signaling. Virtual poster presentation at the 2021 UTMB IHII/McLaughlin Colloquium on Infection & Immunity.
- 2020 Patterson, L. *Ehrlichia chaffeensis* TRP120 Notch Ligand Memetic Motif Interacts with Notch Epidermal Growth Factor Domains to Activate Notch Signaling. Virtual poster presentation at the UTMB 26<sup>th</sup> Annual Pathology Department Trainee Research Day.
- 2020 Patterson, L. *Ehrlichia chaffeensis* TRP120 Notch Ligand Memetic Motif Interacts with Notch Epidermal Growth Factor Domains to Activate Notch Signaling. Virtual poster presentation at the American Society of Cell Biology Virtual 2020 EMBO Meeting.

- 2020 Patterson, L. *Ehrlichia chaffeensis* TRP120 Notch Ligand Memetic Motif Interacts with Notch Epidermal Growth Factor Domains to Activate Notch Signaling. Virtual poster presentation at the American Society of Microbiology.
- 2019 Patterson, L. *Ehrlichia chaffeensis* TRP120 Notch Ligand Memetic Motif Interacts with Notch Epidermal Growth Factor Domains to Activate Notch Signaling. Poster presentation at the American Society of Cell Biology EMBO Meeting, Washington, D.C.
- 2019 Patterson, L. *Ehrlichia chaffeensis* TRP120 Notch Ligand Memetic Motif Interacts with Notch Epidermal Growth Factor Domains to Activate Notch Signaling. Poster presentation at the UTMB 24th Annual Trainee Research Day, Galveston, TX.
- 2019 Patterson, L. *Ehrlichia chaffeensis* TRP120 Interacts with Notch Epidermal Growth Factor Domains to Activate Notch Signaling. Oral Presentation at the 30<sup>th</sup> Meeting of the American Society for Rickettsiology, Sante Fe, NM.
- 2019 Patterson, L. *Ehrlichia chaffeensis* activation of Notch signaling increases XIAP expression to inhibit intrinsic apoptosis. Poster Presentation at the 30<sup>th</sup> Meeting of the American Society for Rickettsiology, Sante Fe, NM.
- 2019 Patterson, L. *Ehrlichia chaffeensis* TRP120 Notch Ligand Memetic Motif Interacts with Notch Epidermal Growth Factor Domains to Activate Notch Signaling. Poster presentation at the UT Health San Antonio Mikiten Graduate Research Symposium, San Antonio, TX.
- 2018 Patterson, L. Identification of a Notch Activation Motif in the *Ehrlichia chaffeensis* TRP120 Effector. Oral Presentation at the 29<sup>th</sup> Meeting of the American Society for Rickettsiology, Milwaukee, WI.
- 2015 Patterson, L. Impact of Autophagy Inhibition on Anticancer Drug Treatment in Ovarian Cancer Cells. Oral Presentation at Texas Southern University Biology Graduate Research Seminar Series.
- 2015 Irwin, M.E., Hornbaker, M., Patterson, L., Zweidler-McKay, P.A., Chandra, J. Targeting the NRF2/HO-1 Antioxidant Pathway with Consequences for Notch Signaling in FLT3-ITD Positive AML: A Novel Therapeutic Approach. Accepted for a poster presentation. 2015 American Society of Hematology Annual Meeting.
- 2015 Patterson, L., Irwin, M.E., Hornbaker, M., Patterson, L., Zweidler-McKay, P.A., Chandra, J. Examining the Cooperation Between the Notch Signaling and HO-1 Mediated Antioxidant Pathways in Acute Myeloid Leukemia. MD Anderson Summer Experience Final Event: Poster Session & Elevator Speech Competition.

## **TEACHING/MENTORSHIP**

- 2019 UTMB High School Summer Biomedical Research Program  
Graduate Mentor  
Office of Educational Outreach and Committee in Support of Science  
Education  
University of Texas Medical Branch, Galveston, TX  
Department of Pathology
- 2018 UTMB High School Summer Biomedical Research Program  
Outstanding Support as a Guest Lecturer  
Office of Educational Outreach and Committee in Support of Science  
Education  
University of Texas Medical Branch, Galveston, TX
- 2017 Biomedical Research Training for High School Students  
Graduate Mentor  
Office of Educational Outreach and Committee in Support of Science  
Education  
University of Texas Medical Branch, Galveston, TX  
Department of Pathology
- 2015 – 2016 Teacher's Assistant, Developmental Biology  
Texas Southern University, Houston, TX  
Department of Biology
- 2014 – 2016 Teacher's Assistant, Immunology  
Texas Southern University, Houston, TX  
Department of Biology

## **PROFESSIONAL CERTIFICATIONS**

- 2019 Good Laboratory Practice (GLP) Training 3 sessions: Basic GLP Training; Certificate of Training, University of Texas Medical Branch, The Office of Regulated Nonclinical Studies.
- 2018 Making Medicines: The Process of Drug Development eLearning Course, Certificate of Completion, Lilly USA, LLC
- 2018 Animal Biosafety Level 2 International Biosafety Training, Certificate of Completion, University of Texas Medical Branch, International Biosafety Training Center

## **PROFESSIONAL AFFILIATIONS/ACTIVITIES**

- 2019 The American Society for Cell Biology, Student Member
- 2018 - 2019 The Society of Cell Biology, President, Department of Cell Biology, University of Texas Medical Branch

2017- 2018	The Society of Cell Biology, Secretary, Department of Cell Biology, University of Texas Medical Branch
2016 - 2017	Graduate School Organization Cell Biology Board of Ambassador at University of Texas Medical Branch – Galveston
2015 – 2016	Founder and President of Texas Southern University’s Inaugural Biology Graduate Student Association (BGSA) Graduate Seminar Series
2007 – 2011	Black Student Council Member
2006 - 2007	President of the National Honors Society for Messmer High School
2004 - 2007	National Honors Society Member, Messmer High School

## RESEARCH SUPPORT

1F31 AI152424-01 (L Patterson, PI) 09/01/2020-  
 Current  
 NIH/NIAID  
 “Characterizing Notch Ligand Mimic Function of the *Ehrlichia* TRP120 Effector in Suppression of Host Cell Apoptosis”  
 This proposal aims to uncover the molecular and functional interactions and mechanisms responsible for *E. chaffeensis* TRP120 Notch activation.

McLaughlin Pre-doctoral Fellowship Fund (L Patterson, PI) 09/01/2019-Current  
 UTMB  
 “Characterizing Notch Ligand Mimic Function of the *Ehrlichia* TRP120 Effector in Suppression of Host Cell Apoptosis”  
 This proposal aims to uncover the molecular and functional interactions and mechanisms responsible for *E. chaffeensis* TRP120 Notch activation.

## SCHOLARSHIPS

2021	Edith and Robert Zinn Presidential Scholarship- The University of Texas Medical Branch, Galveston, TX
2020	Robert Shope Endowed Scholarship- The University of Texas Medical Branch, Galveston, TX
2019	Eva Yznaga Seger, MD Presidential Scholarship- The University of Texas Medical Branch, Galveston, TX
2019	The Arthur V. Simmang Scholarship Fund GSBS- The University of Texas Medical Branch, Galveston, TX

2018

The Arthur V. Simmang Scholarship Fund GSBS- The University  
of Texas Medical Branch, Galveston, TX

2007 – 2019

Bill and Melinda Gates Millennium Scholarship Recipient